

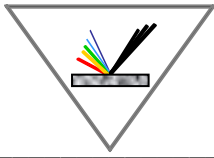
**18th International School
on Quantum Electronics**

LASER PHYSICS AND APPLICATIONS



Book of abstracts

**29 September – 03 October 2014
Sozopol, Black sea, Bulgaria**



БЪЛГАРСКА АКАДЕМИЯ НА НАУКИТЕ

ИНСТИТУТ ПО ЕЛЕКТРОНИКА "АКАДЕМИК ЕМИЛ ДЖАКОВ"

BULGARIAN ACADEMY OF SCIENCES

INSTITUTE OF ELECTRONICS "ACADEMICIAN EMIL DJAKOV"

***EIGHTEENTH INTERNATIONAL SCHOOL ON QUANTUM
ELECTRONICS***

"LASER PHYSICS AND APPLICATIONS"

29 September – 3 October, 2014,

Sozopol, Black Sea, Bulgaria

BOOK OF ABSTRACTS

ABOUT THE ACADEMICIAN EMIL DJAKOV INSTITUTE OF ELECTRONICS

72 Tsarigradsko Chaussee, 1784 Sofia, Bulgaria

<http://www.ie-bas.dir.bg>

The Institute of Electronics at the Bulgarian Academy of Sciences (IE-BAS) was established in 1963 as a non-profit state organization conducting research, education and dissemination of scientific knowledge in the fields of Physical Electronics, Photonics and Quantum Electronics and Radio Sciences. Soon, the Institute of Electronics evolved as a leading scientific institution in these areas of applied physics and engineering within the Bulgarian Academy of Sciences and in Bulgaria.

It was in the IE-BAS where the first Bulgarian laser, lidar, plasma torch, ultra-high vacuum pump, microchannel electron-optical convertor, microwave parametric amplifier, Josephson junction and SQUID, portable microwave moisture meter, magnetometer, electron-beam melting and welding installations were developed, together with state-of-the-art electron-beam, laser and plasma technologies.

Through the years, the Institute's research field and structure have developed dynamically in response to the changes taking place in the main trends in applied physics and technologies. IE-BAS aims to sustain and advance previous pioneering work by promoting the theory, basic science and technology of photonics, optoelectronics, environmental monitoring, laser bio-medical research and applications. This involves searching for new materials, new techniques, new devices and new applications.

**EIGHTEENTH INTERNATIONAL SCHOOL ON QUANTUM
ELECTRONICS**

“LASER PHYSICS AND APPLICATIONS”

ORGANIZED BY

the Institute of Electronics, Bulgarian Academy of Sciences

in cooperation with



***The international society advancing an interdisciplinary
approach to the science and application of light***

www.spie.org



***European Office of Aerospace Research and Development
We wish to thank the following for their contribution to the
success of this conference: European Office of Aerospace
Research and Development, Air Force Office of Scientific
Research, United States Air Force Research Laboratory***

www.london.af.mil



***Ministry of Education, Youth and Science
Republic of Bulgaria***

www.mon.bg



Bulgarian Academy of Sciences

www.bas.bg



The European Physical Society

www.eps.org



NTUA

*The National Technical University of Athens
School of Applied Mathematical and Physical Sciences*

www.ntua.gr



AMERICAN ELEMENTS

www.americanelements.com

COMMITTEES

INTERNATIONAL ADVISORY COMMITTEE

Name	Affiliation	Country
Chairmen:		
Prof. Alexander Serafetinides	National Technical University of Athens (NTUA), Applied Physics Department	GREECE
Members:		
Dr. Peter Balling	Department of Physics and Astronomy, Aarhus University	DENMARK
Prof. Pradip Narayan Ghosh	Jadavpur University, Department of Physics, University of Calcutta	INDIA
Prof. Malgorzata Glodz	Institute of Physics, Polish Academy of Sciences, Warszawa	POLAND
Prof. David Sarkisyan	Laser Spectroscopy Laboratory, Institute for Physical Research, Armenian Academy of Sciences	ARMENIA
Prof. Gerard Sliwinski	The Szewalski Institute, Polish Academy of Sciences	POLAND
Prof. Luigi Moi	Department of Physics - University of Siena	ITALY
Prof. Ludger Wöste	Freie Universität Berlin, FB Physik, Berlin	GERMANY
Prof. V. N. Serkin	Benemerita Universidad Autonoma de Puebla	MEXICO
Prof. Victor Zadkov	International Laser Center, M.V. Lomonosov, Moscow State University	RUSSIA
Prof. S. A. Shlenov	International Laser Center, M.V. Lomonosov, Moscow State University	RUSSIA
Prof. Dimitris Balis	Laboratory of Atmospheric Physics, Aristotle University of Thessaloniki	GREECE
Dr. Stefano Lettieri	Universita degli Studi di Napoli Federico II, Department of Physics, Naples	ITALY

COMMITTEES

PROGRAM COMMITTEE

Name	Affiliation	Country
Prof. Peter Atanasov	Institute of Electronics, Bulgarian Academy of Sciences	BULGARIA
Prof. Latchezar Avramov	Institute of Electronics, Bulgarian Academy of Sciences	BULGARIA
Prof. Ion Mihailescu	National Institute for Laser, Plasma and Radiation Physics	ROMANIA
Dr. Stefka Cartaleva	Institute of Electronics, Bulgarian Academy of Sciences	BULGARIA
Dr. Lyubomir Kovachev	Institute of Electronics, Bulgarian Academy of Sciences	BULGARIA
Prof. Lucas Alados Arboledos	Applied Physics Department Science Faculty, University of Granada	SPAIN
Prof. Dimitar Angelov	Ecole Normale Supérieure de Lion	FRANCE
Prof. Emilio Mariotti	Unità di Siena, Dipartimento di Fisica Università di Siena	ITALY
Prof. Arlene Wilson- Gordon	Department of Chemistry, Bar-Ilan University, Ramat Gan	ISRAEL
Prof. Dimitar Stoyanov	Institute of Electronics, Bulgarian Academy of Sciences	BULGARIA

COMMITTEES

LOCAL ORGANIZING COMMITTEE

Chair: Assoc. Prof. Dr. Sanka Gateva

Vice-Chair:

Assoc. Prof. Dr. Mihaela Koleva

Secretary: Dr. Petko Todorov

Members:

Assoc. Prof. Dr. Tanja Dreischuh

Dr. Irina Bliznakova

Ivan Grigorov

Chavdar Ghelev

ADDRESS FOR COMMUNICATION

Institute of Electronics
Bulgarian Academy of Sciences
72, Tsarigradsko Chaussee Blvd.
1784 Sofia, Bulgaria

www.ie-bas.dir.bg, www.isqe2014.dir.bg

tel. (+359 2) 979 5851

e-mail: isqe.2014@gmail.com

SCHOOL TOPICS

- A. Laser - matter interactions
- B. Laser spectroscopy and metrology
- C. Laser remote sensing and ecology
- D. Lasers in biology and medicine
- E. Laser systems and nonlinear optics

*The organizers are very pleased to acknowledge the co-operating organizations
for their support of the school organization.*

TABLE OF CONTENTS

INVITED LECTURES

LASER-MATTER INTERACTION

- L1.** PHOTONIC FUNCTIONALIZATION AT NANOSCALE,
G. Śliwiński, A. Białous, K. Grochowska 18
- L2.** SYNTHESIS AND CHARACTERIZATION OF SILICON NANOWIRES BY
LASER METHODS,
N. Fukata 19
- L3.** METAL-OXIDE SEMICONDUCTOR NANOPARTICLES AND
MICROSTRUCTURES FOR PHOTOLUMINESCENCE-BASED CHEMICAL
SENSING: FUNDAMENTAL ISSUES AND APPLICATIONS,
*Stefano Lettieri, Pasqualino Maddalena, Deborah Pallotti, Salvatore Amoruso,
Riccardo Bruzzese, Maria Cristina Carotta* 20

LASER SPECTROSCOPY AND METROLOGY

- L4.** SPECTROSCOPY OF ATOMS IN STRONG MAGNETIC FIELDS AND
APPLICATIONS BASED ON MICRO AND NANO-CELLS,
D. Sarkisyan, G. Hakhumyan, A. Sargsyan 21
- L5.** SELECTIVE REFLECTION OF LIGHT FROM A VAPOR OF ALKALI DIMERS,
S. Shmavonyan, A. Khanbekyan, A. Gogyan, M. Movsisyan, A. Papoyan 22
- L6.** VELOCITY ANISOTROPY EFFECT IN PUMP-PROBE SPECTRA OF CESIUM IN
A MICROMETRIC THICKNESS OPTICAL CELL,
P N Ghosh, S Mitra and B Ray, A. Krasteva, D. Slavov, P. Todorov and S. Cartaleva 23
- L7.** SIMULATION OF LIGHT INTERACTION WITH ALCALI ATOMS IN COATED
OPTICAL CELLS,
K. Nasyrov 24
- L8.** DEGENERATE TWO- AND THREE-LEVEL SYSTEMS IN PRESENCE OF
LONGITUDINAL AND TRANSVERSE MAGNETIC FIELDS,
A. D. Wilson-Gordon, L. Margalit, M. Rosenbluh 25
- L9.** SATURATION EFFECTS IN REFLECTION SPECTROSCOPY OF DILUTE
RESONANCE VAPORS,
T. A. Vartanyan 26
- L10.** NON-CLASSICALLY PAIRED PHOTONS FROM SOURCES BASED ON COLD
ATOMS,
Małgorzata Głódź, Maciej Janowicz, Krzysztof Kowalski, Jerzy Szonert 27

TABLE OF CONTENTS

- L11.** THE LNL – Fr MOT: LOADING EFFICIENCY OPTIMIZATION AND SEARCH FOR NEW LINES,
E. Mariotti, S. Agustsson, G. Bianchi, A. Khanbekyan, C. Marinelli, L. Marmugi, L. Moi, R. Calabrese, G. Mazzocca, L. Tomassetti, L. Corradi, A. Dainelli, L. Ricci 28

LASER REMOTE SENSING AND ECOLOGY

- L12.** OPTICAL AND MICROPHYSICAL PROPERTIES OF AEROSOLS OVER SOUTHEASTERN EUROPE USING LIDAR AND SUNPHOTOMETER MEASUREMENTS,
Dimitris Balis 28

LASERS IN BIOLOGY AND MEDICINE

- L13.** PLASMON ASSISTED OPTICAL TRAPPING: FUNDAMENTALS AND BIOMEDICAL APPLICATIONS,
Alexander Serafetinides 29
- L14.** CHROMATIN DYNAMICS AND EPIGENETIC REGULATION,
Dimitar Angelov 30

LASER SYSTEMS AND NONLINEAR OPTICS

- L15.** QUANTUM OPTICS OF QUANTUM EMITTERS NEAR PLASMONIC NANOPARTICLES,
Victor Zadkov and Julia Vladimirova 32
- L16.** FEMTOSECOND LASER FILAMENT AND PLASMA CHANNELS IN THE FOCUSED BEAM IN AIR,
S. A. Shlenov, A. A. Dergachev, A. A. Ionin, V.P. Kandidov, D. V. Mokrousova, L. V. Seleznev, D. V. Sinitsyn, E. S. Sunchugasheva, A. P. Shustikova 34
- L17.** HIDDEN SYMMETRIES AND WAVE-PARTICLE DUALITY OF OPTICAL AND MATTER-WAVE SOLITONS,
V. N. Serkin 35

TABLE OF CONTENTS
ORAL AND POSTER PRESENTATIONS

A - LASER – MATTER INTERACTIONS

- PA1.** MATRIX DESCRIPTION OF THE BEHAVIOR OF DEPENDENT LOSSES IN POLARIZED HIGH-SPEED OPTICAL COMMUNICATION LINES,
Vanya Plachkova, Tinko Eftimov, Georgi Dyankov, Ilya Makrelov 37
- PA2.** FEMTOSECOND LASER SYSTEM FOR MICROMACHINING OF THE MATERIALS,
R. Barbucha, M. Kocik, K. M. Tański, Garasz, T. Petrov, C. Radzewicz 38
- PA3.** ESTIMATION OF ULTRASHORT LASER IRRADIATION EFFECT OVER THIN TRANSPARENT BIOPOLYMER FILMS MORPHOLOGY,
A. Daskalova, C. Nathala, I. Bliznakova, D. Slavov, W. Husinsky 39
- PA4.** FABRICATION OF ZnO NANOSTRUCTURES BY PLD,
A. Og. Dikovska, G. B. Atanasova, G. V. Avdeev, M. E. Koleva, N. N. Nedyalkov, P. A. Atanasov 40
- PA5.** INFLUENCE OF THE SCANNING CONDITIONS ON THE CHARACTERISTICS OF THE NANOSTRUCTURES FABRICATED BY LASER ABLATION IN LIQUID,
A. S. Nikolov, R. G. Nikov, N. N. Nedyalkov, M. T. Alexandrov, D. B. Karashanova, N. E. Marinkov, I. Z. Dimitrov, I. I. Boevski 41
- PA6.** FABRICATION AND CHARACTERIZATION OF METAL SUBSTRATES,
Ru. G. Nikov, N. N. Nedyalkov, P. A. Atanasov 42
- PA7.** EFFECTS OF LASER INTERACTION WITH HISTORICAL COPPER ALLOY COVERED BY PATINA LAYERS,
Iwona Żmuda-Trzebiatowska, Katarzyna Schaefer, Mirek Sawczak, Gerard Śliwiński 42
- PA8.** MORPHOLOGICAL AND OPTICAL PROPERTIES OF NOBLE METAL NANOPARTICLES PRODUCED BY LASER ABLATION,
A. Og. Dikovska, M. Alexandrov, G. Atanasova 43
- PA9.** OPTICAL PROPERTIES OF Ag-ZnO NANOSTRUCTURES,
M. E. Koleva, N. N. Nedyalkov, P. A. Atanasov, N. Fukata, M. Dutta 44
- PA10.** LASER DISPERSING OF WC AND TIC POWDERS IN LIGHT METAL ALLOYS FOR WEAR RESISTANCE ENHANCEMENT,
Rafał Jendrzejewski, Gerard Śliwiński 45

TABLE OF CONTENTS

PA.11	PULSED LASER DEPOSITION OF ORGANIC SEMICONDUCTOR RUBRENE THIN FILMS, Katarzyna Grochowska, Sayani Majumdar, Mirosław Sawczak and Gerard Śliwiński	46
OA1.	THE INTERACTION OF HIGH-POWER LASER PULSE WITH MULTICOMPONENT POLYCRYSTALLINE ROCKS, <i>I. S. Timofeev, I. N. Burdonsky, A. Yu. Goltsov, K. N. Makarov, A. G. Leonov, V. N. Yufa</i>	47
B - LASER SPECTROSCOPY AND METROLOGY		
PB1.	PHASE RECOVERY FROM FRINGE PATTERNS: APPROACH BASED ON HILBERT TRANSFORM AND WAVELET DE-NOISING TECHNIQUES, <i>Peter Sharlandjiev and Natalia Berberova</i>	49
PB2.	AN ANISOTROPIC STRATIFIED STRUCTURE FOR SURFACE PLASMON EXCITATION, <i>Katerina Zhelyazkova and Georgi Dyankov</i>	49
PB3.	ENHANCED VELOCITY SELECTIVE OPTICAL PUMPING IN BI-CHROMATIC EXCITATION OF CS VAPOR IN MICROMETRIC OPTICAL CELL, <i>A. Krasteva, B. Ray, D. Slavov, P. Todorov, P. N. Ghosh, S. Mitra, V. Nikolova and S. Cartaleva</i>	50
PB4.	RUBIDIUM VAPOUR DENSITY MODIFICATION DUE TO LIGHT INDUCED ATOMIC DESORPTION EFFECT, <i>C. Marinelli, E. Mariotti, L. Marmugi, L. Moi, S. Gateva, A. Krasteva, S. Cartaleva</i>	51
PB5.	CONVERSION BETWEEN ELECTROMAGNETICALLY INDUCED ABSORPTION AND TRANSPARENCY IN A FOUR-LEVEL SYSTEM, <i>D. Sarkisyan, A. Sargsyan, A. D. Wilson-Gordon, S. Cartaleva</i>	52
PB6.	MECHANISMS OF NH-PHOTODISSOCIATION IN THE NUCLEOBASE ANALOGUE 2,4-DIAMINOPYRIMIDINE: EXPLORING CONICAL INTERSECTIONS, <i>Pavlina Kancheva, Deniz Tuna, Wolfgang Domcke, Vassil B. Delchev</i>	53
PB7.	INVESTIGATION OF THE INFLUENCE OF STRONTIUM CARBONATE ON FLUORESCENCE SPECTRA OF OXY-FLUORIDE GLASSES DOPED WITH SAMARIUM OXIDE AND SAMARIUM FLUORIDE, <i>Teodora Pashova, Tinko Eftimov, Irena Kostova, Dancho Tonchev, Daniel Brabant</i>	54
PB8.	OBSERVATION OF POLARIZATION DEPENDENT EFFECTS IN MULTILEVEL EIT LAMBDA SYSTEM IN COLD RB ATOMS, <i>K. Kowalski, M. Głódź, J. Szonert, S. Gateva</i>	54

TABLE OF CONTENTS

PB9. ROBUST NARROWING OF DARK RESONANCES IN RB VAPOR WITH COAXIAL COUNTER-PROPAGATING LASER BEAMS, <i>I. Radojičić, M. Radonjić, Z. Grujić, M. Lekić, D. Lukić and B. M. Jelenković</i>	55
PB10. SENSITIVITY AND RESOLUTION OF DYNAMIC LASER SPECKLE METROLOGY, <i>Elena Stoykova, Tanya Nikova</i>	56
PB11. STRUCTURE OF THE FLUORESCENCE MAGNETO-OPTICAL RESONANCE IN A PARAFFIN-COATED 87Rb VACUUM CELL, <i>E. Taskova, E. Alipieva and G. Todorov</i>	57
PB12. SIMPLE METHOD FOR CHARACTERIZATION OF ANTI-RELAXATION COATING OF OPTICAL CELLS, <i>K. Nasyrov, V. Entin, N. Nikolov, N. Petrov, S. Cartaleva</i>	58
PB13. SUB-DOPPLER SPECTROSCOPY ON THE D1 LINE OF POTASSIUM, <i>S. Gozzini, A. Lucchesini, C. Marinelli, L. Marmugi, S. Gateva, S. Tsvetkov, S. Cartaleva</i>	59
PB14. LIGHT-INDUCED ATOMIC DESORPTION DYNAMICS IN CELLS WITH DIFFERENT PDMS COATINGS, <i>S. Tsvetkov, M. Taslakov, E. Mariotti, S. Gateva</i>	61
PB15. PARAMETRIC NON-DEGENERATE FOUR WAVE MIXING IN HOT POTASSIUM VAPOR, <i>B. Zlatković, A.J. Krmpot, N. Šibalić, B. M. Jelenković</i>	62
PB16. MODELING OF THE NONLINEAR ABSORPTION OF CS ATOMS IN AN EXTREMELY THIN CELL - AN ITERATION APPROACH, <i>G. Todorov, D. Slavov, A. Krasteva, S. Cartaleva, V. Polischuk, T. Vartanyan</i>	63
OB1. PHOSPHORESCENCE OF BILIRUBIN, <i>V.Yu. Plavskii, V.N. Knyuksho, A.I. Tretyakova, A.V. Mikulich, L.G. Plavskaya, I.A. Leusenko, B.M. Dzhagarov</i>	64
OB2. INVESTIGATION OF SURFACES OF DRYING EVAPORATING MICRODROPLET CONTAINING SILICA AND SDS ADMIXTURES, <i>J. Archer, M. Kolwas, G. Derkachov, M. Woźniak, D. Jakubczyk and K. Kolwas</i>	65

TABLE OF CONTENTS

C- LASER REMOTE SENSING AND ECOLOGY

- PC1.** ÅNGSTRÖM COEFFICIENTS CALCULATED FROM AEROSOL OPTICAL DEPTH DATA OBTAINED OVER SOFIA, BULGARIA,
Tsvetina Evgenieva, Nikolay Kolev, Doyno Petkov 66
- PC2.** CEILOMETER OBSERVATION OF SAHARAN DUST OVER MOUNTAIN VALLEY OF SOFIA, BULGARIA,
Nikolay Kolev, Tsvetina Evgenieva, Ivan Grigorov, Atanaska Deleva, Danko Ivanov, Ventsislav Danchevski, Plamen Savov, Doyno Petkov 67
- PC3.** TWO-WAVELENGTH LIDAR CHARACTERIZATION OF OPTICAL, DYNAMICAL, AND MICROPHYSICAL PROPERTIES OF SAHARAN DUST LAYERS OVER SOFIA, BULGARIA,
Zahary Y. Peshev, Tsvetina T. Evgenieva, Tanja N. Dreischuh, and Dimitar V. Stoyanov 68
- PC4.** CONSIDERATIONS ABOUT THE LOG-NORMALITY OF THE AEROSOL LIDAR SIGNAL FLUCTUATIONS,
L. Gurdev, T. Dreischuh, Z. Peshev, D. Stoyanov 69
- PC5.** FINITE SYSTEM RESPONSE SHAPE DUE DISTORTIONS OF THE TEMPERATURE AND DENSITY PROFILES IN FUSION PLASMAS RECOVERED USING THOMSON SCATTERING LIDAR,
L. Gurdev, T. Dreischuh, D. Stoyanov 70
- PC6.** LIDAR DETECTION OF FOREST FIRE SMOKE ABOVE SOFIA,
Ivan Grigorov, Atanaska Deleva, Dimitar Stoyanov, Nikolai Kolev and Georgi Kolarov 71

D - LASERS IN BIOLOGY AND MEDICINE

- PD1.** IMPACT OF QUATERNIZATION OF PHTHALOCYANINES FOR ANTIMICROBIAL PHOTODYNAMIC THERAPY,
Meliha Aliosman, Ivan Angelov, Vesselin Kussovski, Vanya Mantareva 73
- PD2.** ANTIBACTERIAL PHOTODISINFECTION BASED ON THE CONJUGATE ZN(II) PHTHALOCYANINE-METAL OXIDE UPON UV AND RED LIGHT EXPOSURE,
Vanya Mantareva, Ivelina Eneva, Ekaterina Borisova, Ivan Angelov, Vesselin Kussovski 74
- PD3.** EXCITATION-EMISSION MATRICES (EEMS) AND SYNCHRONOUS FLUORESCENCE SPECTROSCOPY (SFS) INVESTIGATIONS OF GASTROINTESTINAL TISSUES,
Ts. Genova, E. Borisova, Al. Zhelyazkova, O. Semyachkina-Glushkovskaya, M. Keremedchiev, B. Vladimirov, L. Avramov 75

TABLE OF CONTENTS

PD4.	LASER CLEANING OF PAPER SAMPLES COLONIZED WITH FUNGI SPORES, <i>Evangelini Zekou, Elias Chatzitheodoridis, Alexander A. Serafetinides</i>	76
PD5.	LASER INDUCED AUTOFLUORESCENCE FOR DIAGNOSIS OF NON-MELANOMA SKIN CANCER, <i>E. Drakaki, M. Makropoulou, A. A. Serafetinides, N. Merlemis, I. Kalatzis, I.A. Sianoudis, O. Batsi, E. Christofidou, A. J. Stratigos, A. D. Katsambas, Ch. Antoniou</i>	77
PD6.	LASER CLEANING TREATMENT OF BURNT PAINTINGS, <i>N. Antonopoulou-Athera, E. Chatzitheodoridis, M. Doulgerides, Ch. Evangelatos, A. A. Serafetinides</i>	78
PD7.	DEVELOPING A TIMING CONTROL SYSTEM FOR LASER INDUCED FLUORESCENCE (LIF) IN MEDICAL APPLICATIONS, <i>Ioannis Karachalios, Dimitrios Mathes, Ioannis Valais, Georgios Mitsou and Ioannis Sianoudis</i>	79
PD8.	CHARACTERIZATION OF NEW DRUG DELIVERY NANOSYSTEMS BY USING ATOMIC FORCE MICROSCOPY, <i>Ellas Spyratou, Elena A. Mourelatou, Costas Demetzos, Mersini Makropoulou, Alexander A. Serafetinides</i>	80
PD9.	DENTAL COMPOSITE POLYMERIZATION PROCESS: DIGITAL HOLOGRAPHIC INTERFEROMETRY METHOD, <i>D. Ž. Grujić, D. V. Pantelić, D. M. Vasiljević</i>	81
PD10.	TOTAL ATTENUATION COEFFICIENT OF INTRALIPID® DILUTIONS FOR DISCRETE LASER WAVELENGTHS BETWEEN 405 AND 1315 nm, <i>T. Dreischuh, L. Gurdev, O. Vankov, L. Avramov, D. Stoyanov</i>	82
PD11.	SYNCHRONOUS FLUORESCENT SPECTROSCOPY FOR ANALYSIS OF WINES AND WINE DESTILATES, <i>Ya. Andreeva, E. Borisova, Ts. Genova, Al. Zhelyazkova, L. Avramov</i>	83
PD12.	TISSUE FLUORESCENCE ORIGINS EVALUATION USING EXCITATION-EMISSION MATRICES, <i>A. Zhelyazkova, E. Borisova, L. Angelova, E. Pavlova, M. Keremedchiev, L. Avramov</i>	84
PD13.	QUANTUM YIELDS OF THE PHOTODISSOCIATION OF HbO ₂ AND HbCO IN THE VISIBLE SPECTRAL REGION, <i>S. A. Mamilov, S. S. Esman, M. M. Asimov, A. I. Gisbrecht</i>	85
PD14.	DIFFUSION OF NEAR-INFRARED LASER RADIATION IN TOOTH ROOT CANAL, <i>Tz. Uzunov, I. Angelov, A. Gisbrecht</i>	86

TABLE OF CONTENTS

PD15. COMBINED OPTO-ULTRASOUND METHOD OF TISSUE OXYGENATION AND ITS APPLICATION IN MEDICINE, <i>M. M. Asimov, D. B. Vladimirov, A. N. Rubinov, R. M. Asimov, A. I. Gisbrecht</i>	86
PD16. COMPARATIVE CLINICAL STUDY OF ANTIMICROBIAL ACTIVITY OF PAD WITH FOTOSAN, Nd : YAG LASER AND NAOCL AND EDTA USED FOR TREATMENT OF CHRONICAL PERIODONTITIS, <i>Tzvetelina Gueorgieva, Slavcho Dimitrov, Raina Gergova</i>	87
PD.17 BENT OPTICAL FIBER TAPERS FOR REFRACTOMETRY AND BIOSENSING, <i>Emil Penchev, Tinko Eftimov, Wojtek Bock</i>	88
OD1. REGULATORY BIOLOGICAL ACTION OF CONTINUOUS, QUASI-CONTINUOUS AND PULSED LASER RADIATION OF NANO- AND PICOSECOND RANGES, <i>V. Yu. Plavskii, N. V. Barulin, A. I. Vodchits, I. A. Khadasevich, L. E. Batay, A.S. Grabchikov, A. I. Tretyakova, L. G. Plavskaya, A. V. Mikulich, V. A. Orlovich</i>	89
OD2. 3D IMAGING OF CHITINOUS STRUCTURES USING NONLINEAR LASER SCANNING MICROSCOPY, <i>Aleksandar Krmpot, Mihailo Rabasović, Branislav Jelenković, Srećko Ćurčić, Maja Vrbica, and Dejan Pantelić</i>	90

E - LASER SYSTEMS AND NONLINEAR OPTICS

PE1. IMPROVED FAR-FIELD MODEL OF SIMPLE TWO-LEVEL ANNULAR BEAMS, <i>Dimo N. Astadjov</i>	92
PE2. DETERMINATION OF SPATIALLY-RESOLVED ELECTRON TEMPERATURE IN POWERFUL GAS-DISCHARGE LASERS, <i>K. A. Temelkov, T. P. Chernogorova, S. I. Slaveeva, N. K. Vuchkov</i>	93
PE3. COMPARISON BETWEEN A LASER Nd: YAG AND Nd, Cr: YAG PUMPED BY FLASH LAMP, <i>R. Bouadjemine, D. Louhibi</i>	94
PE4. POLYMERS IN LENS DESIGN FOR LASER APPLICATIONS, <i>Stefka Kasarova, Nina Sultanova, Ivan Nikolov</i>	95
PE5. DYNAMIC LASER SPECKLE MEASUREMENT WITH ENHANCED VIZUALIZATION OF ACTIVITY MAP, <i>Elena Stoykova, Nataliya Berberova, Tania Nikova</i>	96
PE6. BIREFRINGENCE INDUCED IN AZOPOLYMER (PAZO) FILMS WITH DIFFERENT THICKNESS, <i>Lian Nedelchev, Dimana Nazarova, Georgi Mateev, Nataliya Berberova</i>	97

TABLE OF CONTENTS

PE7. AQUEOUS SOLUTIONS OF $MgSO_3 \cdot 6H_2O$: M (M = Co, Ni OR Co+Ni) AND NONLINEAR OPTICS, <i>P. Petkova, M. Mustafa, P. Vasilev, V. Nedkov, J. Tacheva, and Youri Tzukrovski</i>	98
PE8. GENERATION OF MODULATED MICROCHIP LASER PULSES, <i>F. Almabouada, D. Louhibi</i>	98
PE9. ANALOGIES AND DISTINCTIONS BETWEEN HYDRODYNAMIC SUPERCONTINUUM AND SUPERCONTINUUM GENERATION IN OPTICAL FIBERS, <i>Armando Mena Contla, Ricardo Darío Peña Moreno, V.A. Pinaev, and V. N. Serkin</i>	100
PE10. ANALOGIES BETWEEN SOLITONIC BIO-ENERGY TRANSPORT ALONG POLYPEPTIDE CHAINS AND NONAUTONOMOUS OPTICAL SOLITONS IN STRUCTURATED NONUNIFORM FIBERS, <i>Laura Moreno Lara, Ricardo Darío Peña Moreno, V.A. Pinaev, and V. N. Serkin</i>	101
PE11. “WATER WAVES” IN OPTICAL FIBERS: NONLINEAR TUNNELING OF HYDRODYNAMICAL AND OPTICAL SOLITON SUPERCONTINUA, <i>Armando Mena Contla, Ricardo Darío Peña Moreno, V.A. Pinaev, and V. N. Serkin</i>	102
PE12. FORMATION OF STABLE LORENTZIAN TYPE FILAMENT FROM INITIAL FS PULSE WITH GAUSSIAN SHAPE, <i>V. Slavchev, L. Kovachev</i>	103
PE13. FILAMENT AS VECTOR SOLITON WITH LORENTZIAN PROFILE. CONDITIONS FOR STABILITY, <i>A. Dakova and L. Kovachev</i>	103
PE14. COMPARISON OF SOLITON SOLUTIONS OF THE NONLINEAR SCHRÖDINGER EQUATION AND THE NONLINEAR AMPLITUDE EQUATION, <i>A. Dakova and D. Dakova</i>	104
PE15. INTRAPULSE RAMAN SCATTERING IN THE PRESENCE OF LINEAR AND NONLINEAR GAIN AS WELL AS SPECTRAL FILTERING, <i>Ivan M. Uzunov, Zhivko D. Georgiev, Todor N. Arabadzhev</i>	105
PE16. SOLITON SELF-FREQUENCY SHIFT IN THE PRESENCE OF LINEAR AND NONLINEAR GAIN, THIRD-ORDER DISPERSION AND SELF-STEEPENING EFFECT, <i>Ivan M. Uzunov, Todor N. Arabadzhev, Zhivko D. Georgiev</i>	106

TABLE OF CONTENTS

PE17. FAR-FIELD DIFFRACTION OF SINGULAR DARK BEAMS BY COMPUTER-GENERATED HOLOGRAMS WITH ENCODED OPTICAL VORTICES, <i>L. Stoyanov, S. Topuzoski, G. Maleshkov, I. Stefanov, L. Janicijevic, A. Dreischuh</i>	107
PE18. PULSE FRONT TILT MEASUREMENT OF FEMTOSECOND LASER PULSES, <i>N. Dimitrov, L. Stoyanov, I. Stefanov, A. Dreischuh, P. Hansinger, G. G. Paulus</i>	108
PE19. SPATIAL FILTERING OF WIRE LASER RADIATION, <i>E. E. Orlova</i>	109
PE20. SUBPICO SECOND Z-SCAN METHOD, <i>G. Yankov, T. Petrov</i>	110
OE1. IONIZATION-FREE FILAMENTATION. VECTOR MODEL AND VECTOR ROTATION, <i>Lubomir M. Kovachev</i>	110
OE2. VECTOR GENERALIZATION OF THE FILAMENTS INTERACTION <i>Daniela A. Georgieva and Lubomir M. Kovachev</i>	111
AUTHOR INDEX	112

18th International School on Quantum Electronics
“Laser physics and applications” 29 September – 3 October 2014, Sozopol, Bulgaria

INVITED LECTURES

PLENARY SESSION

INVITED LECTURES

LASER-MATTER INTERACTION

L1

PHOTONIC FUNCTIONALIZATION AT NANOSCALE

G. Śliwiński, A. Białous, K. Grochowska

*Photophysics Dept, The Szewalski Institute, Polish Academy of Sciences
14 Fiszera St, 80-231 Gdańsk, Poland
e-mail: gerards@imp.gda.pl*

Recently, for a growing number of materials their nanoscale counterparts can be synthesized and are showing promise of high functional relevance. Functionalized materials of dimensions in-between the atomic and macromolecular scale evoke growing interest because interactions at nanoscale determine the important material properties such as thermal and electrical conductivities, magnetic permeability, optical response (color), etc.

An intensive research is observed in area of nano-devices based on use of the plasmonic effect. Results show that the required optical properties can be engineered not only by cavities of precisely controlled geometries but also by structures obtained from template-free synthesis. Here, besides methods such as the wet chemical ones, microwave- and DC-sputtering the advantages of the laser nanostructuring which result in the characteristic semi-regular (self-organized) nanostructures are frequently indicated [1,2]. The production and properties of nanomaterials, e.g. fabricated by means of pulsed laser irradiation of thin metal films are discussed in this report. Basing on experimental data it is shown that despite relatively broad distributions in the nanoparticle size and shape the self-organized nanostructures reveal short-range order symptomatic for the Rayleigh-Taylor instability-driven mechanism due to fast melting and solidification. Examples reveal that the discussed process represents the cost-effective production path of functionalized materials for light harvesting, catalysis and highly sensitive detection [3].

References:

- [1] M. Bora et al., Appl. Phys. Lett. 102, 251105, (2013).
- [2] Y. Nishijama, L. Rosa, S. Juodkasis, Opt. Express 20(10), 114661477, (2012).
- [3] K. Grochowska et al, Plasmonics, 8, 105-113, (2013).
- [4] D. Grojo et al. ‘Monitoring photonic nanojets from microsphere arrays by femtosecond laser ablation of thin films’, Journal of Nanoscience and Nanotechnology 11 (10), 9129-9135, (2011).
- [5] A. Pereira et al. “Laser-fabricated porous alumina membrane (LF-PAM) for the preparation of metal nanodot arrays”, Small, 4, 572-575, (2008).
- [6] L. Rapp et al., ‘Pulsed-laser printing of silver nanoparticles ink: control of morphological properties’, Optics Express 19 (22), 21563–21574, (2011).

Acknowledgements: We thank French ANR agency for financial support through the FELINS-ANR-10-BLAN-946 project.

L2

SYNTHESIS AND CHARACTERIZATION OF SILICON NANOWIRES BY LASER METHODS

N. Fukata

*International Center for Materials Nanoarchitectonics, National Institute for Materials Science, 1-1 Namiki, Tsukuba, 305-0044, Japan
e-mail: FUKATA.Naoki@nims.go.jp*

Silicon nanowires (SiNWs) are of great interest in the fields of both fundamental and application research. In order to realize nanoscale silicon devices using SiNWs, it is important to investigate the growth of SiNWs and their functionalization by impurity doping.

SiNWs were synthesized by laser ablation of a Si target with nickel as a metal catalyst and boron (B) and phosphorus (P) as dopants which were placed in a quartz tube heated at 1200°C in a flowing Ar gas. A frequency-doubled NdYAG laser (532 nm, 7ns pulse width, 10 Hz, 150 mJ/pulse) was used to ablate the targets. Micro-Raman scattering measurements were performed at room temperature with a 532-nm excitation laser light. Electron spin resonance (ESR) measurements were carried out at 4.2 K to investigate the state of P donors in SiNWs.

Large amount of SiNWs were grown by our laser ablation method. Impurity doping B and P atoms into SiNWs were successfully done during the laser ablation. The characterization of the states of B atoms can be clarified by Raman measurements.

Raman peaks were observed at about 618 and 640 cm⁻¹ for SiNWs synthesized by using a Si target with B. The peak frequencies are in good agreement with those of local vibrational modes of ¹¹B and ¹⁰B in Si crystal. The Fano broadening due to a coupling between the discrete optical phonon and a continuum of interband hole excitations was also observed in the optical phonon peak, which indicates heavily B doping. The observation of B local vibrational peaks and Fano broadening were observed for the first time in our experiments [1-3]. These results prove that B atoms were doped in substitutional sites of the crystalline Si core of SiNWs [1-3]. ESR measurements were performed to investigate defects and P donor/conduction electrons in P-doped SiNWs. The observation of ESR signal due to conduction electrons clearly showed the formation of n-type SiNWs [2,4]. The segregation behaviors of B and P were also investigated [5]. The results showed that the segregation of B is faster than that of P.

References:

- [1] N. Fukata et al., “Doping and hydrogen passivation of B in silicon nanowires synthesized by laser ablation”, *Appl. Phys. Lett.* 89, 203109, (2006).
- [2] N. Fukata, “Impurity doping in silicon nanowires”, *Adv. Mater.*, 21 (27), 2829-2832, (2009).
- [3] N. Fukata, “Doping and characterization of impurity atoms in Si and Ge nanowires”, *Phys. Status Solidi C11* (2), 320-330, (2014).
- [4] N. Fukata et al., “Phosphorus doping and hydrogen passivation of donors and defects in silicon nanowires synthesized by laser ablation”, *Appl. Phys. Lett.* 90, 153117, (2007).
- [5] N. Fukata et al., “Segregation behaviors and radial distribution of dopant atoms in silicon nanowires”, *Nano Lett.* 11, 203106, (2008).

Acknowledgements: This work was in part supported by a Funding Program for Next Generation World-Leading Researchers (NEXT Program) and Kakenhi, MEXT, Japan. This study was also supported by the Japan Science and Technology Agency.

L3

METAL-OXIDE SEMICONDUCTOR NANOPARTICLES AND MICROSTRUCTURES FOR PHOTOLUMINESCENCE-BASED CHEMICAL SENSING: FUNDAMENTAL ISSUES AND APPLICATIONS.

Stefano Lettieri¹, Pasqualino Maddalena^{1,2}, Deborah Pallotti^{1,2}, Salvatore Amoruso^{1,2},
Riccardo Bruzzese^{1,2}, Maria Cristina Carotta³

¹ *Institute for Superconductors, Oxides and Innovative Materials and Devices, National Research Council (CNR-SPIN), U.O.S. Napoli, Via Cintia, I-80126 Napoli, Italy.*

² *Dipartimento di Fisica, Università degli Studi di Napoli “Federico II”, Via Cintia, I-80126 Napoli, Italy*

³ *CFR, Consorzio Ferrara Ricerche, Via Saragat 1, Ferrara, Italy
e-mail: stefano.lettieri@spin.cnr.it*

In this contribution, I will review some recent results regarding the peculiarities of photoluminescence (PL) properties of some metal-oxide semiconductors, as they interact with oxidizing gas molecules. I will focus in particular on Zinc Oxide (ZnO) and Titanium Oxide (TiO₂): both of them are well-known gas-sensitive materials, allowing the realization of low-cost solid-state gas sensors based on chemo-resistive effects. The main scientific goal of the present contribution will be to discuss another gas-detection route, namely the *opto-chemical* one, employing the PL modulation induced by molecular adsorption as transduction mechanism for gas detection [1].

In particular, I will first discuss the phenomenon of suppression of ultraviolet emission of ZnO once exposed to nitrogen dioxide (NO₂). A careful study involving charge transport characterization, static photoluminescence analysis and exciton lifetime measurements allows to sketch a mechanism explaining the experimental findings. Moreover, interesting and preliminary results will be presented regarding the possibility to obtain *multi-parametric* chemical sensing in TiO₂ nanoparticle systems grown by femtosecond pulsed laser deposition [2,3], thanks to the different responses to oxidation of its two polymorph phases (anatase and rutile).

References:

[1] S. Lettieri, “Optical Sensing by Metal Oxide Nanostructures: Phenomenology and Basic Properties”, in: “Chemical Sensors: Simulation and Modelling, vol. 4: Optical sensors”, edited by G. Korochenkova (Momentum Press, New York), p. 71, (2013).

[2] S. Amoruso, S. Tuzi, D. K. Pallotti, C. Aruta, R. Bruzzese, F. Chiarella, R. Fittipaldi, S. Lettieri, P. Maddalena, A. Sambri, Appl. Surf. Sci. 270, 307, (2013).

[3] D. K. Pallotti, E. Orabona, S. Amoruso, C. Aruta, R. Bruzzese, F. Chiarella, S. Tuzi, P. Maddalena and S. Lettieri, J. Appl. Phys. 114, 043503, (2013).

Acknowledgements: The work has been partially supported by the European Union through the FIRB Project *RBAP115AYN* “Oxides at the nanoscale: multifunctionality and applications”.

LASER SPECTROSCOPY AND METROLOGY

L4

SPECTROSCOPY OF ATOMS IN STRONG MAGNETIC FIELDS AND APPLICATIONS BASED ON MICRO AND NANO-CELLS

D. Sarkisyan, G. Hakhumyan, A. Sargsyan

*Institute for Physical Research, Academy of Sciences of Armenia, Ashtarak-2, Armenia
e-mail: davsark@yahoo.com*

Since Cs and Rb atoms, are commonly used for investigations of optical and magneto-optical processes in atomic vapors, as well as for cooling of atoms, for Bose–Einstein condensation, and in a number of other problems, therefore, detailed knowledge of the behavior of atomic levels in external magnetic fields is of a high interest [1,2].

The implementation of recently developed technique based on narrowband laser diodes, strong permanent magnets and micro-and nano- thin cells (MTC and NTC) make studies of the atomic transitions behavior in an external strong magnetic field (in the range of 3 kG- 9 kG) simple and robust, and allows one to study behavior of any individual atomic transition of the ⁸⁵Rb and ⁸⁷Rb atoms for D_{1, 2} lines [3]. Particularly, it is demonstrated that from 20 (12) Zeeman transitions allowed at low *B*-field in ⁸⁵Rb (⁸⁷Rb) D₁ line absorption spectra in the case of σ^+ polarized laser radiation, only 6 (4) remain at $B > 3$ kG, caused by decoupling of the total electronic momentum *J* and the nuclear spin momentum *I* (so called hyperfine Paschen-Back (HPB) regime), while for the Rb D₂ line in the case of $B > 3$ kG and σ^+ polarized laser radiation, only 20 Zeeman transitions remain while there are 60 allowed Zeeman transitions at low *B*-field. At $B > 4.5$ kG in the absorption spectrum these 20 atomic transitions are regrouped to form two completely separate groups of 10 atomic transitions each with the frequency slopes *s*₁ and *s*₂ correspondingly.

Also, the technique based on MTC and NTC use has been successfully implemented to study behavior of individual atomic transition of the Cs atoms for D₂ line. Particularly, it is demonstrated that from 54 Zeeman transitions allowed at low *B*-field in Cs atomic vapor absorption spectrum in the case of σ^+ polarized laser radiation, only 16 atomic transitions (which are contain in two groups of 8 atomic transitions each) remain at $B > 5$ kG, which is manifestation of HPB regime. Theoretical models perfectly well described the experiment. Possible applications will be described [4].

References:

[1] M. Auzinsh, D. Budker, S.M. Rochester, *Optically Polarized Atoms: Understanding Light-Atom Interactions* (Oxford University Press), ISBN 978-0-19-956512-2, (2010).

[2] A Sargsyan, A Tonoyan, G Hakhumyan, A Papoyan, E Mariotti, D. Sarkisyan, "Giant modification of atomic transitions probabilities induced by magnetic field: forbidden transitions become predominant", *Laser Phys. Lett.*, Vol. 11, 055701, (2014).

[3] A. Sargsyan, G. Hakhumyan, C. Leroy, Y. Pashayan-Leroy, A.Papoyan, D. Sarkisyan, "Hyperfine Paschen-Back regime realized in Rb nanocell" *Opt. Lett.*, Vol. 37, 1379, (2012).

[4] A. Sargsyan, A. Tonoyan, R. Mirzoyan, D. Sarkisyan, A. Wojciechowski, W. Gawlik, “Revision of saturated-absorption spectroscopy: implementation for atomic transitions study in strong magnetic fields (> 20 mT)”, *Opt. Lett.*, Vol.39, 2270, (2014).

Acknowledgements: This work has received partial funding from the EU 7-th Framework Programme (FP7/2007-2013), Grant Agreement n° 295264-COSMA.

L5

SELECTIVE REFLECTION OF LIGHT FROM A VAPOR OF ALKALI DIMERS

S. Shmavonyan, A. Khanbekyan, A. Gogyan, M. Movsisyan, A. Papoyan

*Institute for Physical Research, NAS of Armenia, Ashtarak-2, 0203, Armenia
e-mail: papoyan@ipr.sci.am*

Selective Reflection (SR), a Fresnel reflection of radiation from a boundary between transparent dielectric window and atomic vapor in the frequency region of a resonance line, is known in atomic spectroscopy as a powerful tool for studies of interatomic collision mechanisms and determination of the homogeneous linewidth, van der Waals interaction of atoms with a dielectric surface, coherent and magneto-optical processes, determination of isotopic abundance, locking the laser frequency to atomic resonance lines, spectral filtering, controlling thin film formation, etc. The applied value of SR technique is notably higher for the case of a dense media when resonant radiation gets absorbed already on wavelength-scale thickness; it allows studying development of interparticle interactions ending up with formation of molecules.

Realization of SR from molecular vapor, notably diatomic molecules (dimers) of alkali metals, which have transitions from electronic ground state in visible and near-IR region of spectrum, would significantly extend the area of applications, mainly due to substantially wider spectral coverage. Meanwhile to our knowledge, no observation of selective reflection for molecular vapor was reported so far in spite of obvious interest. The difficulties in realization of molecular SR are caused by several reasons: (i) alkali metal dimers are thermally formed at high-density chemically aggressive saturated vapor, which makes impossible the usage of sealed-off glass cells (the heat pipe systems can not be used because of absence of hot vapor-window interface); (ii) transition strength of rovibronic lines is significantly weaker as compared with atomic lines; (iii) rovibronic transitions of molecules are located very close to each other causing problems with spectral resolution of individual SR signals, especially at high vapor density (where one can expect high signal amplitude) because of collisional broadening. The results obtained in our previous study on SR from Cs₂ molecular vapor [1] have been later attributed to Fabry-Pérot behavior of a Cs cell.

We report the first observation of selective reflection of light from an interface of a dielectric window and molecular vapor of Rb₂ dimers formed in all-sapphire sealed-off rubidium vapor cell (temperature up to 520 °C, atomic and molecular densities up to 10¹⁸ and 3×10¹⁶ cm⁻³, respectively). The selective reflection signals were recorded on various rovibronic components of 1(X)¹Σ_g⁺ – 1(A)¹Σ_u⁺ bound-bound electronic transition of Rb₂ by scanning a diode laser frequency in a spectral range of 851 – 854 nm. Only selective reflection signals corresponding to groups of several individual transitions have been recorded, which was

attributed to high spectral density, large collisional broadening, and low oscillator strength of individual rovibronic transitions.

The reported results became possible due to significantly higher vapor density and wider laser frequency tuning as compared with the regime exploited in [1].

References:

[1] M. Movsisyan, S. Shmavonyan, A. Papoyan, “Selective reflection studies of molecular cesium vapor”, Proc. SPIE Vol. 7998, 79980U1, 1-9, (2011).

Acknowledgements: The authors thank D. Sarkisyan for stimulating discussions. The present study has been performed in the frame of Armenian National thematic program No.13-1C089.

L6

VELOCITY ANISOTROPY EFFECT IN PUMP-PROBE SPECTRA OF CESIUM IN A MICROMETRIC THICKNESS OPTICAL CELL

P. N. Ghosh¹, S. Mitra¹ and B. Ray¹, A. Krasteva², D. Slavov², P. Todorov² and S. Cartaleva²

¹*Department of Physics, University of Calcutta, 92 A P C Road, Kolkata 700009, India*

²*Institute of Electronics, Bulgarian Academy of Sciences, boul. Tzarigradsko shosse 72, 1784 Sofia, Bulgaria*

e-mail: pradipnghoshg@gmail.com

The pump-probe spectra in a cell of micrometric thickness containing cesium are reported. The line shape and non-linear features observed in the case of fluorescence in the direction parallel to the cell windows and the transmission spectra observed along the propagation direction of the probe beam show considerable differences in the spectral profiles. We observed Electromagnetically Induced Transparency (EIT) and enhanced Velocity Selective Optical Pumping (VSOP) signals. Atoms moving nearly parallel to the windows and perpendicular to the collinear pump and probe beams will see much lower Doppler shift of incident frequencies and hence will lead to considerable narrowing of the Doppler background in the fluorescence spectra. The coherence decay rate is also low for such atoms as they do not meet with the cell walls. A theoretical model based on five level optical Bloch equations is used to simulate the spectra. The Doppler convolution includes all possible orientation of atomic velocities with respect to the laser beam direction. The simulated curves reproduce the observed sharp EIT peaks and enhanced broad VSOP signals for the closed probe transition in the fluorescence and absorption spectra. The observed effect of detuning of the pump frequency on the non-linear features is also reproduced by the simulation. We also report the temperature and beam intensity effect on the spectra.

L7

SIMULATION OF LIGHT INTERACTION WITH ALCALI ATOMS IN COATED OPTICAL CELLS

K. Nasyrov

*Institute of Automation and Electrometry SB RAS, Novosibirsk, Russia
e-mail: nasyrov@iae.nsk.su*

Optical cells with atomic spin preserving coatings are used for observation of large variety of physical phenomena such as Light Induced Drift of atoms and molecules [1], Light Induced Atoms Desorption from the coatings [2], optical and magneto-optical resonances [3]. Particularly, the optical cells with anti-relaxation coatings are promising for designing and building of miniaturized optical magnetometers tailored for medical applications.

In the simulation of laser light-atom interaction, it is usually assumed that the atom before entering the laser beam is in an equilibrium state, i.e. the atomic ground states are equally populated. However, such assumption is correct only for conventional evacuated glass cells without coating. Inside the laser beam the atomic dynamics is described by the Optical Bloch Equations [4]. Due to optical pumping effect (including hyperfine pumping), after crossing the laser beam atoms have a non-equilibrium distribution of ground states population. In case of uncoated cell, such non-equilibrium distribution is destroyed in result of atomic collisions with cell wall.

In opposite, after collisions with the coated cell wall most of atoms return back to the laser beam in non-equilibrium state. Mathematically it means that initial state of atom entering laser beam depends on the state of atom escaping the laser beam. This fact significantly complicates the numerical solving of obtained equations for laser light-atom interaction in coated cell. In the presented work, we propose several approximations and simplifications, in order to overcoming this problem.

Our method allows direct examination of the dependence of fluorescence spectra on quality of coating that determines the magneto-optical resonance spectral narrowing. In addition, we have found that the magneto-optical resonance becomes asymmetric when observed in alkali vapor contained in coated cell that are illuminated by elliptically polarized light.

Based on this theoretical approach, we propose a simple method for experimental measurement of the quality of cell coating.

References:

- [1] F. Kh. Gel'muchanov, A. M. Shalagin “Theory of optically induced diffusion of gases” JETP, Vol.51, No 5, 839-846, (1980).
- [2] S. N. Atutov, V. Biancalana, P. Bicchi et al. “Light induced diffusion and desorption of alkali metals in a siloxane film: theory and experiment”, Phys. Rev. A, Vol. 60, No 6, 4693-4707, (1999).
- [3] E. B Alexandrov, M. V. Balabas, D. Budker et al. “Light-induced desorption of alkali-atoms from paraffin coating”, Phys. Rev. A, Vol. 66, No 4, 042903, (2002).
- [4] K. Nasyrov, S. Cartaleva, N. Petrov et al. “Coherent population trapping resonances in Cs atoms excited by elliptically polarized light”, Phys. Rev. A, Vol. 74, No 1, 013811, (2006).

Acknowledgements: This work was supported by Marie Curie International Research Staff Exchange Scheme Fellowship within the 7th European Community Framework Programme.

L8

DEGENERATE TWO- AND THREE-LEVEL SYSTEMS IN PRESENCE OF LONGITUDINAL AND TRANSVERSE MAGNETIC FIELDS

A. D. Wilson-Gordon^{1*}, L. Margalit¹, M. Rosenbluh²

¹*Department of Chemistry, Bar-Ilan University, Ramat Gan 52900, Israel*

²*The Jack and Pearl Resnick Institute for Advanced Technology,
Department of Physics, Bar-Ilan University, Ramat-Gan 52900, Israel
e-mail: gordon@biu.ac.il*

We discuss the effect of static and time-dependent longitudinal and transverse magnetic fields on degenerate two-level and three-level systems in Rb atomic vapor.

The effect of a transverse magnetic field (TMF) on the absorption spectra of degenerate two-level systems in the D₂ line of ⁸⁷Rb is investigated both analytically and numerically [1]. We compare the effect of the TMF on the absorption of a polarized pump in the Hanle configuration with that of a σ^- probe in the presence of a σ^+ pump in the pump-probe configuration, and show that the absorption spectra in both configurations is split in the presence of a TMF and that the splitting is proportional to the magnitude of the TMF.

Coherent population trapping (CPT) transients induced by a modulated longitudinal magnetic field (LMF) are investigated theoretically for a realistic three-level system in the D₁ line of ⁸⁷Rb [2]. The contributions to the transient probe absorption from the various subsystems that comprise the realistic atomic system are examined and the absorption of each subsystem is compared to that of a simple system.

We present theoretical results of CPT transients induced by a modulated TMF [3]. The application of a TMF leads to the appearance of new subsystems, the creation of new dark states and the rearrangement of the population among the Zeeman sublevels. We show that transients appear as the system is switched between various steady-state situations and we identify the various level system components of the total probe absorption.

Finally, the differences between TMF modulation and LMF modulation are discussed.

References:

[1] L. Margalit, M. Rosenbluh, and A. D. Wilson-Gordon, "Degenerate two-level system in the presence of a transverse magnetic field," *Phys. Rev. A* 87, 033808, (2013).

[2] L. Margalit, M. Rosenbluh, and A. D. Wilson-Gordon, "Coherence-population-trapping transients induced by an ac magnetic field," *Phys. Rev. A* 85, 063809, (2012).

[3] L. Margalit, M. Rosenbluh, and A. D. Wilson-Gordon, "Coherent-population-trapping transients induced by a modulated transverse magnetic field," *Phys. Rev. A* 88, 023827 (2013).

L9

SATURATION EFFECTS IN REFLECTION SPECTROSCOPY OF DILUTE RESONANCE VAPORS

T. A. Vartanyan

*ITMO University, St. Petersburg 197101, Russian Federation
e-mail: Tigran.Vartanyan@mail.ru*

Ultra-narrow cells filled with pure alkali atoms or alkali-rare gas mixtures are widely used for spectroscopy and nonlinear optics [1] as well as for the studying of the collisions of the excited atoms with the walls [2]. The shapes of the spectral lines in the sub-wavelength thick cells undergo considerable changes as compared to that registered under ordinary conditions in many-wavelength thick spectroscopic cells. They are Doppler-free already in the linear domain. The crossover resonance are absent from the Doppler-free spectra obtained in the ultra-narrow cells.

Frequent collisions of atoms with the cell walls modify considerably the linear as well as nonlinear properties of the atomic vapor confined to the ultra-narrow cell. Even in the presence of a single wall, the saturation effect differs from that in the volume of the resonance vapors [3].

The reason for the considerable changes of the linear and nonlinear optical properties of the narrow slices of atomic vapors adjacent to the surface of a transparent dielectric material is the transient behavior of the atomic polarization that occurs unavoidably after an atom sticks to the surface and desorbes from it or just collides with the surface and then flies back into the vapor volume. In both cases, the atoms are not in the steady state and their polarization is correctly described by a dielectric constant provided the effects of spatial dispersion are accounted for. As usual, spatial dispersion leads to the existence of additional normal waves. To find the unique solution one needs additional boundary conditions. Contrary to the situation in the solid state optics where the problem of additional boundary conditions is not solved yet, in the case atomic vapors a microscopic theory is readily available. Hence the boundary conditions for atomic polarization may be formulated and used for solution of the wave equations.

In this contribution, I present the peculiarities of electrodynamics in the rarefied atomic vapors. It will be shown how the interplay of the saturation and transient effects defines the spectroscopic features and creates periodic structures of atomic inversion near the solid surface that confines the vapor.

References:

- [1] S. Cartaleva, A. Krasteva, L. Moi, A. Sargsyan, D. Sarkisyan, D. Slavov, P. Todorov, K. Vaseva, “Laser spectroscopy of sub-micrometre- and micrometre-thick caesium-vapour layers” *Quantum Electronics*, Vol. 43, No 9, 875-884, (2013).
- [2] T. A. Vartanyan, A.E. Logunov, A.S. Pazgalev, S.G. Przhibel'skii, D. Sarkisyan, V.V. Khromov, “Change in the states of optically excited Rb atoms near sapphire surface”, *Optics and Spectroscopy*, Vol. 115, No 9, 875-884, (2013).
- [3] T. A. Vartanyan, “Resonant reflection of intense optical radiation from a low-density gaseous medium”, *Sov. Phys. JETP*, Vol. 61, No 4, 674 – 677, (1985).

Acknowledgements: This work was partially financially supported by Government of Russian Federation, Grant 074-U01, and RFBR, research project No. 13-02-90601 Arm-a.”

L10

NON-CLASSICALLY PAIRED PHOTONS FROM SOURCES BASED ON COLD ATOMS

Małgorzata Głódź¹, Maciej Janowicz¹, Krzysztof Kowalski¹, Jerzy Szonert¹

¹ *Institute of Physics, Polish Academy of Sciences, Al. Lotników 32/46, 02-668 Warsaw, Poland*
e-mail: glodz@ifpan.edu.pl

The subject of this lecture is creation and propagation of non-classical optical fields, especially paired/entangled photons in an atomic ensembles. Well-established techniques of generation of paired photon (biphotons), which are based on spontaneous parametric down conversion (SPDC) in nonlinear crystals, produce intrinsically broadband (\sim THz) biphotons (unless some tricks are used for combining resonators with crystal-based parametric oscillators). As a result, they tend to have small coherence time, in sub-picosecond range, and short coherence length (\sim 100 μ m) [1]. In contrast, the more recently developed sources based on atomic transitions enable direct generation of narrowband (\sim 10 MHz) correlated photon pairs which are well suited for strong atom-photon interactions needed in quantum information processing and for long-distance quantum communication [2].

The possibility to create sources of non-classically correlated and possibly entangled photons in atomic media has attracted attention of many prestigious laboratories since about the middle of the past decade and soon biphoton generation methods associated with cold-atoms sources have enjoyed vigorous progress. The early studies of biphotons created in atomic media were performed in the pulsed "write-read" regime *e.g.*, [3]. In this talk attention will be focused on sources of non-classically paired photons, which are based on the spontaneous four-wave-mixing process (SFWM) in continuous mode under conditions of electromagnetically induced transparency (EIT), in cold atoms sample produced in a magneto-optical trap (MOT). A review of some experimental achievements in this field, can be found in Ref. [4].

References:

- [1] C. K. Hong, L. Mandel, "Theory of parametric frequency down conversion of light," *Phys. Rev. A* 31, 2409-2418, (1985).
- [2] M. D. Lukin, A. Imamoglu, "Nonlinear Optics and Quantum Entanglement of Ultraslow Single Photons", *Phys. Rev. Lett.* 84, 1419-1422, (2000).
- [3] A. Kuzmich, W. P. Bowen, A. D. Boozer, A. Boca, C. W. Chou, L.-M. Duan, H. J. Kimble, "Generation of nonclassical photon pairs for scalable quantum communication with atomic ensembles", *Nature* 423, 731-734, (2003).
- [4] J. F. Chen, S. Du, "Narrowband photon pair generation and waveform reshaping", *Front. Phys.* 7, 494-503, (2012).

L11

THE LNL – Fr MOT: LOADING EFFICIENCY OPTIMIZATION AND SEARCH FOR NEW LINES

E. Mariotti¹, S. Agustsson¹, G. Bianchi¹, A. Khanbekyan¹, C. Marinelli¹, L. Marmugi¹, L. Moi¹, R. Calabrese², G. Mazzocca², L. Tomassetti², L. Corradi³, A. Dainelli³, L. Ricci⁴

¹*CNISM and DSFTA – UniSiena, via Roma 56, 53100 Siena*

²*INFN and University of Ferrara, via Saragat 1, 44122 Ferrara*

³*INFN – Laboratori Nazionali di Legnaro, viale dell'Università 2, 35020 Legnaro (PD)*

⁴*Physics Department – University of Trento, via Sommarive 14, 38123 Povo (TN)*

e-mail: mariotti@unisi.it

We present here the last achievements of the Weak transition Amplitude DEtection (WADE) project, devoted to the study of symmetries in atomic systems. The basic motivation of this research is the development of experimental techniques useful for a future high precision measurement of Atomic Parity Violation (APV) in Francium isotopes, as a low energy test of the Standard Model for ElectroWeak Interactions. The project is based on the facility already built in INFN Legnaro Laboratories and prepared for Francium production and trapping. We basically discuss two main points: 1. the application of Light – Induced Atom Desorption to the loading efficiency of the Fr MOT and 2. The demonstration of a flexible, wavelength independent, high-sensitivity detection technique based on the direct imaging of MOT population changes upon excitation with a resonant beam.

Acknowledgements: This work was funded by INFN through the CSNV WADE experiment.

LASER REMOTE SENSING AND ECOLOGY

L12

OPTICAL AND MICROPHYSICAL PROPERTIES OF AEROSOLS OVER SOUTHEASTERN EUROPE USING LIDAR AND SUNPHOTOMETER MEASUREMENTS

Dimitris Balis

Laboratory of Atmospheric Physics, Aristotle University of Thessaloniki, Greece

e-mail: balis@auth.gr

Combined Raman/elastic backscatter lidar observations are carried out at the EARLINET station of Thessaloniki, Greece, during the period 2001–2014. The largest optical depths are observed for Saharan dust and smoke aerosol loads. For these aerosol types it is found that the mean free tropospheric contribution is also maximum. For ‘local’ and ‘continental polluted’ aerosols the measurements indicate moderate aerosol loads. The lowest value of aerosol optical depth is observed for ‘continental clean’ aerosols. The largest lidar ratios, of the order of 70 sr are found for biomass burning aerosols. A significant and distinct correlation between lidar ratio and backscatter related Ångström exponent values was estimated for well defined

aerosol categories, which provides a statistical measure of the lidar ratio's dependency on aerosol-size, which is a useful tool for elastic lidar systems. More explicitly, the influence of smoke on the aerosol loading in the free troposphere from EARLINET observations are examined. Several cases during 2001-2011 were identified over Thessaloniki and Athens, Greece, when very high aerosol optical depth values in the free troposphere were observed. Particle dispersion modeling (FLEXPART) and satellite hot spot fire detection (ATSR) showed that these high free tropospheric aerosol optical depths are mainly attributed to the advection of smoke plumes from biomass burning regions. The biomass burning regions were found to extend across Russia in the latitudinal belt between 45°N – 55°N, as well as in Eastern Europe. The highest frequency of agricultural fires occurred during the summer season (mainly in August). Emphasis is also given on the 2007 wild fires surrounding Athens and earlier studies performed in the frame of EARLINET. The data collected allowed the optical and microphysical characterization of the smoke aerosols that arrived over Greece, where limited information has so far been available and in synergy with AERONET and CALIPSO observation an attempt is made for the vertically resolved mass concentration of the smoke plumes.

Acknowledgements: The contributions from Elina Giannakaki and Vassilis Amiridis are greatly acknowledged. Most of the work presented has been supported by the EU projects EARLINET, EARLINET-ASOS and ACTRIS.

LASERS IN BIOLOGY AND MEDICINE

L13

PLASMON ASSISTED OPTICAL TRAPPING: FUNDAMENTALS AND BIOMEDICAL APPLICATIONS

Alexander A. Serafetinides

*Physics Department, School of Applied Mathematical and Physical Sciences, National Technical University of Athens, Zografou Campus, Athens, 15780 Greece
e-mail: aseraf@central.ntua.gr*

The field of optical trapping has dramatically grown due to implementation in various arenas including physics, biology, medicine and nanotechnology. Certainly, optical tweezers are an invaluable tool to manipulate a variation of particles, such as small dielectric spheres, cells, bacteria, chromosomes and even genes, by highly focused laser beams through microscope. The optical trapping forces depend on the intensity of the laser beam, the shape of the laser focus, the size and shape of the trapped particles and the index of refraction of the trapped particles relative to the surrounding medium. Moreover, the morphology of the substrate, including any microstructures that exist on it, plays an important role on the effectiveness of the trapping. The main disadvantage of the conventional optical trapping systems is the diffraction limit of the incident light (therefore the spatial resolution in trapping is ordinarily limited to more than several hundreds of nanometers). Increasing laser power can enhance the trapping force, but the threshold of optical breakdown poses a limitation on maximum trapping power that can be used, especially in the case of sensitive biological specimens. Therefore, other modalities are searched, as for example the plasmon assisted nanotrapping, reported as a suitable technique for trapping sub-wavelength metallic or dielectric particles.

Plasmonic traps do not require elaborate optical setups and, therefore, may play a key role in the development of modern applications, such as lab-on-a-chip, with increased functionalities. For example, plasmonic nanostructures can be integrated in a microfluidic chip and can be used to trap different types of dielectric structures, including living cells.

In this work, we review the basic theory of plasmon excitation, focusing on the interaction of nanoscale metallic structures with laser light. The use of localized fields of metallic structures for efficient trapping, with various patterns (spikes, dots, squares etc.) will be discussed. Experimental results (obtained mostly with a c.w. Nd:YAG laser), showing a significant enhancement of the trapping efficiency, will be presented. The patterns were produced by different methods such as Lithography and FIS (Fracture Induced Structuring) and the materials of the nanostructures were mostly Au and Ag, either as thin films or as nanospheres. These materials had been placed on the surface of glass or SiO₂. The optical forces were calculated by measuring the particle's escape velocity. The results show that the effective quality factor Q in the patterned metal film is enhanced by a factor >10 with respect to the unpatterned metal film and a factor >100 with respect to the uncoated glass. In addition, numerical simulations, performed to determine the dependence of the optical trapping forces on the shape, size and material of the structures, will be also presented. Finally, representative applications of plasmon assisted optical trapping will be discussed, from cancer therapeutics to fundamental biology and cell nanosurgery.

References:

[1] Kotsifaki D.G., Polyzos D., Serafetinides A.A., Makropoulou M., Tsigaridas G., Peláez R.J., Afonso C.N., “Enhanced optical forces in plasmonic micro-structures”, International Multidisciplinary Microscopy Congress – INTERM 2013, Antalya, Turkey, 2013, Springer Proceedings in Physics, V. 154, pp 177-184, (2014).

[2] Huang L., Maerk S.J. and Martin O. J. F., “Integration of plasmonic trapping in a microfluidic environment”, Optics Express, Vol. 17, No. 8 / 6018, (2009).

[3] Roxworthy B.J., Johnston M.T., Lee-Montiel F.T., Ewoldt R.H., Imoukhuede P.I., et al., “Plasmonic Optical Trapping in Biologically Relevant Media”, PLoS ONE 9(4): e93929. doi:10.1371/journal.pone.0093929, (2014).

[4] Boulais E., Lachaine R., Hatef A., Meunier M., “Plasmonics for pulsed-laser cell nanosurgery: Fundamentals and applications”, Journal of Photochemistry and Photobiology C:Photochemistry Reviews 17 26–49, <http://dx.doi.org/10.1016/j.jphotochemrev.2013.06.001>, (2013).

L14

CHROMATIN DYNAMICS AND EPIGENETIC REGULATION

Dimitar Angelov

*Ecole Normale Supérieure de Lyon, Laboratoire de Biologie Moléculaire de la Cellule, UMR
CNRS 5239 46, allée d'Italie, 69364 Lyon Cedex 7, France,
e-mail: dimitar.angelov@ens-lyon.fr*

In eukaryotic cells the DNA is packaged into chromatin which acts as a barrier to vital cellular processes including transcription and repair. The chromatin structure, and thus DNA accessibility, may be altered by the incorporation of linker histones and histone variants, by transcription regulators, by the posttranslational modification of histone tails, by the action of

ATP-dependent molecular motors and histone chaperones. My research is orientated to understand at a molecular level the fundamental question of how transcription and repair take place within chromatin. To address these fundamental biological processes, we are employing a combinational approach using state of the art biochemical, molecular and cellular biology methods in conjunction with physical-chemistry techniques including UV laser DNA-protein crosslinking & footprinting, x-ray scattering in crystals, cryo-EM, AFM, live cell confocal microscopy imaging etc.

Although the fundamental element of the organization of the nucleosome particle is now well-characterized, how nucleosomes are positioned, how they are influenced by other DNA-binding proteins, and how this leads to higher-order structuring of the genome remains largely unknown. It is nevertheless clear that these processes are vital for our health and for the transmission of epigenetic information. Cells use ATP-dependent chromatin-remodeling factors to overcome the general repression of transcription, repair, recombination, etc. associated with DNA packaging into nucleosomes. Our recent discovery of the metastable remodeling intermediate we termed “the remosome” (1-3) might explain the “quasi-stochastic” (diffusion driven) intergenetic transcription and global genome repair versus the “regulated” DNA transcription and transcription-coupled repair.

The incorporation of various histone variants, such of H2A.Bbd, CENP-A, into nucleosomes has diverse effects on nucleosome structure, stability, and the ability of nucleosomal arrays to condense into chromatin higher order structures and to incorporate the linker histone H1. A consequence of the variant nucleosome instability is the interference with the ATP-dependent nucleosome remodeling. While macroH2A chromatin is refractory to transcription and histone acetylation, H2A.Bbd is more accessible. Our findings that histone variants interfere with nucleosome and chromatin structure and stability, the remodeling of the nucleosome, the initiation of transcription and repair gave novel ideas that help deciphering histone variants functions (4).

My current work also includes the determination of the high-resolution 3D structure and dynamic organization of the chromatosome and the 30 nm chromatin fiber which is of primary importance for understanding the epigenetic aspects of cell functioning. I will present some published (5) as well as some new preliminary results obtained by our biochemical and structural studies.

References:

[1] MS Shukla et al., Remosomes, RSC generated non-mobilized particles with approximately 180 bp DNA loosely associated with the histone octamer. *Proc. Natl. Acad. Sci. USA* 107(5), 1936-1941, (2010).

[2] H Menoni et al., Base excision repair of 8-oxoG in dinucleosomes. *Nucleic Acids Res.* 40(2), 692-700, (2012).

[3] IN Lone et al., Binding of NF- κ B to nucleosomes: effect of translational positioning, nucleosome remodeling and linker histone H1. *Plos Genetics* 9(9), e1003830, (2013).

[4] C-M Doyen et al., Dissection of the unusual structural and functional properties of the variant H2A.Bbd nucleosome, *EMBO J.* 25, 4234-4244, (2006).

[5] SH Syed et al., Single base resolution mapping of H1-nucleosome interactions and 3D organization of the nucleosome, *Proc. Natl. Acad. Sci. USA* 107(21), 9620-9625, (2010).

Funding: FP7 Grant 289611 “HEM_ID”; ANR-12-BSV5-0017-03- Blanc “CHROME”

LASER SYSTEMS AND NONLINEAR OPTICS

L15

QUANTUM OPTICS OF QUANTUM EMITTERS NEAR PLASMONIC NANOPARTICLES

Victor Zadkov and Julia Vladimirova

*M.V. Lomonosov Moscow State University, Lenin Hills, Moscow 119991, Russia
e-mail: zadkov@phys.msu.ru*

Nonclassical behavior of light reveals already at the single-atom-level in resonance fluorescence both as the sub-Poissonian behavior of the photon-number statistics and as the phenomenon of antibunching of scattered photons [1]. The antibunching of photons is associated with two-photon correlation measurements and results from the fact that after emitting a photon an atom has to be re-excited in order to emit next photon. Therefore, the probability of joint detection of two photons increases with increasing the time interval between detections from zero to a lifetime of the atomic transition. The antibunching of photons in resonance fluorescence is opposite to that one in thermal beams, which show photon bunching. Antibunching is also closely related to sub-Poissonian behavior of the photon-number statistics, i.e., the distribution function of the emission probability of n photons in a given time interval T . For the time intervals much longer than the atomic spontaneous decay time the sub-Poissonian behavior converges to a Gaussian one. First experimental confirmation of the antibunching of photons in resonance fluorescence was made in 1977 by Kimble, Dagenais, and Mandel [2] and the sub-Poissonian photon number statistics was later on verified by Short and Mandel in 1983 [3]. Most recent observation of the nonclassical properties of resonance fluorescent from a single trapped atomic ion was made by Diedrich and Walther [4].

Over two last decades, such a single-atom level of experiments for studying nonclassical light from isolated atoms or ions was also achieved in emerging field of nanophotonics [5], which demonstrates reliable sources of nonclassical light from single molecules, quantum dots (QD), NV-centers in nanodiamond, including those embedded in different nanostructures. In this case, the radiative properties of an emitter (atom, molecule or quantum dot) are strongly modified in confined geometries [6]. Plasmonic nanostructures, specifically metal nanoparticles (MNP), not only convert the incoming radiation to localized, but they also change the radiative frequency of the emitter and its decay rate. This leads to one of the important applications of nanooptics-using plasmonic nanostructures for changing and controlling fluorescence.

The resonance fluorescence, which features nonclassical behavior of fluorescent light, occurs when the quantum emitter is driven by an electromagnetic wave with the frequency close to the emitter's resonant frequency [1] and studying the resonance fluorescence of a quantum emitter near a MNP is just at start [7] and no attention is paid to the nonclassical behavior of the scattered light.

In this talk, we study quantum-optical effects in the system of “quantum emitter (atom, molecule, quantum dot) + metal nanoparticle” driven by an external near-resonant laser field.

First, we will give an overview of the mechanisms of modification of the local field and radiative and nonradiative decay rates of the two-level atom located in close proximity to a metal nanoparticle. Simple analytical expressions are given for both the local field enhancement, the modified total decay rate of the atom near the metal nanosphere and the frequency shift of the atomic transition.

Then, we will analyze in more detail the polarization distribution at the nanoscale around the nanoparticle. Near-field being formed by the interference of the incident electromagnetic field with the local field of the nanoparticle strongly depends both on the frequency and polarization of the incident field. Dependence of the near-field intensity distribution on these parameters has been studied in detail, however how its polarization distribution depends on them still remains largely a challenging question, being crucial for experiments on interaction of a quantum emitter (atom, molecule, quantum dot) with plasmonic nanoparticles, which lies in the basis of a number of nowadays nanotechnologies. Specifically, we will study in detail the near-field polarization distribution of a plasmonic prolate nanospheroid in an incident electromagnetic field versus its polarization and frequency. Polarization properties of the near-field are described with the help of the 3D generalized Stokes parameters, which allow simple visualization. It is shown that this distribution has a complex structure, which drastically depends on the polarization of the incident laser field and on the parameters of the plasmon resonance of the nanoparticle. For the incident plane electromagnetic wave of arbitrary polarization, the near-field of a prolate nanospheroid has areas with its polarization opposite to the polarization of the incident field. For instance, for the linearly polarized plane electromagnetic wave with the frequency tuned into the plasmon resonance of the nanoparticle the near-field polarization distribution features two symmetric tori in the center of which the near-field polarization is circular and vice versa: when the incident field polarization is circular, the near-field polarization distribution has a complex structure in the center of which the near-field polarization is linear. These results cover the whole set of particles whose shape varies from the spherical one to the nanoneedles and nanorods simply by changing the aspect ratio of the spheroid. A simple experiment is proposed to measure the near-field polarization distribution around a plasmonic nanoparticle.

After that, we will describe the photon-number statistics in resonance fluorescence of a two-level atom (quantum dot, molecule) near a MNP, which we consider for simplicity a metal nanosphere, driven by a laser field with finite bandwidth, as a function of atom's location around the nanoparticle, the intensity of the incident laser field, its bandwidth, detuning from the atomic resonance, and polarization. We have restricted ourselves to the two-level atom because we want to study the principal features of the nonclassical light from resonance fluorescence near a MNP. However, our approach can be also generalized to multilevel atoms in a manner analogous to the method applied for multilevel atoms in free space [8].

We will show that the distribution function $p(n, T)$ of the emission probability of n photons in a given time interval T strongly depends on the local field intensity in the point of space the atom is located at and can be controlled by a few key parameters—the atom's location around the metal nanosphere, the intensity of the incident laser field, its bandwidth, detuning from the atomic resonance, and polarization. Analytical expressions for the mean and the variance of the number of photons are derived for the case when T is much longer than the atomic transition lifetime. It is also shown that by analogy with the atom in free space [1], this distribution function showing sub-Poissonian character and antibunching of the emitted photons at short T converges to a Gaussian one when T is much longer than the modified by

the nanoparticle natural lifetime of the excited atom. As a result, the typical convergence timescale becomes three orders of magnitude longer than for a free atom.

Finally, we will analyze the antibunching effect of photons from the resonance fluorescence in the system “metal nanosphere and a two-level atom” driving by the incident laser field.

In conclusion, we summarize the received results and discuss some possible applications.

References:

[1] L. Mandel, E. Wolf, “Optical Coherence and Quantum Optics”, Cambridge Univ. Press, (1995).

[2] H. J. Kimble, M. Dagenais and L. Mandel, “Photon antibunching in resonance fluorescence”, *Phys. Rev. Lett.* **39**, 691, (1977).

[3] R. Short and L. Mandel, “Observation of sub-Poissonian photon statistics”, *Phys. Rev. Lett.* **51**, 384, (1983).

[4] F. Diedrich and H. Walther, “Nonclassical radiation of a single stored ion”, *Phys. Rev. Lett.* **58**, 203, (1987).

[5] S. V. Gaponenko, “Introduction to Nanophotonics”, Cambridge Univ. Press, New York, (2010).

[6] V. V. Klimov, “Nanoplasmonics: Fundamentals and applications”, Pan Stanford Publishing, Singapore, (2014).

[7] Y. V. Vladimirova, V. V. Klimov, V. M. Pastukhov, and V. N. Zadkov, “Modification of two-level-atom resonance fluorescence near a plasmonic nanostructure”, *Phys. Rev. A* **85**, 053408, (2012).

[8] Yu. V. Vladimirova, B. A. Grishanin, V. N. Zadkov, N. N. Kolachevskii, A. V. Akimov, N. A. Kisilev, S. I. Kanorskii, “Spectroscopy of coherent dark resonances in multilevel atoms for the example of samarium vapor”, *J. Exp. Theor. Phys.* **96**, 629, (2003).

Acknowledgements: The authors acknowledge financial support from the Russian Foundation for Basic Research (grant No. 13-02-00446).

L16

FEMTOSECOND LASER FILAMENT AND PLASMA CHANNELS IN THE FOCUSED BEAM IN AIR

S. A. Shlenov¹, A. A. Dergachev¹, A. A. Ionin², V.P. Kandidov¹, D. V. Mokrousova², L. V. Seleznev², D. V. Sinitsyn², E. S. Sunchugasheva², A.P. Shustikova²

¹*Lomonosov Moscow State University, Physics Department and International Laser Center,
Leninskie Gory, Moscow, Russia*

²*P.N.Lebedev Physical Institute of RAS, 53 Leninsky pr., Moscow, Russia
e-mail: shlenov@physics.msu.ru*

The propagation of high-power femtosecond laser pulse in air is accompanied by self-trapping of the beam and the formation of filaments [1-3]. The high intensity of the optical field in the filaments leads to photoionisation of the molecules of air and the formation of the plasma channels. These channels can be used to create a guiding system for microwave radiation [4], and to control high-voltage discharge [5-6]. It is therefore important to know the characteristics of these channels and be able to control them.

In this paper we study both experimentally and numerically the filamentation of focused beams at wavelength of 800 and 248 nm in a wide range of focal length. The results indicate that relatively tight focusing can lead to the coalescence of individual regions of high fluence and high plasma density that result from multiple refocusing, whereas in the case of weak focusing such regions are separated in the pulse propagation direction. The lower multiphoton ionisation order in the case of UV radiation leads to a stronger effect of geometric focusing on filament formation.

We show the possibility to control the parameters of femtosecond laser plasma filaments by introducing astigmatism in laser beam wavefront. Plasma channel length increases in the presence of weak astigmatism compared with the case of aberration-free focusing. Strong astigmatism can lead to the splitting of the channel into two separate regions.

The influence of the Kerr nonlinearity of a thin quartz plate, placed in the path of the laser beam, on the process of filamentation was investigated. It is shown that the thin quartz plate reduces the distance to the start of filamentation and increases the length of the plasma channel as well as the number of refocusing peaks in the filament.

References:

- [1] S. L. Chin., S. A. Hosseini, W. Liu et al. "The propagation of powerful femtosecond laser pulses in optical media: physics, applications and new challenges", *Can. J. Phys.*, Vol. 83, 863-905, (2005).
- [2] A. Couairon, A. Mysyrowicz, "Femtosecond filamentation in transparent media" *Phys. Rep.*, Vol. 441, 47-189, (2007).
- [3] V. P. Kandidov, S. A. Shlenov, O. G. Kosareva, "Filamentation of high-power femtosecond laser radiation", *Quantum Electronics*, Vol. 39, 205-228, (2009).
- [4] A. E. Dormidonov, V. V. Valuev, V. L. Dmitriev, S. A. Shlenov, V. P. Kandidov, "Laser filament induced microwave waveguide in air" *Proc. SPIE* Vol. 6733, 67332S, (2007).
- [5] B. La Fontaine, D. Comtois, C.-Y. Chien et al. "Guiding large-scale spark discharges with ultrashort pulse laser filaments", *J. Appl. Phys.*, Vol. 88, 610-615, (2000).

Acknowledgements: This work was supported by the Russian Foundation for Basic Research Grant No 14-02-00489.

L17

HIDDEN SYMMETRIES AND WAVE-PARTICLE DUALITY OF OPTICAL AND MATTER-WAVE SOLITONS

V. N. Serkin

Benemerita Universidad Autonoma de Puebla, 72001, Puebla, Mexico
e-mail: vserkin@yahoo.com

"Coming events cast their shadows before them". We start with this famous proverb to describe the historical development of the subject and provide a background to the so-called hidden symmetries and wave-particle duality of optical solitons, and we present the primary literature in the field and the results of the most significant experiments with optical and matter-wave solitons in Bose-Einstein condensates (BEC).

We would like to emphasize that Louis de Broglie in his Letter to Einstein dated 8 March 1954, specially underlined: "in my current research I have come to the idea that in order to

explain the wave-particle duality, one must develop a wave mechanics, which is based on nonlinear equations".

As the self-localized wave object, the soliton, by virtue of the Galilean symmetry, is characterized by its own solitonic analog of the de Broglie wavelength, sending us in search of a solitonic analog of the Ramsauer–Townsend effect. On the other hand, as the extended particle-like object, the soliton, because of the nonlinear self-interaction, becomes a bound state in its own self-induced trapping potential and, as a consequence, acquires a negative self-interaction (binding) energy. The soliton binding energy provides the shape and structural stability of solitons and, similar to the nuclear binding energy, can be considered as the degree of how strongly the quasi-particles that make up the soliton are bound together, for example, photons in optical spatial or temporal solitons, or Bose atoms trapped in matter–wave solitons in a BEC. This form of soliton energy (that is yet hidden from us) is sending us in search of the analogs of the Geiger–Nuttall law for solitons.

May 2011 marked the 100th anniversary of the most important experiments conducted in the history of science – the Rutherford α -particle scattering and the discovery of the atomic nucleus.

In our Lecture, inspired by many remarkable (but, obviously, only formal) analogies with modern Rutherford experiments and nuclear sub-barrier reactions (where the most important innovations are related with quantum tunneling of a composite particle, in which the particle itself has an internal structure), we provide a new framework for understanding of nonlinear tunneling mechanisms, and clarify the profound physical linkage between the Gamow scenario of quantum-mechanical tunneling and soliton tunneling through classically forbidden and localized potential barriers. Guided by this constructive (but obviously only formal) analogy, we have revealed the ‘hidden’ role of the soliton self-interaction (binding) energy in the nonlinear soliton tunneling dynamics and its dramatic impact on the wave-particle duality of tunneling solitons.

The results collected in this Report are of general physics interest and offer many opportunities for further scientific studies: although many different types of solitons have been discovered already in different branches of science (today, approximately one hundred models have been found to have soliton-like solutions), the understanding of the leading role of the soliton self-interaction energy in their scattering dynamics still remains ‘hidden’ and continues to open up unexpected directions of studies. In particular, since related dynamics governed by the NLSE model are also observed in many other physical systems from plasmas and BECs to monster (rogue) waves in oceans and soliton transport in nonlinear networks, our results are expected to stimulate new research directions in many branches of physics and technology.

18th International School on Quantum Electronics
“Laser physics and applications” 29 September – 3 October 2014, Sozopol, Bulgaria

ORAL AND POSTER SESSIONS

ORAL AND POSTER SESSIONS

PRESENTED CONTRIBUTIONS

A - LASER –MATTER INTERACTIONS

PA1

**MATRIX DESCRIPTION OF THE BEHAVIOR OF DEPENDENT LOSSES IN
POLARIZED HIGH-SPEED OPTICAL COMMUNICATION LINES**

Vanya Plachkova¹, Tinko Eftimov¹, Georgi Dyankov¹, Ilya Makrelov¹

¹ *Physics Faculty, Plovdiv University "P. Hilendarski", Plovdiv 4000
e-mail: vania_plachkova@abv.bg*

With increasing speed of information bit rate above 1 Gb/s and successfully minimizing chromatic dispersion in the infrared range, interest in polarization is increased dramatically because one of the limiting factors of the transmission rate are the polarization dependent losses (PDL). Accurate measurement of PDL is essential to determine the propagation characteristics of high-speed (over 2.5 Gb / s) optical systems for long distances (over 100 km). Therefore, various methods have been proposed with commercial measuring devices for characterization of this parameter.

The goal of this paper is to design mathematical models for the simulation of polarization dependent losses. The Mueller matrix model we have used can simulate the spectrum in the line affected by polarization dependent active components. We simulate these spectra as a function of random losses inherent to polarization dependent components. After statistical treatment of spectra we get information about PDL. We show that our theoretical results coincide with experimental ones reported in the literature.

Modeling of the PDL aims at an evaluation of the dispersion group delay changes (DGD) of a long-haul optical communication line in the presence of PDL thus avoiding the use of expensive devices for its measurement. This can help optimize the high-bit-rate performance of a real long-haul communication system.

References:

- [1] H. Dong and P. Shum, "Single-end Measurement of Polarization Mode Dispersion in Optical Fibers with Polarization-dependent Loss", Vol. 3, No. 6, 842-846, (2007).
- [2] Chen, L., O. Chen, S. Hadjifaradji, and X. Bao, "Polarization-mode dispersion measurement in a system with polarization-dependent loss or gain," IEEE Photon. Technol. Lett., Vol. 16, 206-208, (2004).
- [3] Gisin, N. and B. Huttner, "Combined effects of polarization mode dispersion and polarization dependent losses in optical fibers," Opt. Comm., Vol. 142, 119-125, (1997).
- [4] Dong, H., P. Shum, M. Yan, G. Ning, Y. Gong, and C. Wu, "Generalized frequency dependence of output Stokes parameters in an optical fiber system with PMD and PDL/PDG", Opt. Express, Vol. 13, 8875-8881, (2005).

PA2

FEMTOSECOND LASER SYSTEM FOR MICROMACHINING OF THE MATERIALS

R. Barbucha¹, M. Kocik¹, K. M. Tański¹, Garasz¹, T. Petrov², C. Radzewicz³

¹*Institute of Fluid Flow Machinery PAS*

²*Institute of Solid State Physics, BAS*

³*Institute of Physical Chemistry, PAS*

e-mail: brobert@imp.gda.pl

Femtosecond-pulse laser processing is based on a laser ablation phenomenon, i.e. total evaporation of material from the target surface during laser irradiation. It is the most precise method of material removal. Moreover it does not require any post processing. Removal of the material occurs only in the laser focus, since the lack of thermal interaction, neither heat affected zone (HAZ) nor debris occur [1]. Research results have shown that shortening the duration of the laser pulse significantly reduces HAZ, which translates into the high quality of the machined structures [2]. It is the main argument for the use of femtosecond-pulse lasers in the precise micromachining. The heart of the prototype presented here is a femtosecond laser consisting of a solid-state oscillator and the ytterbium-doped pulse fiber amplifier. The source of a high-power femtosecond pulses is the Yb:KYW crystal-based oscillator with a z-type resonator. In the laser presented, we used a passive mode-locking technique, which is implemented with a semiconductor saturable absorber mirror (SESAM). Saturating the absorbent causes modulation losses in the resonator, which leads to synchronization of the modes and generation of the ultra-short pulses. In a SESAM-type construction the absorber mirror is a periodic structure (diffraction grating), reflecting light due to Bragg diffraction phenomenon [3]. From the oscillator output, femtosecond pulses go directly to the amplifier. Due to the high peak power values in a single pulse, significant damages of the optical elements can be caused during the amplification process. Therefore, chirped pulse amplification (CPA) technique needs to be applied. In CPA, an ultra short laser pulse is stretched out in time prior to introducing it to the gain medium using a pair of gratings, then the laser pulse becomes positively chirped. Subsequently the stretched pulse is safely introduced to the gain medium and amplified. Finally, the amplified laser pulse is recompressed to the original pulse width through the reversal process of stretching [4-5]. Average beam power with mode-locking is 4W @25A and pulse length at the oscillator output is 500 fs. Laser micro and nano-machining has found application in different fields. It's primary use is industrial micromachining of metals, ceramics, polymers, glass, biological material for medical use in eye surgery, and photovoltaic cells.

References:

- [1] B. N. Chichkov, C. Momma, S. Nolte, F. van Alvensleben, A. Tunnerman, Femtosecond, picosecond and nanosecond laser ablation of solids, Applied Physics A, 63, Springer-Verlag, (1996).
- [2] N. M. Bulgakova, I. M. Bourakov, Phase explosion under ultrashort pulsed laser ablation: modeling with analysis of metastable state of melt, Applied Surface Science, 197-198, Elsevier Inc., (2002).

[3] O. E. Martinez, 3000 Times Grating Compressor with Positive Group Velocity Dispersion: Application to Fiber Compensation in 1.3-1.6 μm Region, IEEE Journal of Quantum Electronics, 23, (1987).

[4] N. P. Mahalik, Micromachining and Nanotechnology, Springer Science, Nowy Jork, (2006).

[5] B. Tan, A. Dalili, K. Venkatakrishnan, High repetition rate femtosecond laser nano-machining of thin films, Applied Physics A, Materials Science & Processing 95: 537–545, (2009).

PA3

ESTIMATION OF ULTRASHORT LASER IRRADIATION EFFECT OVER THIN TRANSPARENT BIOPOLYMER FILMS MORPHOLOGY

A. Daskalova¹, C. Nathala^{2,3}, I. Bliznakova¹, D. Slavov¹, W. Husinsky²

¹ Institute of Electronics, Bulgarian Academy of Sciences, 72,
Tsarigradsko Chaussee Blvd., 1784 Sofia, Bulgaria

² IAP, Vienna University of Technology, Wiedner Hauptstrasse 8-10, 1040 Vienna, Austria

³ Femtolasers Productions GmbH, Fernkorngasse 10, 1100 Vienna, Austria
e-mail: a_daskalova@code.bg

Recently, laser surface modification of self – standing biopolymers thin films from natural substrates like collagen, elastin and gelatin as an appropriate artificial scaffold matrix, represent an alternative technique to conventional chemical based methods. Several groups reported that the morphological changes of the biofilms affect the cell behavior (growth, adhesion, proliferation and differentiation) and their propagation on laser irradiated and non – irradiated surfaces. Laser modification method is a promising technique for surface microprocessing which allows three – dimensional structure creation with high accuracy, retaining material functionality and modification of surface morphological properties with minimal thermal damages.

In this paper, collagen – elastin surface modifications after femtosecond laser irradiation have been shown. The thin films were treated by CPA Ti:Sapphire laser (Femtopower-Compact Pro) emitting at 800 nm central wavelength with 10 fs and 30 fs pulse duration and 1 kHz repetition rate. A process of microporous scaffold creation by ultrashort laser interaction with transparent biopolymer films has been observed. Numerical evaluations of single-shot ($N = 1$) and multi-shot ($N > 1$) threshold laser fluences by studying the diameter and “height” of porous surface modification formations are also performed. After experimental estimation of the properties of modified zone (D_N) with different pulse numbers (N), we have calculated the incubation coefficient ξ for multi –shot fluence threshold and by power-law relationship form $F_{th}(N) = F_{th}(1)N^{\xi-1}$ estimated the $F_{th}(N)$ for both pulse durations.

The analysis of obtained results allows more detail information concerning the surface changes of thin transparent biopolymer films properties after ultrashort laser treatment.

References:

[1] A. Daskalova, Chandra S. R. Nathala, I. Bliznakova, E. Stoyanova, A. Zhelyazkova, T. Ganz, S. Lueftenegger, W. Husinsky, “Controlling the porosity of collagen,

gelatin and elastin biomaterials by ultrashort laser pulses”, Applied Surface Science, Vol. 292, pp. 367-377, (2014).

[2] L. Rusen, M. Cazan, C. Mistaciosu, M. Filipescu, S. Sandel, M. Zamfirescu, V. Dinca, M. Dinescu, “Tailored topography control of biopolymer surfaces by ultrafast lasers for cell – substrates studies”, Applied Surface Science, Vol. 302, pp. 256 – 261, (2014).

[3] S. Lazare, V. Tokarev, A. Sionkowska, M. Wisniewski, “The Influence of KrF Excimer Laser Irradiation on the Surface of Collagen and Collagen/PVP Films”, Applied Physics A, Vol. 81, pp. 465-470, (2005).

[4] A. Ben-Yakar, R. L. Byer, “Femtosecond laser ablation properties of borosilicate glass”, Journal of Applied Physics, Vol. 96, No 9, pp. 5316-5323, (2004).

Acknowledgements: This work was supported by the Bulgarian National Science Fund (NSF) under bilateral contract No. DNTS/Austria/01/1/2013 – 2015. The SEM measurements were carried out using facilities at the University Service Centre for Transmission Electron Microscopy, Vienna University of Technology, Austria.

PA4

FABRICATION OF ZnO NANOSTRUCTURES BY PLD

A. Og. Dikovska¹, G. B. Atanasova², G. V. Avdeev³, M. E. Koleva¹, N. N. Nedyalkov¹, P. A. Atanasov¹

¹*Institute of Electronics, Bulgarian Academy of Sciences,
72 Tsarigradsko Chaussee, Sofia 1784, Bulgaria*

²*Institute of General and Inorganic Chemistry, Bulgarian Academy of Sciences,
Acad. G. Bonchev str., bl. 11, 1113 Sofia, Bulgaria*

³*Rostislav Kaischew Institute of Physical Chemistry, Bulgarian Academy of Sciences,
Acad. G. Bonchev Str., Bl.11, 1113 Sofia, Bulgaria
e-mail: dikovska@ie.bas.bg*

The synthesis of ZnO nanostructures, such as nanowires, nanorods and nanotubes, has acquired considerable interest due to their potential importance in nanodevice fabrication. Among the various growth methods, pulsed laser deposition (PLD) has been proven to be a suitable method for the synthesis of nano-scale materials. A large number of studies have been reported on the growth of ZnO nanostructures by PLD. These studies investigated the role of various experimental parameters, such as substrate temperature, background oxygen pressure and laser fluence, on the nanostructures growth. A variety of different growth mechanisms have also been suggested. Generally, the authors have focused their attention on the fabrication of nanostructures using two different growth mechanisms, namely, nucleation with or without a catalyst.

The aim of this work is to fabricate ZnO nanostructures by PLD and a metal (Au or Ag) catalyst layer pre-deposited on the substrate before nanostructure growth. The samples were prepared at substrate temperatures in the range of 300 – 650 °C, oxygen pressure of 5 Pa, and laser fluence $\leq 1 \text{ J.cm}^{-2}$ – process parameters usually used for thin-film deposition. The metal layer is substantial for the preparation of nanostructures. The nanostructures grown at different substrate temperatures showed obvious morphological differences. The substrate temperature increase led to changes in the morphology of the nanostructures from

nanowhiskers to nanowalls when a thin Au layer was used. It was also observed that the type and thickness of the metal layer affect the morphology of the nanostructure.

PA5

INFLUENCE OF THE SCANNING CONDITIONS ON THE CHARACTERISTICS OF THE NANOSTRUCTURES FABRICATED BY LASER ABLATION IN LIQUID

A. S. Nikolov¹, R. G. Nikov¹, N. N. Nedyalkov¹, M. T. Alexandrov², D. B. Karashanova³, N. E. Marinkov⁴, I. Z. Dimitrov⁴, I. I. Boevski⁴

¹ *Institute of Electronics, Bulgarian Academy of Sciences, 72 Tsarigradsko Chaussee, Sofia 1784, Bulgaria*

² *Institute of Experimental Pathology and Parasitology, Bulgarian Academy of Sciences, G. Bonchev Street, bl. 25, Sofia 1113, Bulgaria*

³ *Institute of Optical Materials and Technologies, Bulgarian Academy of Sciences, G. Bonchev Street, bl. 109, Sofia 1113, Bulgaria*

⁴ *Institute of General and Inorganic Chemistry, Bulgarian Academy of Sciences, Acad. G. Bonchev Str., bl.11, 1113, Sofia, Bulgaria*

The method of pulsed laser ablation was used to create Ag nanostructures - nanoparticles and nanowire networks. The trajectory of the laser beam on the target surface was investigated to establish its impact on the characteristics of the ablation process itself and the nanostructures obtained. Two circle trajectories of different diameters and one third of another shape were utilized. The fundamental ($\lambda = 1064$ nm) wavelength and the second harmonic ($\lambda_{\text{SHG}} = 532$ nm) of a Nd-YAG laser system were used for the fabrication procedure. They were selected in order to be study the influence of both processes accompanying the ablation procedure – absorption of the incident light by the liquid medium and by the nanostructures already created (the so-called self-absorption). Both possible nanostructures – nanoparticles and nanowire networks were obtained by appropriate choice of the laser fluence for each of the wavelengths selected. The optical extinction spectra of the fabricated colloids allowed an indirect assessment of the shape and the size-distribution of the nanostructures obtained. By transmission electron microscopy (TEM) was visualized their size and morphology. Measurement of the mass-concentration of the Ag in the colloids by the method of inductively coupled plasma atomic emission spectrometry (ICP-AES) enabled the efficiency of the ablation process to be determined.

PA6

FABRICATION AND CHARACTERIZATION OF METAL SUBSTRATES

Ru. G. Nikov, N. N. Nedyalkov, P. A. Atanasov

*Institute of Electronics, Bulgarian Academy of Sciences,
Tzarigradsko chaussee 72, Sofia 1784, Bulgaria*

In this paper we show experimental and theoretical results on the characterization of metal nanoparticle arrays fabricated on metal substrates. The nanostructures are fabricated by laser processing of thin metal films. The films are deposited on the metal substrates by classical PLD technology. The as deposited films are then annealed by nanosecond pulses delivered from a THG Nd:YAG laser system ($\lambda = 355$ nm). At certain conditions, the laser treatment leads to a formation of nanoparticle discrete structure on the substrate. The optical properties of samples fabricated at different conditions and having different characteristics of the nanostructures are examined by optical spectroscopic measurement. The obtained nanostructures show expressed plasmon resonance behaviour in the optical extinction spectra. Finite difference time domain (FDTD) model is used for theoretical description of the optical properties of the fabricated nanoparticle arrays. The great enhancement observed in the Raman spectra of Rodamine 6G deposited on the fabricated samples makes such structures very appropriate for applications like Surface Enhanced Raman Spectroscopy (SERS) and plasmonic solar cells (PSC).

PA7

EFFECTS OF LASER INTERACTION WITH HISTORICAL COPPER ALLOY COVERED BY PATINA LAYERS

Iwona Źmuda-Trzebiatowska¹, Katarzyna Schaefer², Mirek Sawczak¹, Gerard Śliwiński¹

¹*Photophysics Dept, The Szewalski Institute, Polish Academy of Sciences
14 Fiszera St. 80-231 Gdańsk, Poland, Phone: +48 58 6995313*

²*National Maritime Museum in Gdańsk, 9-13 Ołowianka St., 80-751 Gdańsk, Poland
e-mail: izmuda@imp.gda.pl*

The procedure of laser cleaning of historical copper substrate covered by patina with numerous contamination layers was acquired. The laser cleaning was performed by means of the pulsed Q-switched Nd:YAG laser (Laserblast 1000, Quantel) operated by 1064 nm with pulse length and repetition rate of 10 ns and 120 Hz, respectively. It is shown that for density 1-1.4 J/cm² the correct cleaning of investigated material can be observed. Laser damage threshold of the patina layer on copper starts at fluence of 1.4 J/cm² and exceeding this value removes the patina. The damage threshold may be even lower depending on the state of preservation and chemical composition of the patina. In this work a number of patinated samples was studied by using a variety of analytical techniques. The complementary use of the elemental (XRF, LIBS) revealed the presence of Cu, Fe, Pb by XRF and additionally Ca, Na, Si, and C by LIBS techniques. The stratigraphic data obtained by laser ablation indicated the presence of patina layers of thickness ranging from 40 to 80 μ m depending on the measuring area. Using Raman spectroscopy the brochantite (Cu₄SO₄(OH)₆) was indentified.

The effect of the laser excitation at 514 nm during Raman measurement was studied. It was shown, that in case of patinas the laser power level of 0.5-1% is sufficient for sample identification while higher levels lead to damage and decomposition of the patina. Larger power of the laser takes effects of burnout of patina layer which was observed by microscope and prevents further analysis of the measuring surface. Moreover, the surface mapping as well as the chemical composition of the cleaned/deposit material were analyzed by means of scanning electron microscopes equipped with EDS (SEM-EDS). The surface mapping and EDS spectrum confirmed the presence of elements such a Cu, Fe, Pb, Ca in agreement with other techniques.

PA8

MORPHOLOGICAL AND OPTICAL PROPERTIES OF NOBLE METAL NANOPARTICLES PRODUCED BY LASER ABLATION

A. Og. Dikovska¹, M. Alexandrov², G. Atanasova³

¹*Institute of Electronics, Bulgarian Academy of Sciences,
72 Tsarigradsko chaussee, Sofia 1784, Bulgaria*

²*Institute of Experimental Pathology and Parasitology, Bulgarian Academy of Sciences,
Acad. G. Bonchev Street, bl. 25, Sofia 1113, Bulgaria*

³*Institute of General and Inorganic Chemistry, Bulgarian Academy of Sciences,
Acad. G. Bonchev Street, bl. 11, Sofia 1113, Bulgaria
e-mail: dikovska@ie.bas.bg*

Due to their unique physical and chemical properties, noble metal nanoparticles (Au, Ag etc.) have in recent years attracted considerable interest, as evidenced by the large number of scientific publications. Applications of these particles are expected in many areas, such as surface enhanced Raman spectroscopy, biology, medicine, optical devices, chemistry etc. Among the techniques of preparing such particles, laser ablation stands out because of its simplicity, versatility and cost-effectiveness.

In this paper, we report noble metal (Au and Ag) nanoparticles formation on silica substrates by laser ablation. The influence was investigated of the experimental conditions on the morphological and optical properties of the nanoparticles. Our attention was focused on the dependence of the mean diameter, shape and size distribution of the nanoparticles on the number of the laser pulses applied. The influence of the laser fluence used on the nanoparticles produced was also explored.

The existence of metal nanoparticles was evidenced by transmission electron microscopy (TEM) images. The nanoparticles produced in vacuum have mean diameters in the range from 5 nm to 12 nm. The nanoparticles' size increases with the increase of the number of the laser pulses applied. The presence of the nanoparticles was also confirmed by the appearance of a strong optical absorption band into the measured UV-VIS spectra, associated with surface plasmon resonance (SPR). A shift and widening of the absorption peak at the longer wavelengths was observed as the number of the laser pulses was increased. Some additional investigations were performed in order to clarify the structure of the Ag nanoparticles.

Acknowledgements: The study was performed with financial support of The Ministry of Education and Science of Bulgaria, Operational Program "Human Resources Development",

co-financed by the European Social Fund of the European Union, contracts: BG051PO001-3.306-0050.

PA9

OPTICAL PROPERTIES OF Ag-ZnO NANOSTRUCTURES

M. E. Koleva¹, N. N. Nedyalkov¹, P. A. Atanasov¹, N. Fukata², M. Dutta²

¹*Institute of Electronics, Bulgarian Academy of Sciences,
72 Tsarigradsko Chaussee Blvd., Sofia 1784, Bulgaria*

²*International Center for Materials Nanoarchitectonics, National Institute for Materials
Science, 1-1 Namiki, Tsukuba, 305-0044, Japan
e-mail: mihaela_ek@yahoo.com*

The layered nanocomposites of Ag nanoparticles (NPs) and ZnO were laser fabricated and investigated. The double layer (DL) nanostructures of AgNPs/ZnO and the multilayer (ML) nanostructures of AgNPs/ZnO/AgNPs/ZnO on SiO₂ substrate were produced. The Ag thin films were decomposed into nanoparticles by laser annealing. The samples were characterized by UV-VIS transmission spectroscopy, Raman spectroscopy and photoluminescence (PL) emission study. The characteristic resonance absorption was registered for all the samples at the range of 440 – 530 nm. The red shift of absorption minima was observed with deposition of ZnO as a top layer. The broadening of the resonance absorption was observed by increasing the number of layers. Raman scattering study was carried out to obtain information about the laser surface modifications effects of the composite nanostructures on the optical phonons and the lattice defect modes of ZnO.

Understanding the phonon spectrum change in wurtzite nanostructures is important because the optical phonons affect the light emission and absorption. The Raman spectrum taken for the DL and ML structures significantly differs from the spectrum of bulk ZnO. The 1LO-phonon frequency of bulk ZnO usually is between 574 and 591 cm⁻¹. The 1LO peak of ML nanostructure appears at 564 cm⁻¹, which indicates a redshift of more than 10 cm⁻¹. The observed huge redshift could hardly be attributed to the intrinsic impurity or defects in the sample. The possible reason for the observed redshift is intense local heating induced by UV laser in the intermediate layer of ZnO in the ML nanostructure. The PL enhancement occurs after annealing and is due to the morphology changes in the nanoscale structures. Room temperature photoluminescence spectrum shows green emission enhancement at 560 nm for the DL structure, while the strong characteristic ZnO emission enhancement at 380 nm was registered for the ML structure.

PA10

LASER DISPERSING OF WC AND TiC POWDERS IN LIGHT METAL ALLOYS FOR WEAR RESISTANCE ENHANCEMENT

Rafał Jendrzejewski, Gerard Śliwiński

*Photophysics Dept., The Szewalski Institute, Polish Academy of Sciences
Fiszera 14, 80-231 Gdansk, Poland
e-mail: rafj@imp.gda.pl*

In the case of light metal alloys, the considerable enhancement of the wear resistance can be achieved by laser dispersing of hard particles in the bulk material [1, 2]. Such metal matrix composites (MMC) are of interest for numerous applications ranging from the power plant, aircraft and automotive industries to the medical one.

In this work, formation of MMC surface layers on the titanium-based Ti-6Al-4V and aluminum-based Al 6061 alloys by means of laser dispersing of WC and TiC powder particles is investigated. In the process, the substrate surface is locally melted to the depths up to about several hundreds μm by the slightly defocused high power CO₂ or disk Yb:YAG laser beam. Simultaneously, powder particles of irregular (TiC) or spherical (WC) shape and average size of about 100 microns are injected into the molten material by means of specialized, lateral nozzle (Fig. 1).

The single traces as well as surface layers consisting of several consecutive traces were produced. The influence of the process parameters, such as: laser beam intensity, scanning speed, powder feed-rate and substrate preheating temperature, on the properties of the composite layer was analyzed and discussed. The optical and SEM inspections of the produced MMC materials revealed the homogeneously distributed powder particles in the best samples obtained (Fig. 2). From wear tests performed by means of the "ball-on-disc" method the significantly improved abrasion resistance of the composite layers in comparison to the non-processed alloys was concluded.

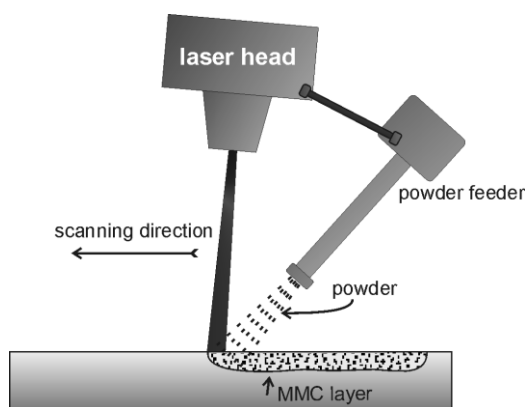


Fig. 1. Laser dispersing scheme

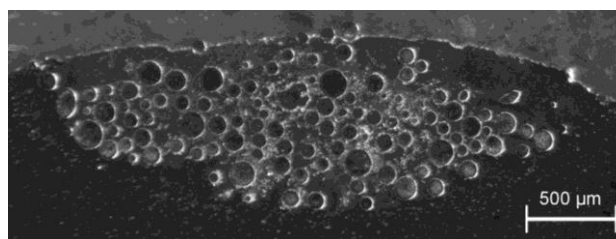


Fig. 2. Cross-sections of the single MMC trace in Al6061 alloy with dispersed WC powder particles

References:

[1] R. Jendrzewski, K. Van Acker, D. Vanhoyweghen, G. Śliwiński, “Metal matrix composite production by means of laser dispersing of SiC and WC powder in Al alloy”, *Applied Surface Science*, 255, 5584-5587, (2009).

[2] R. Jendrzewski, “Laser dispersing of carbide powders in Ti-6Al-4V alloy”, *Proc. SPIE 8703*, 87030K-1 - 87030K-4, (2012).

PA11

PULSED LASER DEPOSITION OF ORGANIC SEMICONDUCTOR RUBRENE THIN FILMS

Katarzyna Grochowska¹, Sayani Majumdar², Mirosław Sawczak¹ and Gerard Śliwiński¹

¹ *Photophysics Department, Szewalski Institute of Fluid-Flow Machinery, Polish Academy of Sciences, 80-231 Gdańsk, Poland*

² *Nanospin, Department of Applied Physics, Aalto University School of Science, FI-00076, Finland*

e-mail: kgrochowska@imp.gda.pl

Pulsed Laser Deposition (PLD) technique is applied to produce multilayers of ferromagnetic oxide thin film and organic semiconductor rubrene for spintronics applications. The aim of the PLD deposition of rubrene on LSMO (Lanthanum Strontium Manganite Oxide) is to avoid the undesired effect of contamination that significantly affects the interface energetics in case of the two-step production of the hybrid structure [1-2]. The organic-inorganic system LSMO/rubrene combines the advantage of 100% spin polarization of the half-metallic oxides and very long spin relaxation lengths of the organic semiconductors and offers control over the spin-polarized signal in hybrid spintronics components. Moreover, the use of organic material is advantageous because of such properties as chemical tuning of electronic functionality, easy structural modifications, ability of self-assembly and mechanical flexibility [3]. Among organic materials, rubrene reveals the highest hole mobility - up to 40 cm²/(V·s) and its properties can be exploited for example in organic light-emitting diodes (OLEDs) or organic field-effect transistors (OFETs) [4]. In this work the rubrene thin films are produced from hardened pellets in vacuum at ~ 10⁻⁵ hPa using Nd:YAG pulsed laser operated at 1064 nm, 2 Hz and energy fluence around 0.19 J/cm². In case of the reference rubrene samples deposited on SiO₂ glass the AFM data reveal a continuous 5-7 nm thick rubrene films with agreement with profilometric measurements. The amorphous structures are confirmed by XRD measurements and also Raman spectra which show tetracene and phenyl bands and a broadband at 1373 cm⁻¹. From XPS and magnetic measurements on the LSMO/rubrene interface the modified electronic structure due to the hybridization of p orbitals of the organic molecule and d electrons of the inorganic ferromagnet leading to modified spin polarization properties is concluded. The preliminary results indicate that continuous, defect-free organic semiconductor for organic-inorganic hybrids can be prepared by means of PLD with flexibility sufficient for the control of spin polarization properties in spintronic devices.

References:

- [1] M. Grobosch, M. Knupfer, "Electronic properties of organic semiconductor/electrode interfaces : the influence of contact contaminations on the interface energetic" *The Open Applied Physics Journal*, 4, 8-18, (2011).
[2] S. Majumdar and S. van Dijken, "Pulsed laser deposition of La_{1-x}Sr_xMnO₃: thin-film properties and spintronic applications" *J. Phys. D : Appl. Phys.*, 47, 034010, (2014)
[3] W.J.M. Naber, S. Faez, W.G. van der Wiel, "Organic spintronics" *J. Phys. D: Appl. Phys.*, 40, R205-R228, (2007).
[4] T. Hasegawa, J. Takeya, "Organic field-effect transistors using single crystals" *Sci. Technol. Adv. Mater.*, 10, 024314, (2009).

OA1

THE INTERACTION OF HIGH-POWER LASER PULSE WITH MULTICOMPONENT POLYCRYSTALLINE ROCKS

I. S. Timofeev, I. N. Burdonsky, A. Yu. Goltsov, K. N. Makarov, A. G. Leonov, V. N. Yufa

MIPT, Dolgoprudny, Russia
e-mail: i.s.timofeev@gmail.com

Research results of laser radiation interaction with multicomponent polycrystalline rocks are described in the paper. It is of considerable interest from the point of view of possible technological applications, in particular, laser modeling of micrometeorite impact, since the properties of such rocks differ drastically from metals properties.

A series of experiments to study the craters formed in andesite targets of various thicknesses (from 250 μm to 1 cm) under the action of laser radiation intensity of 10^{11} - 10^{13} W/cm^2 with a pulse duration of 30 ns was carried out on the "Saturn" [1]. In a simplified model of the shock wave generation by laser radiation [1] theoretical scaling of the shock wave velocity in the target was ~ 10 km/s.

For a detailed study of the mechanism of energy transfer to the rear surface of the target, experiments with thin andesite plates (thickness ~ 300 μm) were carried out. There are two typical cases of spall: with the through channel and without it, depending on the energy of the laser radiation and the target thickness. Analysis of the spall crater matter showed the presence of a large number of solid fragments with characteristic dimensions of 0.1-100 μm .

X-ray diagnostics of the resultant plasma temperature ($T \sim 200$ eV at $I \sim 4 \times 10^{11}$ W/cm^2) allowed to estimate the plasma pressure, which is in a quite satisfactory agreement with the model [1], and to calculate the shock wave velocity. One can expect that at the rear surface of the target velocity of the crater fragments will be around 10 - 20 km/s. It should be noted, that in case of through-channel, plasma glow from the rear surface of the target is registered after 20 ns, that leads to an abnormally high velocity of shock wave front around 17 km/s [2], and may be connected with target porosity and the presence of various cavities.

References:

- [1] I. N. Burdonsky, A. Y. Goltsov, A. G. Leonov, K. N. Makarov, I. S. Timofeev, V. N. Yufa, "Crater formation in multicomponent polycrystalline targets under the action of

ORAL AND POSTER SESSION

high-power laser”, *Problems of Atomic Science and Technology*, Vol. 36, No 2, P. 8-19, (2013).

[2] I. N. Burdonsky, A. Y. Goltsov, A. G. Leonov, K. N. Makarov, I. S. Timofeev, V. N. Yufa, “Spalls formation in thin polycrystalline targets under the action of the high-power laser pulse.”, *Physics of Extreme States of Matter*, P., 123-125, (2014).

B - LASER SPECTROSCOPY AND METROLOGY

PB1

**PHASE RECOVERY FROM FRINGE PATTERNS: APPROACH BASED
ON HILBERT TRANSFORM AND WAVELET DE-NOISING
TECHNIQUES**

Peter Sharlandjiev and Natalia Berberova

*Institute for Optical Materials and Technologies, Bulgarian Academy of Science
e-mail: pete@iomt.bas.bg*

Surface topography estimation of 3-D objects is of interest for many applications in science and engineering. This task can be defined in terms of laser metrology as phase retrieval from registered fringe patterns. Phase Shifting (PS) is one of the best known such techniques, although it needs several frames to be registered and analyzed. Post –processing of the frame data includes three major steps: phase recovery, phase unwrapping and de-noising. Methods based on Fourier Transform (FT), Windowed Fourier Transform (WFT), Hilbert Transform (HT), Wavelet Transform (WT) algorithms are widely implemented. Complex WT can be used for phase retrieval, but real 2-D discrete WT are applied for de-noising.

We have developed an approach based on HT and WT de-noising of a single fringe pattern. Its performance is compared by numeric modeling to that of PS and WT phase extraction. In the three cases considered, the unwrapping and the de-noising procedures were the same. The effect of noise in the fringe pattern was generated by simulation of stochastic white Gaussian noise and non-sinusoidal waveforms (presence of second and third harmonics). In the PS case, based on the so-called “algorithm 5.1”, phase-stepping specific sources of errors were included, too. Results indicate that the proposed approach is robust, effective and outperforms the other two methods.

PB2

**AN ANISOTROPIC STRATIFIED STRUCTURE FOR SURFACE PLASMON
EXCITATION**

Katerina Zhelyazkova¹ and Georgi Dyankov¹

¹*Faculty of Physics, Plovdiv University “Paissi Hilendarski”, 24 Tzar Assen St, Plovdiv 4000,
Bulgaria*

e-mails: katiyajeliazkova@abv.bg, dyankov@uni-plovdiv.bg

In this work, we propose a structure based on an anisotropic thin film for surface plasmon resonance excitation. The theoretical model is based on 4x4 matrix method for solving Maxwell equations for anisotropic media/metal structure. We have simulated light propagation in stratified structure: prism/chiral media/metal/air for conditions, corresponding to plasmon excitation. The simulations have been provided for different thickness, pitch length, and type of the chiral and metal media. The efficiency of excitation depends on the configuration of the structure.

PB3

ENHANCED VELOCITY SELECTIVE OPTICAL PUMPING IN BI-CHROMATIC EXCITATION OF CS VAPOR IN MICROMETRIC OPTICAL CELL

A. Krasteva¹, B. Ray², D. Slavov¹, P. Todorov¹, P. N. Ghosh², S. Mitra², V. Nikolova and S. Cartaleva^{1*}

¹Institute of Electronics, BAS, boul. Tzarigradsko shosse 72, 1784 Sofia, Bulgaria

²Department of Physics, University of Calcutta, 92 A P C Road, Kolkata 700 009, India

e-mail: stefka-c@ie.bas.bg

In this work we study the pump probe spectra of Cs in a micrometric (MM) cell of path length 6λ ($\lambda = 852\text{nm}$). The D_2 line is excited by a pump radiation fixed within the $F_g=3$ to $F_e=4$ transition and the probe one scanned across the $F_g=4$ to $F_e=3,4,5$ transitions. The spectra show sub-natural-width Electromagnetically Induced Transparency (EIT) and Enhanced Velocity Selective Optical Pumping (EVSOP) resonances. The EIT resonance gets broader and its contrast reduces with the pump laser frequency shift from the $F_g=3 \rightarrow F_e=4$ transition [1].

To analyze the EVSOP resonance, its dependence on the pump laser frequency detuning is investigated. When the pump frequency is in exact resonance with the $F_g=3 \rightarrow F_e=4$ transition, the EVSOP resonance is of very high contrast (Fig.1,left). With a small pump frequency

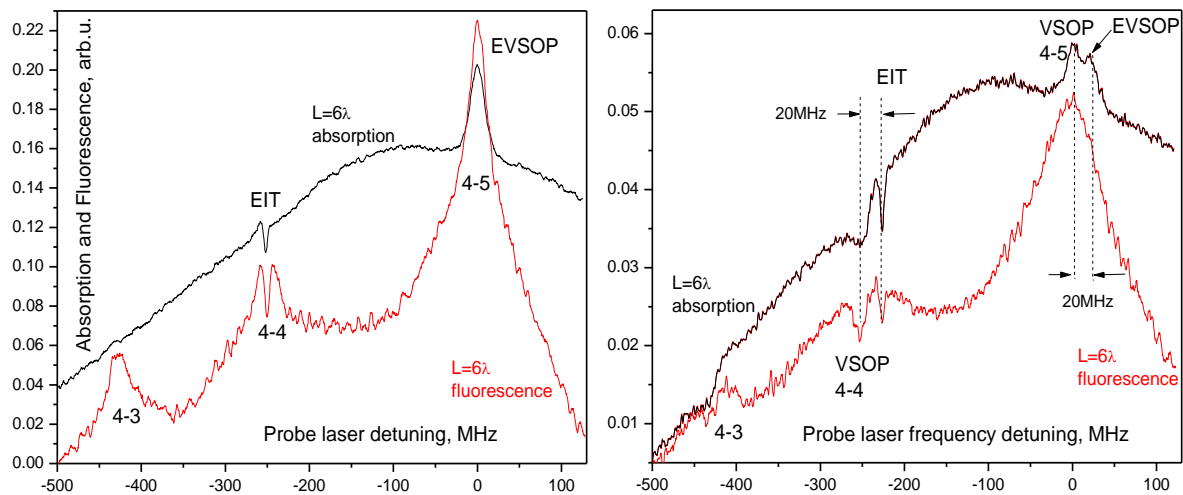


Fig.1. Pump-probe spectra: for (left) the pump fixed exactly at the 3-4 transition and the probe scanned over the $F_g = 4$ set of transitions and (right) the pump frequency is shifted by 20MHz from the 3-4 transition. $T_{MM} = 74^\circ\text{C}$, $W_{\text{probe}} = 0.1\text{mW}/\text{cm}^2$ and $W_{\text{pump}} = 1.5\text{mW}/\text{cm}^2$.

detuning (Fig.1, right), the EIT resonance is slightly broader but its contrast does not change significantly. As the EIT dip is shifted from the 4-4 transition centre by $\Delta = 20\text{MHz}$, larger than the width of the conventional VSOP resonances observed in MM cell by single beam approach [2], it is accompanied by the VSOP (4-4) resonance. At the 4-5 transition a sharp peak, the VSOP (4-5) is observed, while the EVSOP resonance suffers strong damage due to the high selectivity of excitation. Our experiments have shown that the EVSOP resonance is much more critical to the pump laser frequency detuning than the EIT resonance.

References:

- [1] A. Sargsyan, C. Leroy, et al. Opt. Commun, 285, 2090–2095, (2012).
- [2] S. Cartaleva, A. Krasteva, L. Moi et al., Quant. Electr.43 (9), 875 – 884, (2013).

Acknowledgements: This work is supported by a Marie Curie International Research Staff Exchange Scheme Fellowship within the 7th European Community Framework Programme

PB4

RUBIDIUM VAPOUR DENSITY MODIFICATION DUE TO LIGHT INDUCED ATOMIC DESORPTION EFFECT

C. Marinelli¹, E. Mariotti¹, L. Marmugi¹, L. Moi¹, S. Gateva², A. Krasteva², S. Cartaleva²

¹Department of Physical, Geological and Environmental Sciences, University of Siena, via Roma 56, 53100 Siena, Italy

²Institute of Electronics, BAS, boul. Tzarigradsko shosse 72, 1784 Sofia, Bulgaria
e-mail: stefka-c@ie.bas.bg

In this work we report the Rb vapor density modification induced by weak, non-laser light irradiation of paraffin and PDMS coated cells containing pure Rb gas. The natural mixture of Rb atoms were irradiated by a free running diode laser, tuned on the Rb D₂ resonance line. Absorption spectra were measured for different laser frequency scanning rates and laser light intensities. The obtained spectra were compared for two different cases: without and with illumination of the walls of the cell by a UV lamp centered around 404 nm wavelength. It was shown experimentally that without Light Induced Atomic Desorption (LIAD) effect, strong hyperfine optical pumping is observed (Fig.1a). Note that the F_g = 2 level (⁸⁷Rb) is almost completely depleted and the absorption from the F_g = 3 level (⁸⁵Rb) is dramatically reduced as compared to that from the F_g = 2 level. However, the strong flow of atoms from the cell

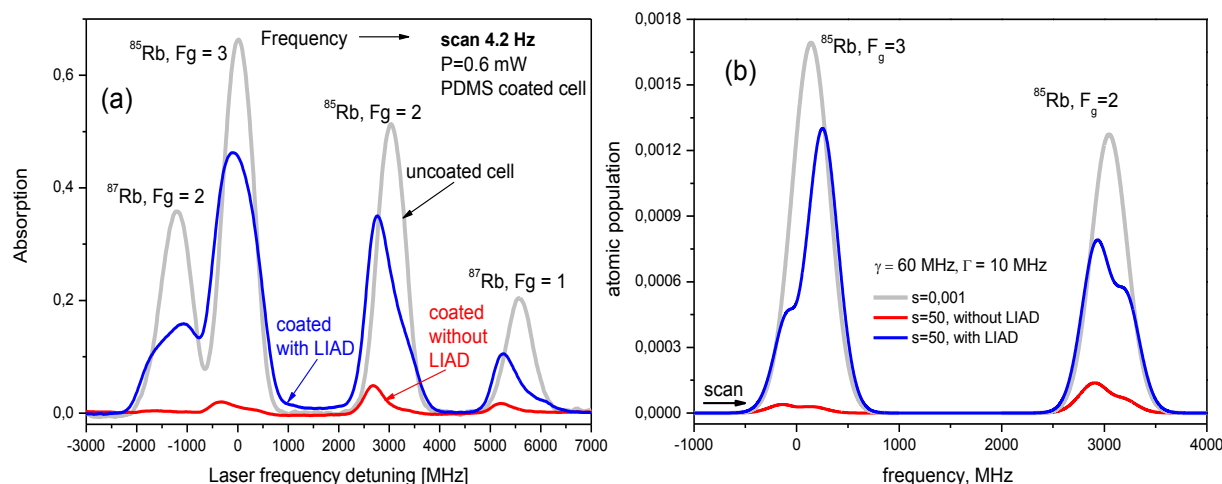


Fig. 1. (a) Experimental spectra: (grey trace) reference spectrum of Rb atoms in an uncoated cell; (red trace) the spectrum of Rb in the PDMS coated cell without LIAD effect, exhibiting strong hyperfine optical pumping; (blue trace) significantly modified spectrum of Rb in the PDMS coated cell, for strong LIAD effect; (b) Theoretical simulation: (gray trace) low saturation parameter; (red and blue traces) high saturation parameter – without and with LIAD, respectively.

coating released by LIAD effects results in significant randomization of atomic spin orientation. The rate of hyperfine optical pumping is reduced and even reversed. A theoretical model based on atomic population rate equations was used to describe the optical pumping processes (Fig.1b), considering the D_2 line of one isotope (^{85}Rb). The theoretical analysis can provide a good description of the property of the coatings (i.e. their ability to significantly reduce the atomic spin relaxation) and on the vapor-surface interaction.

Acknowledgements: This work was supported by Marie Curie International Research Staff Exchange Scheme Fellowship within the 7th European Community Framework Programme.

PB5

CONVERSION BETWEEN ELECTROMAGNETICALLY INDUCED ABSORPTION AND TRANSPARENCY IN A FOUR-LEVEL SYSTEM

D. Sarkisyan¹, A. Sargsyan¹, A. D. Wilson-Gordon², S. Cartaleva³

¹*Institute for Physical Research, Academy of Sciences of Armenia, Ashtarak-2, Armenia*

²*Department of Chemistry, Bar-Ilan University, Ramat Gan 52900, Israel*

³*Institute of Electronics, Bulgarian Academy of Sciences, 72 Tzarigradsko Shosse bld, 1784 Sofia, Bulgaria*

e-mail: davsark@yahoo.com

Continuous interest in coherent population trapping and related electromagnetically induced transparency (EIT) phenomena is stimulated by a number of important applications in a variety of fields such as laser cooling, information storage, magnetometry, spectroscopy, atomic frequency references etc. [1].

Recently, formation of the sub-natural width N -type resonance in a Λ -system, on the D_2 line of Cs atoms has been demonstrated [2]. Two continuous narrow-band diode lasers with $\lambda=852$ nm were used. A 1 cm- long cell filled with the Cs vapor and a buffer gas (neon) was used to investigate the N -type process. N -type resonance demonstrates narrow-band increase in the absorption (i.e. a “bright” resonance) inside the probe laser radiation spectrum in the presence of a coupling laser. The N -type resonance in a magnetic field for ^{133}Cs atoms is shown to split into seven or eight components, depending on the magnetic field and laser radiation directions. Since important characteristics of N -type resonance are similar to those of EIT-resonance (because for both resonances the same ground levels of the Λ -system participate), one expects a similar large number of applications.

For the formation of high-contrast N -type resonance in a Λ -system (ground levels are $F_g=2, 3$), on the D_1 line of the Rb atoms, two continuous narrow-band diode lasers with $\lambda=795$ nm and a 8 mm- long cell filled with the Rb vapor and a buffer gas (20 Torr neon) are used.

We have suggested a new 4-level system based on an additional (3^{rd}) laser radiation (we call it “preparation” radiation). When the frequency ν_{PREP} is in resonance with $5S_{1/2}, F_g=2 \rightarrow 5P_{3/2}$ transitions (D_2 line, $\lambda=780$ nm) via optical pumping process (through $5P_{3/2}$ level) it transfers a large number of Rb atoms from $F_g=2$ to $F_g=3$ and creates the inversion condition with non-thermal atomic population distribution $N_3(F_g=3) > N_2(F_g=2)$. If the probe frequency starts from $F_g=3$, then the amplitude of the “bright” resonance will increase. Meanwhile when

frequency ν_{PREP} is in resonance with $5S_{1/2}, F_g=3 \rightarrow 5P_{3/2}$ transitions it transfers atoms from $F_g=3$ to $F_g=2$ and creates opposite non-thermal atomic population distribution $N_2(F_g=2) > N_3(F_g=3)$. In this case a Raman-type process is switched-on and the initially "bright" resonance is amplified and demonstrates increase in transmission (in the spectrum it looks like a "dark" resonance). Thus, it is possible to control the sign of the resonance.

References:

[1] M. Fleischhauer, A. Imamoglu, J.P. Marangos, "Electromagnetically induced transparency: Optics in Coherent Media", Rev. Modern Physics, Vol.77, pp.633-674 (2005).

[2] D. Slavov, A. Sargsyan, D. Sarkisyan, R. Mirzoyan, A. Krasteva, A. D. Wilson-Gordon, S. Cartaleva "Sub-natural-width N-type Resonance in Cesium Atomic Vapor: splitting in magnetic fields" Journal Phys. B: At. Mol. Opt. Phys. Vol.47, p. 035001(2014).

Acknowledgements: This work has received partial funding from the EU 7-th Framework Programme (FP7/2007-2013) Grant Agreement n° 295264-COSMA.

PB6

MECHANISMS OF NH-PHOTODISSOCIATION IN THE NUCLEOBASE ANALOGUE 2,4-DIAMINOPYRIMIDINE: EXPLORING CONICAL INTERSECTIONS

Pavlina Kancheva¹, Deniz Tuna², Wolfgang Domcke², Vassil B. Delchev¹

¹ Dept. Physical Chemistry, University of Plovdiv, Tzar Assen 24 Str., 4000-Plovdiv, Bulgaria

² Dept. of Chemistry, Technische Universität München, 85747 Garching, Germany
email: pkancheva@uni-plovdiv.net

We performed quantum chemical investigations of the NH-photodissociation reactions of 2,4-diaminopyrimidine at the CASSCF/cc-pVDZ level. Four conical intersections were located, they are accessible through the $^1\pi\sigma^*$ excited-state reaction paths of the compound. Each conical intersection mediates one particular NH-dissociation process and exhibits a planar geometry (see Fig. 1).

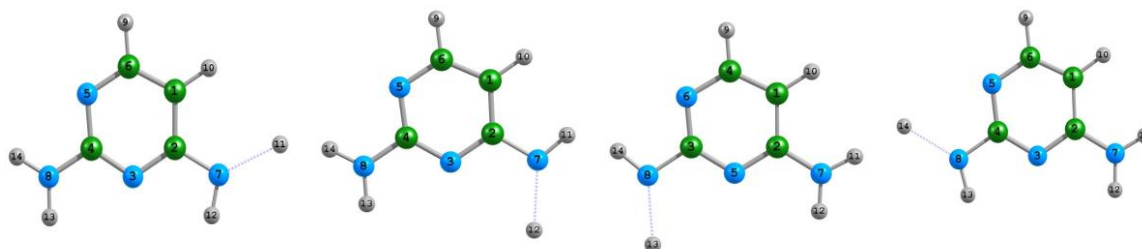


Figure 1. Planar conical intersections for the NH-photodissociation mechanisms of 2,4-diaminopyrimidine

Currently, we are exploring the accessibility of these structures through the repulsive $^1\pi\sigma^*$ excited state by connecting the Franck-Condon geometry of the compound with each conical intersection. These mechanisms constitute the so-called photo-induced dissociation-association (PIDA) mechanism, [1-3] which explains the photostability of biomolecules with respect to tautomerization reactions.

References:

- [1] A. L. Sobolewski, Chem. Phys. Lett., 211, 293, (1993).
[2] B. Chmura, M. Rode, A. Sobolewski, L. Lapinski, M. Nowak, J. Phys. Chem. A, 112, 13655, (2008).
[3] V. B. Delchev, A. L. Sobolewski, W. Domcke, Phys. Chem. Chem. Phys. 12, 5007, (2010).

PB7

INVESTIGATION OF THE INFLUENCE OF STRONTIUM CARBONATE ON FLUORESCENCE SPECTRA OF OXY-FLUORIDE GLASSES DOPED WITH SAMARIUM OXIDE AND SAMARIUM FLUORIDE

Teodora Pashova¹, Tinko Eftimov¹, Irena Kostova², Dancho Tonchev², Daniel Brabant³

¹*Faculty of Physics, Plovdiv University “Paisii Hilendarski”, 24 Tsar Assen Str., 4000 Plovdiv, Bulgaria*

²*Faculty of Chemistry, Plovdiv University “Paisii Hilendarski”, 24 Tsar Assen Str., 4000 Plovdiv, Bulgaria*

³*Photonics Research Center, Universite du Quebec en Outaouais, Gatineau, Quebec, Canada*

Prepared oxy-fluoride glasses contain strontium carbonate doped with samarium. The glasses are sorted with respect to the quantity of strontium carbonate. The fluorescence spectra recorded for different pumping wavelengths are presented. We have investigated the influence of the excitation on the efficiency of the fluorescence, depending on the quantity strontium carbonate in the samples and variety in wavelength of the excitation source. The results of optical pumping in range 370-490 nm show typical fluorescence spectrum of Sm³⁺. When pumped with wavelength above 500 nm a new peak that has not been investigated by us, is appeared in the fluorescence spectrum. From the data analysis, the range of appearance of the fluorescence peak was determined and the most effective source for its excitation was found.

PB8

OBSERVATION OF POLARIZATION DEPENDENT EFFECTS IN MULTILEVEL EIT LAMBDA SYSTEM IN COLD RB ATOMS

K. Kowalski¹, M. Głódź¹, J. Szonert¹, S. Gateva²

¹*Institute of Physics, Polish Academy of Sciences, 02-668 Warsaw, Poland*

²*Institute of Electronics, Bulgarian Academy of Sciences, 1784 Sofia, Bulgaria
e-mail: krkoyal@ifpan.edu.pl*

Coherent coupling of light with atomic samples enables to study the wealth of phenomena. One of them the electromagnetically induced transparency (EIT) causes the otherwise absorptive medium to become transparent. EIT is the quantum interference effect which in the simple approach relies on the mutual interaction between a three-level system and two laser fields. In experiment, however, the real multilevel magnetic structure of the medium and the polarization dependency of the light fields can significantly influence the observations.

In this contribution we investigate the generalized Λ -system based on the $5S_{1/2}(F=2)$, $5S_{1/2}(F=3)$, $5P_{3/2}(F'=4, 3, 2)$ levels of the cold ^{85}Rb atoms interacting with the polarized laser beams: the stronger one (coupling or the pump) and the weaker one (the probe). The sample is produced in the magneto-optical trap. Cold atom environment is used to overcome limitations of conventional systems. Dependence of the probe transmission on the polarizations and detunings of both the probe and pump beams is studied. Results and discussion will be presented.

PB9

ROBUST NARROWING OF DARK RESONANCES IN Rb VAPOR WITH COAXIAL COUNTER-PROPAGATING LASER BEAMS

I. Radojičić, M. Radonjić, Z. Grujić, M. Lekić, D. Lukić and B. M. Jelenković

*Institute of Physics, University of Belgrade, Pregrevica 118, 11080 Belgrade, Serbia
e-mail: milan.radonjic@ipb.ac.rs*

Counter propagating spatially separated hollow pump and coaxial probe laser beams generate narrow Zeeman electromagnetically induced transparency (EIT) resonances in vacuum Rb cell. The lasers were locked to $F_g=2 \rightarrow F_e=1$ transition of either D1 or D2 line of ^{87}Rb . This Ramsey type configuration yields dual-structured resonances having narrow peak on top of broader pedestal [1]. The pedestal becomes more prominent with increase of the probe beam intensity. Interestingly, we observed weak dependence of the narrow peak line-widths on the probe beam intensity and diameter provided dark region between the two beams is kept fixed [2]. Accompanying theoretical model showed good agreement with the measurements and enabled explanation of differences in line shapes for the two D-lines. We also found that very weak probe beam can be transmitted through the Rb cell only if the pump beam is present.

References:

- [1] Z. D. Grujić, M. Mijailović, D. Arsenović, A. Kovačević, M. Nikolić and B. M. Jelenković, “Dark Raman resonances due to Ramsey interference in vacuum vapor cells”, *Phys. Rev. A* 78, 063816, (2008).
- [2] I. S. Radojičić, M. Radonjić, Z. D. Grujić, M. M. Lekić, D. V. Lukić and B. M. Jelenković, In preparation

Acknowledgements: This work was supported by the Ministry of Education and Science of Serbia, under Grants No. III45016 and OI171038 and also by SCOPES JRP IZ73Z0_1

PB10

SENSITIVITY AND RESOLUTION OF DYNAMIC LASER SPECKLE METROLOGY

Elena Stoykova, Tanya Nikova

*Institute of Optical Materials and Technologies, Bulgarian Academy of Sciences,
Acad. Georgi Bonchev Str., Bl.109, 1113 Sofia, Bulgaria
e-mail: t_lubanova@yahoo.com*

Dynamic laser speckle metrology has established itself as a simple means for monitoring speed of processes within various objects by capture and statistical processing of 2D laser speckle patterns formed on their surface. The main reason why this method attracts a lot of research efforts is simplicity of its instrumental implementation which requires only a low-cost laser source and a 2D optical sensor. Processing of the acquired speckle patterns is much more complicated and relies on averaging in the spatial or/and temporal domains. This means that sensitivity and resolution both in space and time crucially depend on the number of data entries used to build an estimate of a given statistical parameter.

There are several tricky things about retrieval of information in dynamic laser speckle metrology that are primarily due to the speckle nature of the acquired raw data. The first one is the choice of the statistical parameter to characterize the speed of the undergoing processes. The goal of the measurement is to compare the values of this parameter at different points or at different moments so the absolute values are of minor importance. This gives some degree of freedom when building the parameter estimate. The strongly fluctuating intensity across the object surface that has variance increasing with the mean intensity is another peculiarity of this type of metrology. Another important issue is the dependence of the estimate variance on the value of the statistical parameter which means that the estimate should be further processed as if it is contaminated with a signal-dependent noise.

The aim of the present paper is to evaluate the impact of speckle nature of images acquired in dynamic laser speckle metrology from the point of view of the achieved sensitivity and resolution. To solve the task we processed both synthetic and experimental speckle patterns which were simulated or recorded for objects with varying activity across their surface. We sought for finding answers to the questions: i) evaluation of sensitivity and resolution of pointwise estimates at averaging in time; ii) evaluation of the same parameters for estimates calculated from two images by averaging within a spatial window. Figure 1 shows for example monitoring of paint drying on the surface of a coin. The captured speckle pattern reveals no structure of the surface beneath the paint. This structure becomes discernible after evaluating correlation at increasing time lag. The maps presented below correspond to a moment when the paint has almost evaporated from the embossed parts of the coin; this means that the activity due to evaporation on the embossments (dark regions) is lower in comparison to the activity observed on the flat surface of the coin and within the grooves.

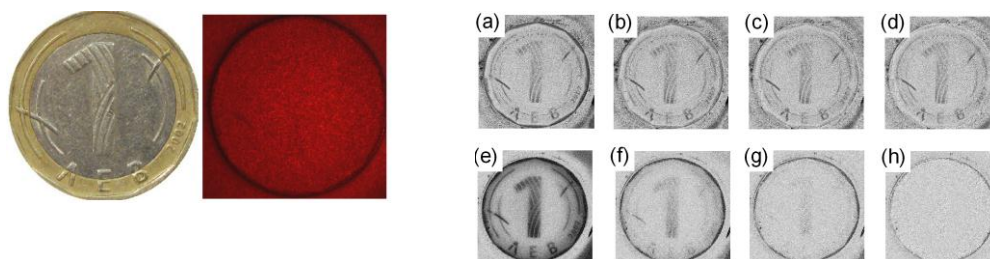


Figure 1. Coin of 1 lev used as a test object and a 2D recorded speckle pattern of the coin covered with a white paint at illumination with a HeNe laser. Gray scale activity maps at $t_1 = 0$ (top) and $t_2 = 75$ s (bottom); the maps are estimated at time lags 0.25 s (a,e), 1.25 s (b,f), 2.5 s (c,g), 5 s (d,h) between the compared speckle patterns. The scale is from 0 to 2.5.

PB11

STRUCTURE OF THE FLUORESCENCE MAGNETO-OPTICAL RESONANCE IN A PARAFFIN-COATED ^{87}Rb VACUUM CELL

E. Taskova, E. Alipieva and G. Todorov

*Academician Emil Djakov Institute of Electronics, Bulgarian Academy of Sciences,
72 Tzarigradsko Chaussee, 1784 Sofia, Bulgaria
e-mail: alipieva@ie.bas.bg*

In this work we investigate the magneto-optical resonance on ^{87}Rb D_1 line. In two-level degenerated system this resonance is due to the interference between the Zeeman sub-levels, created by interaction of resonance linear polarized laser beam with the atoms. The observed signal is detected by sweeping magnetic field \mathbf{B} around its zero value. This phenomenon is known as a Coherent Population Trapping (CPT) in Hanle configuration, too.

In a coated vacuum cell the fluorescence signal has a complex form, because the anti-relaxation coating preserves the created coherence. The ground state coherence is transmitted by the laser field to the upper level, thereby polarization moments with different rank contribute to the fluorescence. The manifestation of the different polarization moments in the observed signal depends on the geometry of the experiment – direction of observation, plane of the laser polarization, polarization of the registered light.

The experiment is performed on the D_1 ^{87}Rb line, $F=2 \rightarrow F=1$ transition in a paraffin-coated cell. The coherence in the two-level atomic system is created by a single frequency diode laser Thorlabs L785P090, polarized in a plane perpendicular to the scanned magnetic field \mathbf{B} .

The magneto-optical resonances, detected in two orthogonal polarizations are measured. The unpolarized fluorescence dependence on the scanned magnetic field, at the same experimental geometry, has been detected too. The resonances, obtained in the both cases, polarized and unpolarized fluorescence, are well described with a sum of two Lorentzian curves. The resonances with different polarization are compared and analyzed in order to clear the contribution of the polarization moments having different rank to the fluorescent signal.

A numerical experiment with parameters, close to the real one are performed by a program, based on the irreducible tensor operator formalism [1]. The results of the modelling are compared with the measured ones at different experimental conditions.

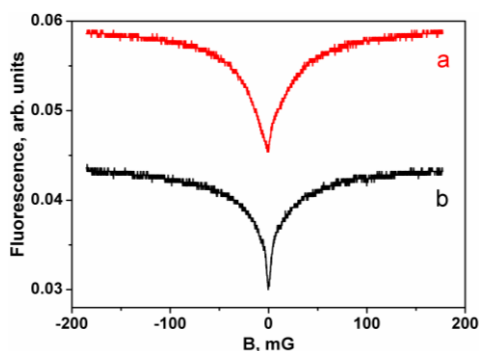


Figure 1. Fluorescence signal detected in two orthogonal polarizations a) $\mathbf{E}_{\text{obs}} \perp \mathbf{B}$ and b) $\mathbf{E}_{\text{obs}} \parallel \mathbf{B}$.

References:

[1] V. Polischuk, V. Domelunksen, E. Alipieva, G. Todorov, “Modelling of nonlinear interaction of ^{87}Rb atoms with polarized radiation”, *Bulg. J. Phys.* **39** 150-164, (2012).

Acknowledgements: This work has received partial funding from the EU 7-th Framework Programme (FP7/2007-2013) Grant Agreement n° 295264-COSMA.

PB12

SIMPLE METHOD FOR CHARACTERIZATION OF ANTI-RELAXATION COATING OF OPTICAL CELLS

K. Nasyrov¹, V. Entin², N. Nikolov³, N. Petrov³, S. Cartaleva³

¹*Institute of Automation and Electrometry SB RAS, Novosibirsk, Russia*

²*Rzhanov Institute of Semiconductor Physics SB RAS, Novosibirsk, Russia*

³*Institute of Electronics, BAS, boul. Tzarigradsko shosse 72, 1784 Sofia, Bulgaria*

e-mail: cartaleva@abv.bg

Optical cells with atomic spin preserving coatings are used in various basic experiments and photonic sensors. Recently many works are devoted to the development of different kinds of anti-relaxation coatings, which allow: (i) using higher cell temperatures and (ii) significant reduction of optical cell dimensions. For characterization of optical cells with different anti-relaxation coatings, an easy applicable methodology will be of great importance.

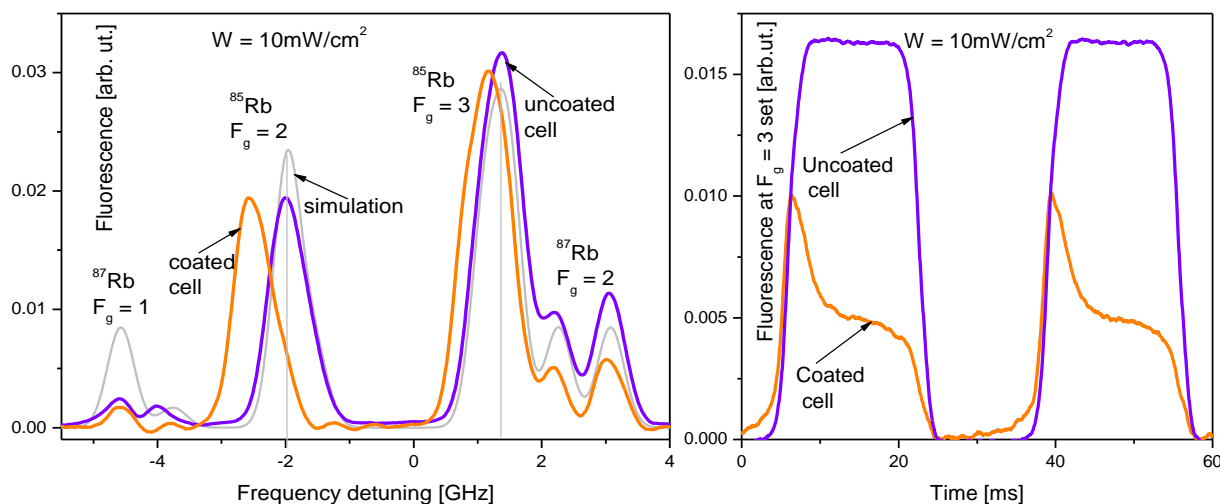


Fig.1 (left) Spectra of D₁ line of Rb: simulated one, experimental spectra of Rb atoms in uncoated and paraffin coated cells. (right) Time dependence of Rb atom fluorescence, induced by intensity modulated laser beam in uncoated and coated cells. In the first case where the optical pumping is negligible, no decay in the fluorescence is observed during the light irradiation, while in the coated cell the fluorescence strongly reduces with time.

We demonstrate a simple method allowing direct study of the dependence of fluorescence spectra on the quality of cell wall coating. The proposed approach is first demonstrated on the D₁ line of Rb. In uncoated cell, the spectrum of D₁ line follows the theoretical spectrum (Fig.1, left). However in the paraffin-coated cell, significant shifts of ⁸⁵Rb fluorescence lines are observed due to hyperfine optical pumping, greatly assisted by the spin preservation during atomic collision with the wall. The influence of optical pumping to the fluorescence signal measured in the orthogonal to the laser beam direction is significant (Fig.1, right). In the coated cell, it is shown that with irradiation of Rb vapor by intensity-modulated laser light, the fluorescence is reduced due to depleting of the excited by the light ground-state level. In order to determine the number of atomic collisions going with spin preservation, a new methodology is proposed, based on the fluorescence decay to steady state.

Acknowledgements: The work is supported by Marie Curie International Research Staff Exchange Scheme Fellowship (7th European Community Framework Programme). V.E. and K.N. thank RASc, and V.E. - RFBR (Grants: 13-02-00283, 14-02-00680), for partial support.

PB13

SUB-DOPPLER SPECTROSCOPY ON THE D₁ LINE OF POTASSIUM

S. Gozzini¹, A. Lucchesini¹, C. Marinelli^{1,2}, L. Marmugi^{1,2}, S. Gateva³, S. Tsvetkov³, S. Cartaleva³

¹*Istituto Nazionale di Ottica CNR – UOS Pisa, Via Moruzzi 1, 56124 Pisa*

²*Department of Physical, Geological and Environmental Sciences, University of Siena, via Roma 56, 53100 Siena, Italy*

³*Institute of Electronics, BAS, boul. Tzarigradsko shosse 72, 1784 Sofia, Bulgaria
e-mail: stefka-c@ie.bas.bg*

The resonance lines of alkali atoms are widely used in laser spectroscopy since sufficient atomic densities are easily achieved in thermal optical cells. They are important due to many applications in basic experiments, laser cooling and optical sensors. The spectrum of potassium is much less studied than those on Na, Rb, and Cs. Several features distinguish K from other alkali atoms. The hyperfine (hf) ground-state splitting is smaller than the Doppler width. As a result, the crossover(CO) resonances that involve both ground state levels, being negligible for Cs and Rb and suppressed for Na, are usually dominant for K.

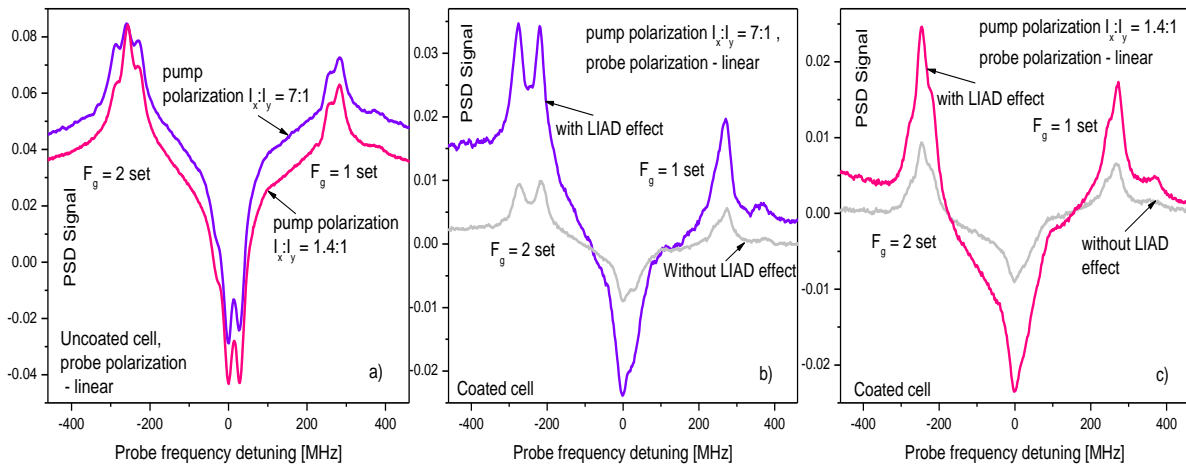


Figure 1. Sub-Doppler spectra of K obtained by counter propagating pump and probe beams with phase sensitive detection modulating the pump beam: (a) influence of the pump beam polarization in case of uncoated optical cell; (b) SA spectrum for linearly polarized pump in coated cell without/with desorbed by the LIAD effect K atoms; (c) strong influence of the pump beam polarization on the amplitude of the CO resonance observed within the $F_g = 2$ set of hf transitions. $F_g = 1$ and $F_g = 2$ are sets of hf transitions starting from the respective ground-state levels.

In this work we will present and discuss about new features observed in the Saturated absorption (SA) spectrum, on the D_1 line of K. In an uncoated optical cell containing pure K atoms, the using of circularly polarized pump beam results in some enhancement of the amplitude of CO resonance occurring within the SA group related to $F_g = 2$ set of hf transitions (Fig.1a). Much stronger this effect is present in the anti-relaxation (PDMS) coated cell. Here, the CO resonance in the $F_g = 2$ set is not observed experimentally with linearly polarized pump (Fig.1b), while in case of circular polarization its amplitude is overwhelming. The Light induced atomic desorption (LIAD) strongly improves the PSD signal.

Acknowledgements: This work was supported by Marie Curie International Research Staff Exchange Scheme Fellowship within the 7th European Community Framework Programm and by the Italian National Research Council and the Bulgarian Academy of Sciences (Bilateral Cooperation Program CNR/BAS 2013-2015).

PB14

LIGHT-INDUCED ATOMIC DESORPTION DYNAMICS IN CELLS WITH DIFFERENT PDMS COATINGS

S. Tsvetkov¹, M. Taslakov¹, E. Mariotti², S. Gateva¹

¹*Institute of Electronics, Bulgarian Academy of Sciences, 72 Tzarigradsko Chaussee, 1784 Sofia, Bulgaria*

²*Department of Physical, Geological and Environmental Sciences, University of Siena, via Roma 56, 53100 Siena, Italy
e-mail: sgateva@ie.bas.bg*

Light-induced atomic desorption (LIAD) is investigated a lot experimentally and theoretically and has different applications - vapor density stabilization, MOT loading, surface nanostructuring etc. [1,2 and references therein]. Many parameters influence LIAD, the developed models take into account various processes and there are still open questions. Reduction of the factors influencing LIAD will help for the better understanding of the process of LIAD and its dynamics.

In [3] a special LED system for homogeneous illumination was developed. Homogeneous illumination enables the investigation of LIAD without the process of lateral diffusion and prevents from cluster formation. The experimental investigation of the transmission spectra under blue light illumination in PDMS coated cells prepared with different concentrations of PDMS in ether has shown a dependence on the PDMS concentration [4]. As the PDMS concentration is raised, the thickness of the PDMS film and the surface roughness increase. The comparison of the measured LIAD rate and the adsorption rate in uncoated and paraffin coated cell has shown that in uncoated cell the rates are about three orders higher than in paraffin coated cell [1,3]. That's why it is of interest to compare the LIAD dynamics in cells with different PDMS coatings.

This paper presents an experimental investigation of the rates of the change of Rb atom density in PDMS coated cells prepared with two different concentrations of PDMS in ether at homogeneous illumination and the dependence of these rates on the illuminating blue-light power. A comparison is carried out with the LIAD effect in other coated and uncoated cells. All measurements were on the Rb D2 line in vacuum cells with similar dimensions and geometry.

The work is interesting not only for the better understanding of LIAD and its dynamics, but for the development of new optoelectronic elements, LIAD-loaded atomic devices and their miniaturization, and new methods for surface and coating diagnostics.

References:

- [1] T. Karaulanov *et al.*, “Controlling atomic vapor density in paraffin-coated cells using light-induced atomic desorption”, *Phys. Rev. A* **79**(1), art. no. 012902 (2009).
- [2] A. Bogi, A. Burchianti, C. de Mauro *et al.*, “Atomic sources controlled by light: Main features and applications”, *Proc. SPIE* **7747**, art. no. 77470D, (2011).
- [3] M. Taslakov, S. Tsvetkov, S. Gateva, “Light-induced atomic desorption under different types of illumination”, *J. Phys.: Conf. Ser.* **514** (1), art. no. 012028 (2014).

[4] S. Tsvetkov, S. Gateva, M. Taslakov, E. Mariotti, S. Cartaleva, “Light-induced atomic desorption in cells with different PDMS coatings”, J. Phys.: Conf. Ser. **514** (1), art. no. 012030 (2014).

Acknowledgements: This work is in the frame of the 7th FP of EC Grant Agreement 295264-COSMA and a Bilateral Cooperation Program CNR/BAS Project “Coherent Ramsey resonance in coated cells for application in optical magnetometry”.

PB15

PARAMETRIC NON-DEGENERATE FOUR WAVE MIXING IN HOT POTASSIUM VAPOR

B. Zlatković¹, A.J. Krmpot¹, N. Šibalić^{1,2}, B. M. Jelenković¹

¹ *Institute of Physics, University of Belgrade, Pregrevica 118, 11000 Belgrade, Serbia*

² *Faculty of Physics University of Belgrade, Studentski trg 12, 11000 Belgrade, Serbia*
e-mail: bojan@ipb.ac.rs

Parametric non-degenerate four wave mixing (4WM) is a nonlinear process in which two pump photons interact in medium with χ^3 nonlinearity producing photons with different frequencies. This process can be realized via double lambda scheme by stimulating a four-stage cyclical transition resulting in the emission of amplified probe and conjugate photons. Photons created by this process are time-correlated and produce relative intensity squeezed beams. Measuring and subtracting the corresponding beam intensities cancels the photon shot-noise [1], enabling measurements beyond the shot-noise limit. [2]

The aim of the experiment is to maximize the gain of the 4WM process since the degree of relative intensity squeezing depends on this gain. In our experiment double lambda scheme is realized at D1 line of potassium. We have investigated the influence of various parameters on the 4WM gain. These are temperature of the vapor cell, intensity of the pump beam, intensity of the probe beam, angle between pump and probe beam, one photon detuning, two photon detuning and the beam diameters of pump and probe beams.

Parameters for 4WM obtained from this measurement will be used further in experiment for relative intensity squeezing.

The laser source used in the experiment is single mode Ti:Sa laser with ring resonator (Coherent MBR 110) that delivers 500 mW used for both, pump and probe beams. The laser frequency is locked at approximately 1GHz blue detuned from the resonance $4S_{1/2} F_g=1 \rightarrow 4P_{1/2}$, using external reference cavity. The probe beam passes through two acoustooptic modulators that enables controllable detuning around 460 MHz (ground state hyperfine splitting) with respect to the pump beam. Such experimental setup enables double asymmetric lambda scheme where the longest “leg” is created conjugate beam that is intensity correlated with amplified probe beam. The potassium vapor cell used in the work is evacuated, without coating, and it is heated up to 180°C. The pump and probe beam intersect at very small angle (about 7mrad) in the cell, in order to fulfill phase-matching conditions.

The efficiency of 4WM process is studied by measuring conjugate beam power and probe beam amplification, simultaneously while varying relevant parameters. Parameters for maximum 4WM gain in hot potassium vapor are determined.

References:

[1] C. F. McCormick, V. Boyer, E. Arimondo, and P. D. Lett, *Optics Letters*, Vol. 32, Issue 2, pp. 178-180, (2007).

[2] R. C. Pooser, A. M. Marino, V. Boyer, K. M. Jones, and P. D. Lett, *Optics Express*, Vol. 17, Issue 19, pp. 16722-16730, (2009).

Acknowledgements: We are thankful for financial support by the Ministry of education and science of Republic of Serbia, under grants III45016 and OI171038, and SNF-Scopes Grant IZ 76Z0 147548/1.

PB16

MODELING OF THE NONLINEAR ABSORPTION OF CS ATOMS IN AN EXTREMELY THIN CELL - AN ITERATION APPROACH

G. Todorov¹, D. Slavov¹, A. Krasteva¹, S. Cartaleva¹, V. Polischuk², T. Vartanyan²

¹*Institute of Electronics, BAS, boul. Tzarigradsko shosse 72, 1784 Sofia, Bulgaria*

²*St.Petersburg University of Information Technologies, Mechanics and Optics, Kronverkskiy pr. 49, St.Petersburg 197101, Russian Federation*
e-maisl: stefka-c@ie.bas.bg, todorov.gt@gmail.com

The nonlinear polarization of atomic vapor confined in Extremely Thin Cells (ETC) is calculated for arbitrary total momentum of the resonance levels in the case of excitation with linearly polarized light. Using the density matrix equations of motion in the Irreducible Tensor Operator (ITO) representation [1, 2], analytical solutions are found for the statistical tensor components ξ_0^K describing the optical coherence with accuracy up to the third-order terms with respect to the laser field. Following the procedure developed in [3, 4], expressions for the polarization and light absorption are obtained for the case of running waves. In contrast with previous works, the characteristic decay constants for the population of the lower resonance levels γ_φ^K and the upper resonance levels γ_f^K as well as for the optical coherences γ_ξ^K are supposed to be different and can be varied. The later allows for phenomenological consideration of the influence of different relaxation processes in ETC. Model calculations and comparison with experimental data for the case of Cs vapor are performed.

References:

[1] M. I. Dyakonov, V. I. Perel, “On the theory of a gas laser in a magnetic field” *Optics and Spectroscopy*, Vol. 20, No. 3, p. 472-480, (Russ), (1966).

[2] B. Decomps, M. Dumont, M. Ducloy, “Linear and nonlinear phenomena in laser optical pumping”, *Laser Spectroscopy of Atoms and Molecules, Topics in Applied Physics*, Vol. 2, ISBN 978-3-540-07324-6, Springer-Verlag, p. 283-347, (1976).

[3] T. A. Vartanyan and D. I. Lin, “Enhanced selective reflection from a thin layer of a dilute gaseous medium” *Phys. Rev. A*, vol 51, No 3, p. 1959-1964, (1995).

[4] T. A. Vartanyan and D. I. Lin, “Nonlinear diffraction due to the transient polarization in a thin film of atomic gases”, *Eur. Phys. J. D*, p. 217-221, (1998).

Acknowledgements: This work was supported by a Marie Curie International Research Staff Exchange Scheme Fellowship within the 7th European Community Framework Programme.

OB1

PHOSPHORESCENCE OF BILIRUBIN

V. Yu. Plavskii, V. N. Knyukshto, A. I. Tretyakova, A. V. Mikulich, L. G. Plavskaya, I. A. Leusenko, B. M. Dzhagarov

*B. I. Stepanov Institute of Physics, National Academy of Sciences of Belarus, 68
Nezavisimosti Ave., Minsk, 220072, Belarus
e-mail: v.plavskii@ifanbel.bas-net.by*

Unsuccessful attempts to detect phosphorescence of bilirubin have lasted for over period 40 years (Cu, 1974, Bonnett, 1975; Matheson, 1975; Barber 1977; Dalton, 1979; Greene, 1981; Lamola, 1985, Plavskii, 2012). The problem is caused by a very low value of quantum yield to triplet state for bilirubin molecules ($\varphi_{isc} \sim 0.005-0.05$) as well as by intensive low-temperature fluorescence of the pigment, against of background of which to detect very weak phosphorescence was very problematic even when using the laser excitation.

Thereupon, we have decided to undertake studies of phosphorescence with using classic phosphoroscope enabling to cut off intensive fluorescence of nanosecond range. To increase the intensity of the excitation the continuous-wave semiconductor lasers with $\lambda = 405$ and 445 nm, output power ~ 100 mW were used. To exclude photolysis of bilirubin its irradiation was carried out only after samples cooling to the temperature of 77 K. Both laser sources and xenon lamp, the required spectral interval from its emission spectrum was isolated with a monochromator, were used for excitation of low-temperature fluorescence. 2-Methyltetrahydrofuran, Triton X-100, N,N-Dimethylformamide, Dimethyl sulfoxide, buffer solutions of HSA were used as solvents.

In this work we, for the first time, have detected the phosphorescence of bilirubin. It was detected at the temperature of 77 K and laser excitation against of background of intensive fluorescence (quantum yield in 2-Methyltetrahydrofuran is $\varphi_{fl} \sim 0.36$, $\tau = 2-3$ ns, $\lambda_{max} = 502$ nm) in all aforementioned solvents with exception of bilirubin-albumin complex. The first maxima in phosphorescence spectra are in the region of 762 nm (Dimethyl sulfoxide); 768 nm (2-Methyltetrahydrofuran), 772 nm (N,N-Dimethylformamide), 774 nm (Triton X-100).

Relevance of ascription of detected luminescence to phosphorescence of bilirubin (but not to luminescence of uncontrolled impurities) is confirmed by increase of its intensity when changing laser excitation with $\lambda = 405$ nm (corresponds to short-wave slope of absorption band of bilirubin) to $\lambda = 445$ nm (corresponds to the maximum of absorption band of the pigment). Furthermore, according to our data, the energy of the triplet state of bilirubin is $E_T \approx 155$ kJ/mole as it in good accordance with value $E_T \approx 150$ kJ/mole obtained from literature under control triplet-triplet transfer with the use of laser flash-photolysis method. It was found that quantum yield of phosphorescence of bilirubin in 2-Methyltetrahydrofuran is $\varphi_{ph} \sim 6.7 \cdot 10^{-6}$, $\tau \sim 100$ μ s. Freezing the solutions leads to reversible changes in the spectral characteristics of the pigment.

It is shown that, as the triplet (T_1) state of bilirubin is located above the S_1 -level of oxygen ($E_\Delta = 94.3$ kJ/mole), it is provided the possibility of bilirubin-sensitized generation of singlet oxygen. At the same time, taking into account that the energy of singlet-triplet splitting for pigment molecule $\Delta E = 82$ -89 kJ/mole is less than $E_\Delta = 94.3$ kJ/mole, it excludes possibility of sensitized formation of singlet oxygen from S_1 -level of bilirubin.

OB2

INVESTIGATION OF SURFACES OF DRYING EVAPORATING MICRODROPLET CONTAINING SILICA AND SDS ADMIXTURES

J. Archer^{*}, M. Kolwas, G. Derkachov, M. Woźniak, D. Jakubczyk and K. Kolwas

*Institute of Physics, Polish Academy of Sciences, Al. Lotników 32/46, 02-668 Poland
e-mail: archer@ifpan.edu.pl*

We analyze the intensities of the copolarized and cross-polarized scattered light from an evaporating single levitated glycol microdroplet containing 450 nm diameter SiO_2 nanoparticles and SDS (Sodium dodecyl sulfate) admixtures. In particular, we focus on the temporal changes of the interaction of elastically scattered light with the surface of an evaporating microdroplet of suspension undergoing nano-spherical aggregate formation. As the liquid evaporates, we observe successive stages of drying processes manifested in the light scattering properties [1]: from light scattering on clean liquid droplet surface (evidenced by whispering gallery modes) to a rapid increase of scattered light accompanied by light depolarization (speckles) on the spherical aggregate. The nanoparticles ordering process on the surface of the evaporating microdroplet can be described as a first-order phase transition like the analogous transition of the atoms or molecules from the gas phase to a liquid or the solid. We present the analysis of the surface phase transitions using the intensities of the copolarized and cross-polarized scattered light via surface pressure isotherms and the temporal evolution of the droplet radius.

Keywords: depolarization, microdroplet evaporation, electrodynamic trapping, and surface pressure isotherm.

Reference:

[1] G. Derkachov, K. Kolwas, D. Jakubczyk, M. Zientara and M. Kolwas, "Drying of a Microdroplet of Water Suspension of Nanoparticles: from Surface Aggregates to Microcrystal", *J Phys Chem C*; 112:16919–23, (2008).

C- LASER REMOTE SENSING AND ECOLOGY

PC1

ÅNGSTRÖM COEFFICIENTS CALCULATED FROM AEROSOL OPTICAL DEPTH DATA OBTAINED OVER SOFIA, BULGARIA

Tsvetina Evgenieva¹, Nikolay Kolev¹, Doyno Petkov²

¹*Institute of Electronics, Bulgarian Academy of Sciences, 72 Tsarigradsko Shosse Blvd., 1784 Sofia, Bulgaria,*

²*Space Research and Technology Institute, Bulgarian Academy of Sciences
e-mails: tsevgenieva@ie.bas.bg, blteam@ie.bas.bg*

The optical and physical properties of aerosols, such as aerosol optical depth (AOD), single scattering albedo, and aerosol size distribution are important parameters that control the aerosol radiative forcing at the surface and at the top of the atmosphere.

The Ångström wavelength exponent α is a commonly used parameter to illustrate the wavelength dependence of AOD and to obtain basic information on the aerosol size distribution. It is also an indicator of the average aerosol particle size in the atmosphere. Thus, $\alpha \leq 1$ indicates aerosol size distribution mainly dominated by coarse mode aerosols of effective radius usually greater than $0.5 \mu\text{m}$. These aerosols mainly originate from dust outflows or sea-spray. On the other hand, $\alpha \geq 1$ usually indicates a size distribution dominated by fine-mode aerosols of effective radius smaller than $0.5 \mu\text{m}$, usually associated with urban pollution and biomass burning. The Ångström turbidity coefficient β is related to the aerosol loading. A value of $\beta > 0.2$ usually indicates heavy pollution while $\beta > 0.4$ indicates extremely heavy pollution [1].

One year (October 2006 – October 2007) continuous measurements of the AOD during the development of planetary boundary layer (followed by lidar) were carried out by 5-channel hand-held sun photometer Microtops II over the city of Sofia, Bulgaria [2]. In order to investigate microphysical properties of aerosols, the Ångström coefficients α and β are calculated from the spectral AOD data using Volz method [3]. The Volz method is preferred from among the existing methods because of the small number of the Microtops II's channels. Daily behavior of Ångström exponent α and turbidity parameter β as well as their seasonal variations will be presented. The variations in the monthly mean α and β have similar behavior as AOD variations. The monthly mean AOD (at 500nm), α and β values are found to be highest in the months March ($\tau = 0.34$, $\alpha = 1.29$ and $\beta = 0.15$) and August ($\tau = 0.42$, $\alpha = 1.61$ and $\beta = 0.16$). The lowest monthly mean α value is found to be $\alpha = 1.07$ in April while the lowest monthly mean AOD and β values are found to be $\tau = 0.22$ (in January and February) and $\beta = 0.09$ (in January and October 2007). The above mentioned values show moderate turbidity of the atmosphere and dominance of fine-mode aerosols over Sofia.

References:

[1] K. Soni, S. Singh, T. Bano, R. S. Tanwar, S. Nath, “Wavelength dependence of the aerosol Angstrom exponent and its implications over Delhi, India”, *Aerosol Science and Technology*, 45, 12, 1488-1498, (2011).

[2] Ts. Evgenieva, N. Kolev, I. Iliev, Pl. Savov, B. Kaprielov, P.C.S. Devara, I. Kolev, “Lidar and spectroradiometer measurements of the atmospheric aerosol optical characteristics over urban area (Sofia, Bulgaria)”, *Int. J. Rem. Sens.*, 30, 24, 6381 – 6401, (2009).

[3] V. E. Cachorro, A. M. de Frutos, J. L. Casanova, “Determination of the Angstrom turbidity parameters”, *Appl. Opt.*, 26, 15, 3069– 3076, (1987).

Acknowledgements: The authors gratefully acknowledge the valuable discussion of the results and suggestions of Assoc. Prof. Ivan Kolev, PhD from Institute of Electronics, Bulgarian Academy of Sciences and Assoc. Prof. Ilko Iliev, PhD from Solar-Terrestrial Influences Laboratory, Bulgarian Academy of Sciences.

PC2

CEILOMETER OBSERVATION OF SAHARAN DUST OVER MOUNTAIN VALLEY OF SOFIA, BULGARIA

Nikolay Kolev^{1,3}, Tsvetina Evgenieva¹, Ivan Grigorov¹, Atanaska Deleva¹, Danko Ivanov², Ventsislav Danchovski², Plamen Savov³, Doyno Petkov⁴

¹*Institute of Electronics, Bulgarian Academy of Sciences, 72 Tsarigradsko Shosse Blvd., 1784 Sofia, Bulgaria,*

²*Department of Meteorology and Geophysics, Faculty of Physics, Sofia University “St. Kliment Ohridsky”, Sofia, Bulgaria*

³*Department of Physics, University of Mining and Geology “St. Ivan Rilski”, Sofia*

⁴*Space Research and Technology Institute, Bulgarian Academy of Sciences*

e-mail: blteam@ie.bas.bg

Atmospheric aerosol is known to considerably influence the Earth’s radiative budget and to make an impact on air quality. The influence of aerosols strongly depends on their spatial distribution and optical properties (such as aerosol optical depth).

The aerosol has natural and anthropogenic origin. Aerosol types can be also classified according to their size, sources or geographical origin (desert, continental, marine etc.). Mineral dust is one of the natural aerosols presented in the atmosphere. Its main source is the Sahara desert region. Saharan aerosol layers are frequently observed in Europe by means of active and passive remote sensing devices, especially in the frame of EARLINET and ACTRIS.

In this paper, observations of vertical distribution of aerosols and assessment of their optical properties will be presented. Two-year (2013-2014) complex measurements were carried out by a ceilometer CHM-15k (Jenoptik) and two lidars in an urban area located in a mountain valley (Sofia, Bulgaria) [1].

The ceilometer works 24 hours in automatic mode and has the following characteristics: light source - a microchip Nd:YAG laser with a central wavelength of 1064nm; measuring range 30-15000m; resolution 15m; measuring time 60s; pulse duration about 1ns; pulse repetition rate 5-7kHz; and energy per pulse 8μJ. Part of the results is compared with results obtained by lidars operating in analog and photon counting modes for specific periods of simultaneous work [2]. Supplementary data from: two meteorological stations; HYSPLIT back trajectory model; BSC-DREAM8b dust model; and the database of atmospheric radio sounding profiles

from Department of Atmospheric Engineering of Wyoming University (USA) are also used in the analysis of the obtained results.

References:

[1] Ts. Evgenieva, B. Wiman, N. Kolev, P. Savov, E. Donev, D. Ivanov, V. Danchovski, B. Kaprielov, V. Grigorieva, I. Iliev, I. Kolev, “Three-point observation in the troposphere over Sofia-Plana Mountain, Bulgaria”, *Int. J. Rem. Sens.*, 32, 24, 9343-9363, DOI:10.1080/01431161.2011.554456, (2011).

[2] D. Stoyanov, I. Grigorov, A. Deleva, N. Kolev, Z. Peshev, G. Kolarov, E. Donev, D. Ivanov, “Remote monitoring of aerosol layers over Sofia during Sahara dust transport episode (April, 2012)”, *Proceedings of SPIE Vol. 8770, Paper # 87700Y*, DOI 10.1117/12.2014154 (ISSN: 0277786X), (2013).

PC3

TWO-WAVELENGTH LIDAR CHARACTERIZATION OF OPTICAL, DYNAMICAL, AND MICROPHYSICAL PROPERTIES OF SAHARAN DUST LAYERS OVER SOFIA, BULGARIA

Zahary Y. Peshev, Tsvetina T. Evgenieva, Tanja N. Dreischuh, and Dimitar V. Stoyanov

*Institute of Electronics, Bulgarian Academy of Sciences,
72 Tsarigradsko Chaussee Blvd., 1784 Sofia, Bulgaria,
e-mail: zypeshev@ie.bas.bg*

Being a subject of intercontinental long-range transport, mineral aerosols resulting from strong dust storms in Sahara desert frequently invade the atmosphere over broad areas of Europe. The desert dust is one of the most important air pollutants, having direct and severe impact on the atmospheric thermal and radiative budget, climatic changes, air quality, human health, etc. The presence and transport of Saharan mineral dust in the atmosphere over the continent has been permanently monitoring by European lidar network during the last decade in the frame of the EC projects EARLINET, ASOS, and ACTRIS. In this work, we present results of two-wavelength lidar observations on Saharan dust layers over Sofia, Bulgaria, during strong dust intrusion events in the fall and winter of the year 2010. Measurements are carried out at a slope angle of 32° at two wavelengths (1064 nm and 532 nm) by using two channels of an aerosol lidar based on a frequency-doubled Nd:YAG laser. Optical, dynamical, and microphysical properties of the dust layers are studied and analyzed, distinguishing specifics of coarse and fine aerosol fractions. Time-averaged height profiles of the atmospheric backscattering coefficient at 1064 nm and 532 nm are presented, showing the dust and aerosol density distribution up to about 10 km AGL, with a range/height resolution of 15/8 m. Dust-loading forecast maps provided by the Barcelona Supercomputing Center (BSC-DREAM8b model), as well as backward trajectories by the NOAA HYSPLIT MODEL for air parcel transport, are presented in order to prove the presence and origin of the Saharan dust layers. Microphysical properties of dust and aerosol particles are characterized qualitatively by using backscatter-related Ångström exponents (BAE). Range-resolved time-averaged height profiles of BAE are shown, particularly for the dust layers, indicating the dominating particle size-modes. Obtained BAE values in the range 0.2-0.5 are typical for desert mineral dust, suggesting coarse particles in the over-micron size range. Frequency-

count analysis of the obtained BAE arrays is performed for typical separate dust-containing layers in the planetary boundary layer and above it, revealing distributions and changes of particle size modes in terms of BAE, as well as effects of dust mixing with finer urban and industrial aerosols present in the atmosphere over Sofia. Some efforts are devoted and focused on characterizing the temporal dynamics of the range distribution and density of dust and aerosols at different time scales, particularly on revealing their short-term dynamics. Multiple series of lidar returns are registered at an average time of 5 s. Obtained lidar data are further statistically processed and analyzed. Relative standard deviation of pre-processed laser-power normalized range-corrected lidar signals is used as a dynamics characterizing parameter. The observed spatial-temporal evolution of atmospheric aerosol/dust density fluctuations is shown on height-time coordinate color-map plots for each of the two wavelengths. Peculiarities of spatial distribution, size composition, and temporal evolution of Saharan dust aerosols are revealed, analyzed, and discussed as compared to results of others.

Acknowledgements: This work is supported by the FP7 Project "Aerosols, Clouds, and Trace gases Research Infrastructure Network" (ACTRIS), INFRA-2010-1.1.16.

PC4

CONSIDERATIONS ABOUT THE LOG-NORMALITY OF THE AEROSOL LIDAR SIGNAL FLUCTUATIONS

L. Gurdev, T. Dreischuh, Z. Peshev, D. Stoyanov

*Institute of Electronics, Bulgarian Academy of Science
72 Tzarigradsko shosse blvd., Sofia 1784, Bulgaria
e-mail: lugurdev@ie.bas.bg*

The knowledge of the statistics of the lidar signals, under different environment, is important for the right interpretation and estimation of the accuracy of the results from laser remote sensing of the atmosphere. It is of importance as well in the process of modeling the lidar signals. It is frequently assumed that the aerosol-lidar signal fluctuations or those of the optical depth of an atmospheric layer have log-normal statistics (e.g. [1,2]). Such an assumption is supported to some extent by some experimental and/or modeling-based results [3,4]. There is no however clear-cut physical and mathematical substantiation of this “log-normality hypothesis”.

The main purpose of the present work is to analyze physically the factors conditioning the formation and the fluctuations of the aerosol lidar signals, and to express mathematically the deductions derived from the analysis. The considerations performed are based on the assumption of incoherent aerosol scattering from aerosol particles occupying a scattering volume determined by the radius and the length of the sensing laser pulse-beam. Poisson and non-Poisson statistics of the number of scattering particles (of different sizes) is considered. The radii of the scattering volume and the aperture of the lidar receiving optical system and the distance between them are also taken into account as essential factors influencing the level of fluctuations.

As a whole, it is shown that the aerosol lidar signal fluctuations can indeed be considered as (nearly) log-normal under various environment conditions. The fluctuation level is expressed

ORAL AND POSTER SESSION

through the above-mentioned factors of importance, namely, the mean number and variance of the scattering particle number, the radius of the scattering volume, the radius of the aperture of the lidar receiving optical system, and the distance between them. Thus, the modeling of aerosol lidar signals and the interpretation of aerosol lidar data may be based on the assumption of log-normal statistics of the signal fluctuations whose level is derived on the basis of reasonable physical concepts and determined by the above-indicated geometrical parameters of concern.

References:

- [1] H. Gerber, “Probability distribution of aerosol backscatter in the lower marine atmosphere at CO₂ wavelengths”, *J. Geophysical Research: Atmospheres* 96(D3), 5307–5314 (1991).
- [2] F. Wagner and A. Silva, “Some Considerations about Angstrom Exponent Distributions”, *Atmospheric Chemistry and Physics* 8, 481-489, (2008).
- [3] N. T. O'Neill, A. Ignatov, B. N. Holben and T. F. Eck, “The lognormal distribution as a reference for reporting aerosol optical depth statistics; Empirical tests using multi-year, multi-site AERONET Sunphotometer data”, *Geophysical Res. Lett.* 27 (20), 3333–3336, (2000).
- [4] S.A Gyngazov, S.I. Kavkanyanov, and G.M. Krekov, *Izvestiya AN SSSR: Fizika Atmosfery i Okeana*, vol. 21(8), 841-848 (1985) (in Russian).

PC5

FINITE SYSTEM RESPONSE SHAPE DUE DISTORTIONS OF THE TEMPERATURE AND DENSITY PROFILES IN FUSION PLASMAS RECOVERED USING THOMSON SCATTERING LIDAR

L. Gurdev, T. Dreischuh, D. Stoyanov

*Institute of Electronics, Bulgarian Academy of Science
72 Tzarigradsko shosse blvd., Sofia 1784, Bulgaria
e-mail: lugurdev@ie.bas.bg*

The analytical consideration of the distortion effect of the system response function of a Thomson scattering (TS) lidar facility on recovered temperature and density profiles in fusion plasmas is of importance for a better understanding of the direct experimental results and the results obtained after applying distortion-reducing deconvolution procedures.

The performed analysis reveals interesting and useful features of the distortions of the measured lidar profile, and the corresponding temperature and density profiles, due to convolution of the response function with the maximum-resolved lidar profile obtainable at a delta-like system response. So, it is shown that in the case of a symmetric, say Gaussian pulse response, far from the pedestal area at the plasma edge, the convolution does not distort the information about the smooth-enough line-of-sight (LOS) distributions of the electron temperature and density. In the pedestal area such distortions exist. They concern mainly the steep density profiles and depend on the temperature profile steepness. In practice, the temperature profiles are slanting-enough around the pedestal, and the distortions may be negligible. In this case, the center-of-mass wavelength (CMW) [1] and the fitting [2]

approaches provide the undistorted temperature profile. At the same time, the latter approach provides a convolution of the density profile with the response function.

In the case of an asymmetric, say exponentially-shaped pulse response, distortions of the information about the density distribution exist along the whole LOS within the plasma torus. They depend on the variability of the electron temperature and density profiles and could be minimal at relatively high temperatures (above 5 – 10 keV), slanting-enough temperature profiles, and relatively near (the incident wavelength) spectral intervals. In the pedestal, the distortions may decrease additionally. Then, both above-mentioned approaches can be used to obtain the undistorted temperature and convolved density profiles. Under general conditions, deconvolution procedures are necessary for improving the accuracy and resolution of the recovered electron temperature and density profiles. The analytical conclusions deduced in the work are supported by numerical results.

References:

- [1] L. Gurdev, Dreischuh, D. Stoyanov, Proc. SPIE 7027, 702711 (2008).
- [2] T. Dreischuh, L. Gurdev, D. Stoyanov, Proc. SPIE 8770, 877012 (2013).

PC6

LIDAR DETECTION OF FOREST FIRE SMOKE ABOVE SOFIA

Ivan Grigorov, Atanaska Deleva, Dimitar Stoyanov, Nikolai Kolev and Georgi Kolarov

*Institute of Electronics – Bulgarian Academy of Sciences,
72 Tzarigradsko Shose Blvd., 1784-Sofia, Bulgaria
e-mail: ivangr@ie.bas.bg*

The distribution of aerosol load in the atmosphere due to three forest fires near Sofia (the capital city of Bulgaria) was studied using two aerosol lidars operated at 510.6 nm and 1064 nm. Experimental data is presented as 2D-heatmaps of the evolution of attenuated backscatter coefficient profiles and mean profile of the aerosol backscatter coefficient, calculated for each lidar observation. Backscatter related Angstrom exponent was used as a criterion in particle size estimation of detected smoke layers. Calculated minimal values at altitudes where the aerosol layer was observed corresponded to the predominant fraction of large aerosol particles. Dust-transport forecast maps¹ and calculations of backward trajectories² were employed to make conclusions about aerosol's origin. They confirmed the local transport of smoke aerosol over the city and lidar station. DREAM forecast maps predicted neither cloud cover, nor Saharan load in the air above Sofia on the days of measurements. The results of lidar observations are discussed in conjunction with meteorological situation, aiming to better explain the reason for the observed aerosol stratification. The data of regular radio sounding of the atmosphere shows a characteristic behavior with small difference between the air temperature and dew-point temperature profiles, together with a jump of the wind direction at aerosol smoke layer altitude. So the resulting stratification confirmed the existence of atmospheric layers with aerosol trapping properties.

ORAL AND POSTER SESSION

References:

[1] Basart, S., Pérez, C., Nickovic, S., Cuevas, E. & Baldasano, J.M. « Development and evaluation of the BSC-DREAM8b dust regional model over Northern Africa, the Mediterranean and the Middle East », *Tellus B*, 64, 1-23 (2012).

[2] Draxler, R.R. and Rolph, G.D., 2013. HYSPLIT (HYbrid Single-Particle Lagrangian Integrated Trajectory) Model access via NOAA ARL READY Website (<http://www.arl.noaa.gov/HYSPLIT.php>). NOAA Air Resources Laboratory, College Park, MD.

Acknowledgements: This work is supported by the project of FP7 “Aerosols, Clouds, and Trace gases Research Infrastructure Network” (ACTRIS), INFRA-2010-1.1.16. The authors gratefully acknowledge the NOAA Air Resources Laboratory (ARL) for the provision of the HYSPLIT model for air mass transport and dispersion and/or READY website used in this publication. The authors would like also to express their gratitude to the Earth Sciences Division, Barcelona Supercomputing Center, Spain, for the provision of the DREAM model aerosol dust data and to the Department of Atmospheric engineering of Wyoming University (USA), for the rich database of atmospheric radio sounding profiles, used in this publication.

PD1

IMPACT OF QUATERNIZATION OF PHTHALOCYANINES FOR ANTIMICROBIAL PHOTODYNAMIC THERAPY

Meliha Aliosman¹, Ivan Angelov¹, Vesselin Kussovski³, Vanya Mantareva^{1,*}

¹ *Institute of Organic Chemistry with Centre of Phytochemistry, Bulgarian Academy of Sciences, Acad. G. Bonchev, str., Bld. 9, 1113 Sofia, Bulgaria*

² *Institute of Electronics, Bulgarian Academy of Sciences, 72, Tsarigradsko chaussée Blvd, 1784 Sofia, Bulgaria*

³ *The Stephan Angeloff Institute of Microbiology, Bulgarian Academy of Sciences, Bl. 26, 1113 Sofia, Bulgaria*
e-mail: mantareva@yahoo.com

Photodynamic therapy (PDT) is well accepted as a treatment modality for different pathological conditions [1]. Presently the antibacterial PDT is under progress due to fast development of resistance of the human pathogens. The advantages of the new generation photosensitizers such as phthalocyanines are owned on the far red absorption (> 675 nm), long life-time of the triplet state and optimal quantum yield of singlet oxygen quantum yield [2]. The specific functionalization aims high solubility and cellular specificity for enhancement of the selectivity of the photodynamic action.

Cationic metal phthalocyanine (MPc) was synthesized with four peripheral pyridyloxy groups. The suitable quaternization led to water-solubility of the final MPc complex. The new phthalocyanine was characterized by the known spectral methods. The photophysical parameters of absorption and fluorescence were studied. The singlet oxygen generation in a model system and a suspension of cell cultures showed the capacity of the new phthalocyanine for photoinactivation of pathogenic microorganisms.

References:

- [1] M. Durmus, T. Nyokong, *Tetrahedron*, 63, 1385 – 1394, (2007).
[2] V. Mantareva, I. Angelov, D. Wohrle, E. Borisova, V. Kussovski, *Metallophthalocyanines for antimicrobial photodynamic therapy, J. Porphyrins and Phthalocyanines*, 17, 1-18, (2013).

Acknowledgements: This work was supported by Bulgarian Academy of Sciences.

PD2

ANTIBACTERIAL PHOTODISINFECTION BASED ON THE CONJUGATE Zn(II) PHTHALOCYANINE-METAL OXIDE UPON UV AND RED LIGHT EXPOSURE

Vanya Mantareva^{1,*}, Ivelina Eneva¹, Ekaterina Borisova², Ivan Angelov,¹ Vesselin Kussovski³

¹ Institute of Organic Chemistry with Centre of Phytochemistry, Bulgarian Academy of Sciences, Acad. G. Bonchev, str., Bld. 9, 1113 Sofia, Bulgaria

² Institute of Electronics, Bulgarian Academy of Sciences, 72, Tsarigradsko chaussée Blvd, 1784 Sofia, Bulgaria

³ The Stephan Angeloff Institute of Microbiology, Bulgarian Academy of Sciences, Bl. 26, 1113 Sofia, Bulgaria

e-mail: mantareva@yahoo.com

The light exposure on a daily basis has been well accepted as a competitive method for decontamination of wastewater. The great numbers of studies on the photocatalytic action of TiO₂ show the high efficacy in industrial water cleaning including the usefulness against the pathogenic microorganisms [1]. The photodisinfection method offers great potential to reduce the transmission of pathogens in the environment. Although the titanium dioxide shows high activity against pathogens, its general usage in waste water cleaning is limited due to the insufficient excitation natural light (about 3% of the solar spectrum). The specific dopants as metals and broad spectrum light active compositions have been explored for broadening of the irradiation spectrum and enhancement of photo activity [2].

A hydrophobic Zn(II)-phthalocyanine with four peripheral hydrocarbon chains (ZnPcDo) was immobilized on a photocatalyst TiO₂ anatase (P25) and on a ZnO powder. The resulted greenish colored nanoparticles of phthalocyanine adsorbed on metal oxides were characterized by absorption, fluorescence and infrared spectroscopy. The laser scanning confocal fluorescence microscopy was used to visualize the immobilized phthalocyanine by the red fluorescence emission (650 – 740 nm). The intensive Q-band in the far red visible spectral region (~ 680 nm) suggested a monomeric state of phthalocyanine on TiO₂. Two pathogenic bacterial strains associated with wastewater were photoinactivated with the suspensions of the solids. Both species (*methicillin-resistant Staphylococcus aureus* - MRSA and *Salmonella enteritidis*) were effectively photoinactivated with the suspension of TiO₂ anatase nanoparticles (1 g.L⁻¹) and irradiation with UVA 346 nm as well as with two light sources (UVA 346 nm and LED 643 nm). However Zn(II) phthalocyanine adsorbed on TiO₂ is less effective than TiO₂ alone at UVA irradiation. The composite materials of ZnPcDo on TiO₂ and ZnO showed a moderate effect than photocatalyst alone. The gram-negative *Salmonella enteritidis* was fully inactivated with ZnPcDo-TiO₂ and TiO₂ alone at UVA 346 nm and the two light sources (346 nm + 643 nm). The proposed conjugates of phthalocyanine immobilized on metal oxides appear as a useful photoactive composite for antibacterial disinfection of wastewater at irradiation with wide spectral range.

References:

[1] M. N. Cheng, B. Jin, C.W.K. Chow, C. Saint, C., “Recent developments in photocatalytic water treatment technology: a review”, *Wat. Res.* 44(10), 2997-3027, (2010).

[2] H. A. Foster, I. B. Ditta, S. Varghese, A. Steele, “Photocatalytic disinfection using titanium dioxide: spectrum and mechanism of antimicrobial activity”, *Appl. Microbiol. Biotechnol.* 90, 1847-1868, (2011).

ORAL AND POSTER SESSION

Acknowledgements: The work was supported by Bulgarian Academy of Sciences.

PD3

**EXCITATION-EMISSION MATRICES (EEMS) AND SYNCHRONOUS
FLUORESCENCE SPECTROSCOPY (SFS) INVESTIGATIONS OF
GASTROINTESTINAL TISSUES**

Ts. Genova¹, E. Borisova¹, Al. Zhelyazkova¹, O. Semyachkina-Glushkovskaya²,
M. Keremedchiev³, B. Vladimirov³, L. Avramov¹

¹*Institute of Electronics, Bulgarian Academy of Sciences, 72, Tsarigradsko Chaussee Blvd., 1784
Sofia, Bulgaria*

²*Biology Dept., Saratov State University, Physiology of Human and Animals lab., 83
Astrakhanskaya str., Saratov, Russia*

³*Queen Jiovanna-ISUL University Hospital, 8, Bialo More str., 1527 Sofia, Bulgaria
e-mail: ts.genova@gmail.com*

In this report we will present our recent investigations of the fluorescence properties of lower part gastrointestinal tissues using excitation-emission matrix and synchronous fluorescence spectroscopy measurement modalities. The spectral peculiarities observed will be discussed and the endogenous sources of the fluorescence signal will be addressed.

For these fluorescence spectroscopy measurements the FluoroLog 3 system (HORIBA Jobin Yvon, France) was used. It consists of Xe lamp (300 W, 200-850 nm), double monochromators, and PMT detector with a work region at 220-850 nm. Autofluorescence signals were detected in the form of excitation-emission matrices for the samples of normal mucosa, dysphasia and colon carcinoma and specific spectral features for each tissue were found.

Autofluorescence signals from the same samples are observed through synchronous fluorescence spectroscopy, which is a novel promising modality for fluorescence spectroscopy measurements of bio-samples. It is one of the most powerful techniques for multicomponent analysis, because of its sensitivity. In the SFS regime, the fluorescence signal is recorded while both excitation λ_{exc} and emission wavelengths λ_{emm} are simultaneously scanned. A constant wavelength interval is maintained between the λ_{exc} and λ_{emm} wavelengths throughout the spectrum. The resulted fluorescence spectrum shows narrower peak widths, in comparison with EEMs, which are easier for identification and minimizes the chance for false determinations or pretermission of specific spectral feature. This modality is also faster, than EEMs, a much smaller number of data points are required [1].

In our measurements we use constant wavelength interval $\Delta\lambda$ in the region of 10-100 nm. Measurements are carried out in the terms of finding $\Delta\lambda$, which resulting a spectrum with most specific spectral features for comparison with spectral characteristics observed in EEM.

Implementing synchronous fluorescence spectroscopy in optical methods for analyzing biological tissues could result in a better differentiation between normal and dysplastic tissue. Thus could improve fluorescence imaging like diagnostic modality among optical techniques applied in clinical practice.

References:

[1] Quan Liu, Kui Chen, Matthew Martin, Alan Wintenberg, Roberto Lenarduzzi, Masoud Panjehpour, Bergein F. Overholt, and Tuan Vo-Dinh, “Development of a

ORAL AND POSTER SESSION

synchronous fluorescence imaging system and data analysis methods”, *Optics Express*, Vol. 15, No. 20, (2007).

Acknowledgements: This work is supported in part by the National Science Fund of Bulgarian Ministry of Education, Youth and Science under grant #DMU-03-46/2011 and in part by the Ministry of Education and Science of Russian Federation under Grant № 17.488.2014/K.

PD4

LASER CLEANING OF PAPER SAMPLES COLONIZED WITH FUNGI SPORES

Evangelini Zekou¹, Elias Chatzitheodoridis², Alexander A. Serafetinides¹

¹*Physics Department, School of Applied Mathematical and Physical Sciences, National Technical University of Athens, Zografou Campus, Athens, 15780 Greece*

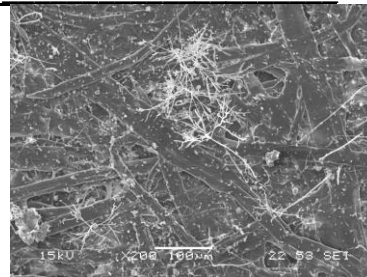
²*School of Mining and Metallurgical Engineering, National Technical University of Athens, Zografou Campus, Athens, 15780 Greece*
e-mail: aseraf@central.ntua.gr

Moving forward in the century of e-books, historical books became significant cultural heritage treasures, and their preservation an important issue for the conservators. However, the conventional methods for cleaning paper and manuscripts still require being improved and upgraded, by the use of modern technologies, such as lasers and analytical methods for diagnosis. Lasers provide controlled energy, thus being an accurate tool for scientists, while several diagnostic techniques are available for visualizing and analyzing the resulting treatment in microscale.

Lasers were utilized for cleaning paper documents in the past decades. The green light of 532 nm from Nd:YAG-2 ω was applied at fungi stains [1]. Initially, *Alternaria solani* and *Penicillium notatum* were removed, and in both of these cases no damage to the paper fibers was observed. The stains associated with *Chaetomium globosum* and *Fusarium oxysporum* appeared to be unaffected by the laser treatment. Laser cleaning investigations on artificially soiled paper samples were performed using 532nm Nd:YAG-2 ω laser and 10.6 μ m CO₂ laser by our group [2]. Following this work, we recently proceeded to the application of Nd:YAG lasers for the cleaning and diagnosis of biological stains from cultural heritage books from the Historical Library of NTUA [3]. A SEM image of paper cellulose fibres contaminated with fungi hyphae and spores is shown in Figure 1.

The current work broadens out this study and focuses on the use of Nd:YAG laser light onto paper samples with *Ulocladium chartarum*. The available wavelengths are 1064 nm, 532 nm, 355 nm, 266 nm and 213 nm, at various fluences and number of pulses. Several samples are prepared with fungi colonies grown on paper substrates, as well as on paper ink texts. Cleaning follows using laser irradiation. The paper samples are characterized, with Optical Microscopy and SEM/EDX analyses, before and after cleaning.

Figure 1: SEM image of fungi stains on a book from the Historical Library of NTUA.



References:

- [1] H. M. Szczepanowska and W. R. Moomow, “Laser Stain Removal of fungus-induced stains from paper”, JAIC, Vol. 33, p.25-p.32, (1994).
- [2] E. Zekou, D. G. Kotsifaki, and A. A. Serafetinides, “Paper surface modification by lasers”, Proc. of SPIE, Vol. 7747, p.774705-1-7, Nessesbar (2010).
- [3] N. Antonopoulou-Athera, E. Chatzitheodoridis, Z. Christodoulopoulos, Ch. Evangelatos, A. A. Serafetinides, E. Zekou, “Use of lasers for cleaning of paper documents and coins”, Proc. Athens Congress, Vol.6, Athens, (2010).

PD5

LASER INDUCED AUTOFLUORESCENCE FOR DIAGNOSIS OF NON-MELANOMA SKIN CANCER

E. Drakaki¹, M. Makropoulou¹, A. A. Serafetinides^{1*}, N. Merlemis² I. Kalatzis²
I.A. Sianoudis², O. Batsi³, E. Christofidou³, A. J. Stratigos³, A. D. Katsambas³, Ch. Antoniou³

¹Physics Department, National Technical University of Athens, Athens, 15780 Greece.

²Technological Educational Institute (TEI) of Athens, Agiou Spiridonos & Dimitsanas str.,
Egaleo, 12210, Greece.

³University of Athens, Department of Dermatology, Hospital A. Syggros
5 Dragoumi Street, Athens 16121, Greece.

e-mail: aseraf@central.ntua.gr

Non melanoma skin cancer is one of the most frequent malignant tumors among humans. A non-invasive technique, with high sensitivity and high specificity, would be the most suitable method for basal cell carcinoma (BCC) or other malignancies diagnostics, instead of the well established biopsy and histopathology examination. In the last decades, a non-invasive, spectroscopic diagnostic method was introduced, the laser induced fluorescence (LIF), which could generate an image contrast between different states of skin tissue. The noninvasiveness consists in that this biophotonic method do not require tissue sample excision, what is necessary in histopathology characterization and biochemical analysis of the skin tissue samples, which is worldwide used as an evaluation gold standard.

The object of this study is to establish the possibilities of a relatively portable system for laser induced skin autofluorescence to differentiate malignant from nonmalignant skin lesions. Unstained human skin samples, excised from humans undergoing biopsy examination, were irradiated with a Nd:YAG-3 ω laser ($\lambda=355$ nm, 6 ns), used as an excitation source for the autofluorescence measurements. A portable fiber-based spectrometer was used to record fluorescence spectra of the sites of interest. To minimize background signal during

ORAL AND POSTER SESSION

fluorescence spectra acquisition, the spectrometer gating was synchronized with the arrival of the fluorescence signal.

The *ex vivo* results, obtained with this spectroscopic technique, were correlated with the histopathology results. After the analysis of the fluorescence spectra of almost 120 skin tissue areas, we developed an algorithm, in order to distinguish different types of malignant lesions, including inflammatory areas. Optimization of the data analysis and potential use of LIF spectroscopy with 355 nm Nd:YAG laser excitation of tissue autofluorescence for clinical applications are discussed.

References:

[1] E. Drakaki, T. Vergou, C. Dessinioti, A.J. Stratigos, C. Salavastru, C. Antoniou, “Spectroscopic methods for the photodiagnosis of nonmelanoma skin cancer” *J Biomed Opt.* 1, 18(6), 61221, (2013).

[2] E. Drakaki, E. Kaselouris, M. Makropoulou, A.A. Serafetinides, A. Tsenga, A.J. Stratigos, A.D. Katsambas, Ch. Antoniou “Laser induced fluorescence and reflectance spectroscopy for the discrimination of basal cell carcinoma from the surrounding normal skin tissue”, *Skin Pharmacol. Physiol.*, 22, 3, 158-165, (2009).

Acknowledgements: This research effort is financially supported by the Project “Grants for research “ARCHIMEDES III”, grant No 021215, Code MIS: 379389, “FluDiaPhoSkin Therapy” funded by the Technological Education Institute (TEI) of Athens.

PD6

LASER CLEANING TREATMENT OF BURNT PAINTINGS

N. Antonopoulou-Athera¹, E. Chatzitheodoridis¹, M. Doulgerides², Ch. Evangelatos³, A. A. Serafetinides³

¹*School of Mining and Metallurgical Engineering, National Technical University of Athens, Heroon Polytechniou 9, Athens, 15780 Greece*

²*National Gallery of Athens, Alsos Stratou, Goudi, Athens, 11525 Greece*

³*Physics Department, National Technical University of Athens, Heroon Polytechniou 9, Athens, 15780 Greece*
e-mail: aseraf@central.ntua.gr

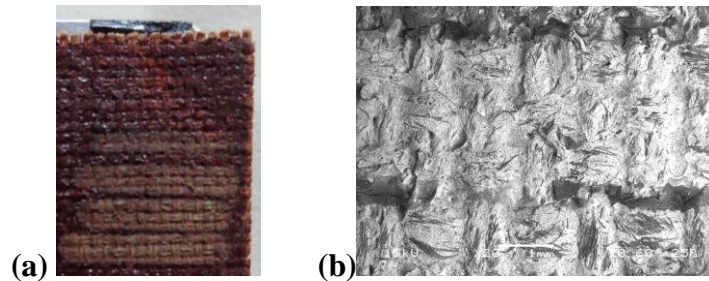
The restoration process of paintings is very difficult due to their complex composition. Lasers are already extensively used as a very promising cleaning method [1,2]. However, special cases still require more investigation in order to achieve optimum results.

In this study, three samples of a painting that belongs to the collection of the National Gallery of Athens and was made by the great Greek artist Konstantinos Parthenis (1878-1967), are investigated for cleaning with lasers. This painting requires a complex cleaning process because it has been partly burnt. The optimum fluence-wavelength values are investigated to achieve an acceptable restoration result. Six different wavelengths with a set of fluences were used, *i.e.*, the five harmonics of a Nd:YAG laser (1064nm, 532nm, 355nm, 266nm, 213nm), a free running 10.6 μ m CO₂ laser and a free running 2.94 μ m Er:YAG laser. Characterisation was performed prior and after the cleaning process by optical and electron microscopy and analysis (SEM/BSE EDX).

ORAL AND POSTER SESSION

The results of this work indicate that the wavelength in the visible spectrum (532nm) with fluences between 0.2J/cm² - 0.4J/cm² show the optimum cleaning (Figure 1). The optical microscopy results show that with these laser parameters the burnt layer was preferentially removed, exposing to the surface the original colors that Parthenis had used in this painting. Electron microscopy imaging and chemical analysis revealed that the original texture and materials of these samples are preserved after irradiation. Since the damage varies along the surface of the painting, more experiments should be performed in order to find and optimize the full cleaning and characterization process for the homogeneous cleaning of the whole surface of the painting.

Figure 1. Result of the cleaning process with fluence of 0.296J/cm² as viewed under (a) the optical microscope, and (b) with the SEM.



References:

- [1] R. Bordalo, P. J. Morais, H. Gouveia, Ch. Young, “Laser Cleaning of Easel Paintings: An Overview”, Laser Chemistry, Vol. 2006, 90279, 9 pages, (2006).
- [2] R. Teule, H. Scholten, O. F. van den Brink, R.M.A. Heeren, V. Zafirooulos, R. Hesterman, M. Castillejo, M. Martín, U. Ullenius, I. Larsson, “Controlled UV laser cleaning of painted artworks: a systematic effect study on egg tempera paint samples”, Journal of Cultural Heritage, 4, 209-215, (2003).

Acknowledgements: The samples for this study were provided by the National Gallery of Athens, specifically they came from the collection with burnt paintings of Konstantinos Parthenis.

PD7

DEVELOPING A TIMING CONTROL SYSTEM FOR LASER INDUCED FLUORESCENCE (LIF) IN MEDICAL APPLICATIONS

Ioannis Karachalios¹, Dimitrios Mathes¹, Ioannis Valais¹, Georgios Mitsou²
and Ioannis Sianoudis^{3*}

¹Department of Biomedical Engineering,

²Department of Energy Technology Engineering,

³Department of Optics & Optometry,

Technological Educational Institute (T.E.I.) of Athens, 122 10 Athens, Greece,

e-mails: ivalais@teiath.gr, jansian@teiath.gr

Laser Induced Fluorescence (LIF) as a spectroscopic method is successfully used as optical complementary techniques in medicine, in order to characterize chemical, physical and optical properties in skin tissue and to investigate changes for diagnostic purposes. It is a diagnostic tool for making temporally and spatially resolved measurements. The present study relates to the development of a timing control system adapted on a pulsed Nd:YAG laser and an optical spectrometer setup, used for fluorescence measurement applications. By controlling the

ORAL AND POSTER SESSION

timing between the laser output pulse sequence and the reading of the induced fluorescence pulse, material quality, structure and morphology information can be acquired. The timing control circuitry is based on a microcontroller of RISC technology, programmed to accurately trigger a sequence of emissions and readouts between the pulsed laser and the spectrometer.

Fluorescence measurements of UV-laser excited phosphor screens prepared in our laboratory for X-ray detection and imaging, were performed and the fluorescence spectral response was acquired. The described timing controller offers a low-cost and versatile tool for application of LIF spectroscopy in studying biological samples with fluorescent properties.

References:

[1] C. M. Michail, G. P. Fountos, S. L. David, I. G. Valais, A. E. Toutountzis, N. E. Kalyvas, I. S. Kandarakis, G. S. Panayiotakis, "A comparative investigation of Lu₂SiO₅:Ce and Gd₂O₂S:Eu powder scintillators for use in x-ray mammography detectors", *Meas. Sci. Technol.*, 20, 104008, (2009).

[2] E Drakaki, M Makropoulou, A Serafetinides, E Borisova, L Avramov, JA Sianoudis, "Optical spectroscopic studies of animal skin used in modelling of human cutaneous tissue", *Proc. SPIE Vol. 6604, 66042K.1-66042K*, (2007).

Acknowledgements: This research effort is financially supported by the Project "Grants for research "ARCHIMEDES III", grant No 021215, Code MIS: 379389, "FluDiaPhoSkin Therapy" funded by the Technological Education Institute (TEI) of Athens.

PD8

CHARACTERIZATION OF NEW DRUG DELIVERY NANOSYSTEMS BY USING ATOMIC FORCE MICROSCOPY

Ellas Spyratou¹, Elena A. Mourelatou², Costas Demetzos², Mersini Makropoulou¹, Alexander A. Serafetinides¹

¹*National Technical University of Athens, School of Applied Mathematical and Physical Sciences, Department of Physics, Zografou Campus, Athens, 15780 Greece*

²*University of Athens, School of Pharmacy, Department of Pharmaceutical Technology, Panepistimiopolis Zografou, 15771 Greece*
email: mmakro@central.ntua.gr

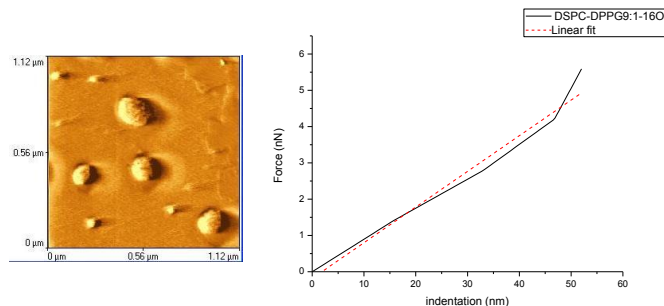
In the field of nanomedicine, a lot of research is focused on the improvement of drug carrier's biopharmaceutical properties including pharmaco-kinetics, pharmaco-dynamics, bioavailability and protein binding behaviour. New classes of drug carriers have emerged derived from the combination of different kinds of biomaterials. Chimeric advanced drug delivery nanosystems (chi-aDDnSs) are mixed nanosystems combining different biomaterials that can offer advantages as drug carriers. Among materials used, the mix of lipidic and polymeric has attracted much attention. A relatively young class of dendritic polymers, named hyperbranched polymers (HBPs), has lately drawn the most attention. HBPs are characterized by a high degree of branching, a three-dimensional architecture, and multiple terminal functional units.

Atomic force Microscopy appears as an essential tool for Chi-aDDnSs characterization. It can provide simultaneously information about size distribution and to probe the biomechanical characteristics of DDnSs by force-spectroscopy application. The biomechanical behaviour of

ORAL AND POSTER SESSION

DDnSs is an important predictor of circulation efficiency through capillaries and the entry into the cell. In our work, polyol hyperbranched polymers (HBPs) have been employed along with liposomes for the preparation of new chi-aDDnSs. Aliphatic polyester HBPs with three different pseudo-generations G2, G3 and G4 with 16, 32, and 64 peripheral hydroxyl groups, respectively, have been incorporated in liposomal formulation. AFM was used for the comparative study of the morphology and the biomechanical properties of Chi-aDDnSs and conventional DDnSs. It was examined the effect of HBPs architecture and the pseudogeneration number in the stability of the chi-aDDnSs. From the force-distance curves of AFM spectroscopy, the Young's modulus was calculated.

Figure 1. (a) AFM image and (b) Force curve analysis of the loading force versus the indentation for DSPC/DPPG/PFH-16OH liposome. From the linear fitting of the curve, Young's modulus was calculated.



References:

- [1] K. N. Kontogiannopoulos, A.N. Assimopoulou, S. Hatziantoniou, K. Karatasos, C. Demetzos, V.P. Papageorgiou, “Chimeric advanced drug delivery nano systems (chi-aDDnSs) for shikonin combining dendritic and liposomal technology”, *Int. J. Pharm.* 422, 381-9, (2012).
- [2] X. Liang, G. Mao and K.Y. Simon Ng, “Mechanical properties and stability measurement of cholesterol-containing liposome on mica by atomic force microscopy” *J. Colloid Interf. Sci.* 278, 53-62, (2004).

PD9

DENTAL COMPOSITE POLYMERIZATION PROCESS: DIGITAL HOLOGRAPHIC INTERFEROMETRY METHOD

D. Ž. Grujić¹, D. V. Pantelić¹, D. M. Vasiljević¹

¹*Photonics Center, Institute of Physics, University of Belgrade, Pregrevica 118, Belgrade, Serbia*
e-mail: dusang@ipb.ac.rs

A biomechanical tooth model with mesio-occluso-distal (MOD) cavity was used to study the polymerization process. We describe a digital holographic interferometry (DHI) technique which was used to obtain an information about shrinkage of dental composite and corresponding deformation on the walls of MOD cavity during polymerization. Experimental results were later compared with finite element method (FEM) calculations.

The model was placed in front of the spherical mirror at a distance of two focal lengths. A single laser beam (532 nm) was used so as to simultaneously illuminate both sides of the subject, while the remainder of the beam was focused in the mirror and served as a reference beam. Therefore, both sides of the subject were observed at the same time [2]. The holographic image was recorded directly on the CCD of a standard SLR: a very high resolution (4752 x 3168 pixels) camera - Canon EOS 50D, without using the objective. Registered holograms were processed calculating the Fresnel transform on the computer with

ORAL AND POSTER SESSION

nVidia (CUDA enabled) card which enables parallel processing. As a result, the processing time of the hologram (size of 2048 x 2048 pixels) is about 5 seconds.

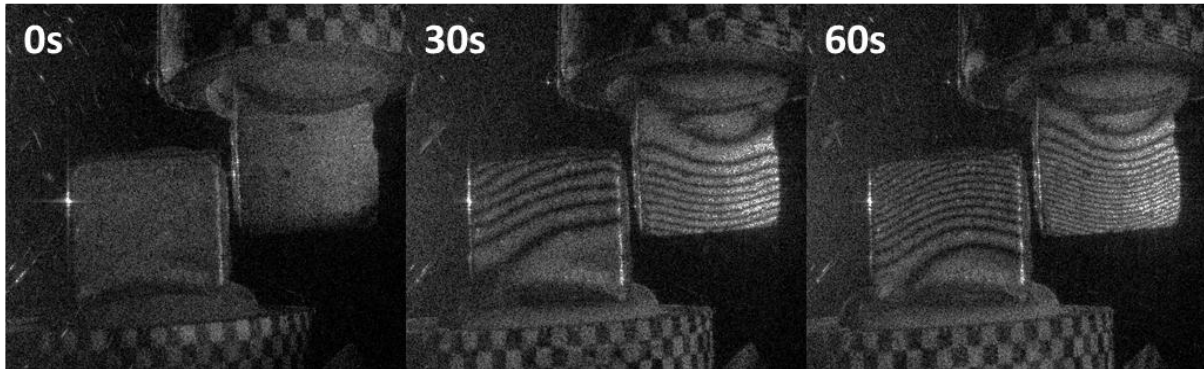


Figure 1. Sequence of holographic interferograms. The model is on the left, its image in a spherical mirror is on the right.

When MOD cavity was filled with dental restoration, the process of polymerization was initiated using the blue lamp; during the polymerization one hologram per second was recorded. The process was finished after approx. 2 minutes. Interferograms were created by comparing the initial with the current state (e. g. an insight into the deformation in twentieth second was gained through comparison of hologram recorded in the twentieth second with hologram recorded in the first second), thus allowing for the dynamic monitoring of the entire process.

References:

[1] G. Undt, K. Wild, G. Reuther, R. Ewers, “MRI-based stereolithographic models of the temporomandibular joint: technical innovation”, *J. Cranio-Maxillofacial Surg.*, Vol. 28, 258–263, (2000).

[2] Pantelić D, Blažić L, Savić-Šević S, Panić B, “Holographic detection of a tooth structure deformation after dental filling polymerization”, *J. Biomed. Opt.*, Vol. 12, 024026–024027, (2007).

Acknowledgements: This research was funded by the Serbian Ministry of Education and Science under contract numbers III 45016 and OI 171038.

PD10

TOTAL ATTENUATION COEFFICIENT OF INTRALIPID[®] DILUTIONS FOR DISCRETE LASER WAVELENGTHS BETWEEN 405 AND 1315 nm

T. Dreischuh, L. Gurdev, O. Vankov, L. Avramov, D. Stoyanov

*Institute of Electronics, Bulgarian Academy of Science
72 Tzarigradsko shosse blvd., Sofia 1784, Bulgaria
e-mail: tanjad@ie.bas.bg*

The experimental investigations on different aspects of optical tomography require the knowledge of the optical parameters of tissues and tissue-like phantoms in order to

ORAL AND POSTER SESSION

unambiguously interpret the experimental data and specify characteristic inhomogeneities in tissue diagnostics. The main optical parameters of interest are the absorption coefficient, μ_a , the scattering, μ_s , backscattering, μ_{bs} , and reduced-scattering, $\mu_{rs}=\mu_s(1-g)$, coefficients, the total attenuation (extinction) coefficient $\mu_e = \mu_a+\mu_s$, and the anisotropy factor, g . The absorption coefficient describes the optical-energy dissipation and respectively the thermal effect on tissues. The backscattering and extinction coefficients determine the informative depth of sensing, from where the backscattered (single-sided tomography) signal is sufficiently strong to be accurately detected [1].

In this work, we extend our investigations of the optical properties of tissue-mimicking phantoms, such as Intralipid-20% fat emulsion, using an approach we have developed recently [2] based on the peculiarities of laser radiation beams propagating through semi-infinite turbid media. The dependence of the total attenuation coefficient on the Intralipid concentration, for laser radiation wavelengths $\lambda=405, 672, 850, \text{ and } 1314 \text{ nm}$, is studied, by using a set of phantoms consisting of different dilutions of Intralipid in distilled water.

The experimental results for the extinction are in agreement with our previous results [2] and with empiric formulae found by other authors [3-5] concerning the wavelength dependence of μ_s of Intralipid -10% and Intralipid - 20%. They are also in agreement with known data of the water absorbance [6,7].

As a whole, the results obtained in the work confirm the consideration of the experimental phantoms as semi-infinite media. They also confirm and extend theoretical and experimental results obtained previously [1-5], and reveal advantages of using longer wavelengths for deeper diagnostics of tissues and mimic turbid media.

References:

- [1] L. Gurdev, T. Dreischuh, D. Stoyanov, Proc. SPIE 6604, 660421 (2007).
- [2] L. Gurdev et al. Appl. Phys. B 115, 427-441(2014).
- [3] H.J. van Staveren et al., Appl. Opt. 30, 4507- 4514 (1991).
- [4] R. Michels, F. Foschum, A. Kienle, Opt. Express 16, 5907-5925 (2008).
- [5] B. Aernouts et al., Opt. Express 21, 32450 (2013).
- [6] K. F. Palmer, D. Williams, JOSA 64, 1107 – 1110 (1974).
- [7] D. M. Wieliczka, S. Weng, M. R. Querry, Appl. Opt. 28, 1714 – 1719 (1989).

PD11

SYNCHRONOUS FLUORESCENT SPECTROSCOPY FOR ANALYSIS OF WINES AND WINE DESTILATES

Ya. Andreeva^{1,2}, E. Borisova¹, Ts. Genova^{1,2}, Al. Zhelyazkova¹, L. Avramov¹

¹*Institute of Electronics, Bulgarian Academy of Sciences, 72, Tsarigradsko chaussee Blvd. 1784 Sofia, Bulgaria; tel: +3592 9795894;*

²*Physics Faculty, Sofia University, 5, James Baucher Blvd, Sofia, Bulgaria
e-mail: borisova@ie.bas.bg*

Fluorescence spectroscopy is a well established and extensively used research and analytical tool in many disciplines. In the recent years, a remarkable growth in the use of fluorescence in food analysis has been observed. The fluorescence detection is used for analysis of different liquids, such as wines, brandies, beers, colorants, vegetable oils, honey, etc.

ORAL AND POSTER SESSION

Fluorescence technique could be successfully applied for analysis of wines. The fluorescent analysis takes advantage of the presence of natural fluorescent components, including tannic acid, vanillic acid, syringic acid, caffeic acid, ferulic acid, p-coumarin acid.

Wines are very complex systems and therefore conventional fluorescent technique, relying on recording of single emission or excitation spectra, is often insufficient, if directly applied. In such case, total luminescence or synchronous scanning fluorescence techniques are used, improving the analytic potential of the fluorescence detection.

Using FluoroLog3 spectrofluorimeter (HORIBA Jobin Yvon, France) measurements using excitation at the region of 220-700 nm were made on a set of wine samples. Emission spectra were detected in the region of 220-700 nm, and $\Delta\lambda$ from 10 to 100 nm, with step of 10 nm for the synchronous scanning was applied.

The present method allows recognition of the geographic region, where the wine is produced, detection of adulteration of the wines and authentication of the products. The method also allows differentiation of beverages. Further studies with increasing of the database and addressing of the fluorescence maxima observed to the chemical content of different types of wines are foreseen.

Acknowledgements: This equipment used in these experiments was purchased in the frames of grant DO-02-112/2008, funded by the National Science Fund of Bulgarian Ministry of Education and Science.

PD12

TISSUE FLUORESCENCE ORIGINS EVALUATION USING EXCITATION-EMISSION MATRICES

A. Zhelyazkova¹, E. Borisova¹, L. Angelova¹, E. Pavlova², M. Keremedchiev², L. Avramov¹

¹*Institute of Electronics, Bulgarian Academy of Sciences, 72, Tsarigradsko Chaussee Blvd.,
1784 Sofia, Bulgaria*

²*Queen Giovanna-ISUL University Hospital, 8, Bialo More str., 1527 Sofia, Bulgaria
e-mail: alexandra_jivkova@abv.bg*

Autofluorescence has been proven to be a very sensitive, accurate, noninvasive method for detection of early changes in tissues. The method has the potential to provide real-time diagnosis of different benign, dysplastic and malignant tissue pathologies.

The second most commonly diagnosed type of cancer is this of skin worldwide, gastrointestinal tract (GIT) tumours also are in the “top ten” positions. Most of them could have better prognoses for the patients, if earlier and precise diagnosis is applied.

Biological tissues, including skin, contain several types of endogenous fluorophores – co-enzymes, such as nicotinamide adenine dinucleotide (NADH), aromatic amino acids like tryptophan, and structural proteins such as collagen and elastin and their cross-links, some of the vitamins also have fluorescent properties and could be detected, such as vitamin A and D. We measured excitation–emission matrices (EEM) for normal and tumours’ human tissue samples of various cutaneous malignant, dysplastic and benign lesions, as well for normal GIT mucosa, polyps and carcinoma. We obtain the samples after surgical excision. Ethical approval for our investigations is received from Ethical Committee of University Hospital “Queen Giovanna-ISUL” – Sofia.

ORAL AND POSTER SESSION

We used spectrofluorimeter FluoroLog 3 (HORIBA Jobin Yvon, France) for our investigations. Excitation applied is in 280-440 nm region. Fluorescence emission were measured between 300 nm and 800 nm.

Based on the received EEM, we determined the main endogenous fluorophores, see table 1.

Endogenous Fluorophores	Excitation [nm]	Emission [nm]
Amino Acids	280-300	350-400
Structural proteins		
Collagen	335	350-450
Elastin cross-links	350-390	400-570
Keratin	480	500-570
Enzymes and co-enzymes		
NADH	360	380-550
Flavins	480	500-570
Porphyrins	390-410	610-700

Table 1. Endogenous Fluorophores-Excitation And Emission Maxima.

PD13

QUANTUM YIELDS OF THE PHOTODISSOCIATION OF HbO₂ AND HbCO IN THE VISIBLE SPECTRAL REGION

S. A. Mamilov¹, S. S. Esman¹, M. M. Asimov², A. I. Gisbrecht*

¹ *Institute of Physics National Academy of Sciences of Belarus, Minsk, Belarus*

² *Institute of applied problems of physics and biophysics NAS of Ukraine,*

³ *Institute of Electronics, Bulgarian Academy of Science.*

e-mail: agiz@abv.bg

In vivo experimental measurements of the quantum yield of the laser-induced photodissociation of oxyhemoglobin (HbO₂) and carboxyhemoglobin (HbCO) in cutaneous blood vessels in the visible spectral range are presented.

The spectral effectiveness of the photodissociation approximately correlates with their absorption spectrum and the transmission spectrum of skin tissue. It is shown that the quantum yield of photodissociation of HbCO is much higher than HbO₂.

Different aspects of biomedical application of this phenomenon are discussed. Non-invasive four-wavelength technique for determination of HbO₂ and HbCO concentrations in blood is also developed.

PD14

DIFFUSION OF NEAR-INFRARED LASER RADIATION IN TOOTH ROOT CANAL

Tz. Uzunov¹, I. Angelov², A. Gisbrecht^{3*}

¹Medical University, Department of Stomatology

²Institute of Organic Chemistry, Bulgarian Academy of Sciences

³Institute of Electronics, Bulgarian Academy of Sciences

e-mail: agiz@abv.bg

Optical methods for endodontic treatment of root canals become important in dental practice. Currently a large numbers of near-infrared lasers applies to endodontic procedures such as decontamination, apicoectomy, etc. In this context, solving safety problem of procedures is most important. Infrared irradiation penetrates deeply into biological tissue and, applying directly into the root canal, it can produce unwanted distant effects.

In this study are presented experimental results of measurements of the infrared laser radiation diffusion through human tooth roots in longitudinal and crosswise directions.

The obtained results can be used in dental practice for determination of the efficiency of therapy treatment and specific limits for each tissue-laser combination.

PD15

COMBINED OPTO-ULTRASOUND METHOD OF TISSUE OXYGENATION AND ITS APPLICATION IN MEDICINE

M. M. Asimov¹, D. B. Vladimirov¹, A. N. Rubinov¹, R. M. Asimov², A. I. Gisbrecht^{3*}

¹Institute of physics of National Academy of Sciences of Belarus, Minsk,

²"Sensotronica Ltd." Belarus Hi - Tech Park, Minsk, Belarus

³Institute of Electronics of Academy of Sciences of Bulgaria, Sofia, Bulgaria

e-mail: agiz@abv.bg

Novel method of tissue oxygenation and restoring normal cell metabolism is proposed. The results of investigation of tissue oxygenation by combination of ultrasound method and laser-induced photodissociation of blood oxyhemoglobin are presented.

Photodissociation of HbO₂ induced by laser radiation and release rate of free molecular oxygen into blood plasma has been measured experimentally at several wavelengths using high sensitive pulse oximeter. The oxygen released from HbO₂ primarily increases the PO₂ of blood plasma and then O₂ diffuses into a tissue.

This effect could be enhanced by applying the ultrasound method. Ultrasound waves have been widely used in medical therapy, in particular for increasing blood circulation. The combination with the method of laser-induced tissue oxygenation can increase the additional value of tissue oxygenation. It has been shown experimentally that an application of combined

ORAL AND POSTER SESSION

methods of tissue oxygenation increases local oxygen concentration at least two times directly in the zone of treatment.

Application of proposed method in modern medicine for increasing the efficiency of therapy treatment is discussed.

References:

[1] K. P. Nielsen, Juzeniene A, Juzenas P, Stamnes K, Stamnes JJ, Moan J. "Choice of optimal wavelength for PDT: The significance of oxygen depletion", *Photochem Photobiol.*,81, 1190-1194, (2005).

[2] J. A. Viator, J. Komadina, L. O. Svaasand, G. Aguilar, B. Choi, J. S. Nelson, "A comparative study of photo acoustic and reflectance methods for determination of epidermal melanin content", *J. Inv. Derm.*, 122, 1432–1439, (2004).

PD16

COMPARATIVE CLINICAL STUDY OF ANTIMICROBIAL ACTIVITY OF PAD WITH FOTOSAN, Nd : YAG LASER AND NaOCL AND EDTA USED FOR TREATMENT OF CHRONICAL PERIODONTITIS

Tzvetelina Gueaorgieva¹, Slavcho Dimitrov², Raina Gergova³

¹*Medical university of Sofia, Faculty of Dental medicine, Department of Conservative Dentistry-Sofia, Bulgaria*

²*Medical university of Sofia, Faculty of Dental medicine, Department of Conservative Dentistry-Varna, Bulgaria*

³*Medical university of Sofia, Faculty of medicine
e-mail:cvettyg@gmail.com*

The methods used recently for eradication of endodontic infection, main cause of apical periodontitis, are not fully effective (2,3). Photoactivation disinfection has a specific mechanism of action, which leads to a significant reduction of the bacterial infection (1). Another modern method is disinfection with high-energy lasers.

The purpose of this study is to make a comparative clinical study of the antibacterial effect of of PAD with FotoSan, Nd:YAG laser and NaOCL and NaOCL and EDTA used for treatment of chronical periodontitis.

The study included 54 teeth of patients diagnosed with chronic periodontitis. After the endodontic access is obtain we take microbiological sample from root canals to determine the types and quantities characteristic of isolated microorganisms. Treated teeth were divided into three groups of 18 teeth: I group – disinfection of roots canals with Nd: YAG laser with pulse mode with a frequency of 15 Hz, the diameter of fiber optic fiber is 200 µm for 1 minute; II group - photoactivation disinfection with . Fotosan. For the PAD is used laser "Laksta-Milon" with a wavelength of 665 nm, power 200 mW, continuous waveof irradiation for 1 minute with fiber-optic fiber with a thickness of 200 µm; III group- disinfection with 2,5% NaOCL% EDTA and 17 using a standard technique. Root canals in all three groups were dried with sterile paper points and microbiological sample is taken to account for the effect.

All three methods show significant differences in the amounts of MO before and after treatment ($p < 0.001$). These results show that the method NaOCL / EDTA has a greater effect

ORAL AND POSTER SESSION

of FAD Fotosan ($p = 0.048$). In the other groups there is no significant different effect on the amount of MO.

FAD with FotoSan can be successfully used as an additional method of disinfection of endodontic treatment.

Reference:

[1] BONSOR S J, NICHOL R, REID TM, PEARSON GJ. Microbiological evaluation of photo-activated disinfection in endodontics (An *in vivo* study). *Brit Dent J*; 200: 337–341, (2006).

[2] BONSOR SJ, NICHOL R, REID TM, PEARSON GJ. An alternative regimen for root canal disinfection. *Brit Dent J*; 201:101-105, (2005).

[3] GUNNEL ST, GUNNAR B. Biofilms in endodontic infections, *Endodon Top*; 9: 27–36, (2004).

Acknowledgements: This work is supported by the Grants projects of National Science Fund, Bulgaria.

PD17

BENT OPTICAL FIBER TAPERS FOR REFRACTOMETRY AND BIOSENSING

Emil Penchev¹, Tinko Eftimov², Wojtek Bock³

¹*University of Food Technology, 26 Maritza BLVD, 4000 Plovdiv, Bulgaria*

²*Faculty of Chemistry, Plovdiv University “Paisii Hilendarski”, 24 Tsar Assen Str., 4000 Plovdiv, Bulgaria*

³*Photonics Research Center, Universite du Quebec en Outaouais, Gatineau, Quebec, Canada*

We report the results of our study of the spectral shifts caused by surrounding refractive index changes (SRI) in bent fibre tapers. Fused and etched fibre tapers were fabricated using a gas burner and HF acid. Spectral shifts as high as 200 nm have been observed for SRI variations from 1.33 to 1.44 and sensitivity as high as 830 nm/r.i.u. around water RI values. We present results for refractometric measurements of cow milk of varying fat content and compare results with those obtained with conventional Abbe refractometers and high sensitivity double resonance LPGs.

OD1

REGULATORY BIOLOGICAL ACTION OF CONTINUOUS, QUASI-CONTINUOUS AND PULSED LASER RADIATION OF NANO- AND PICOSECOND RANGES

V. Yu. Plavskii¹, N. V. Barulin², A. I. Vodchits¹, I. A. Khadasevich¹, L. E. Batay¹, A.S. Grabchikov¹, A. I. Tretyakova¹, L. G. Plavskaya¹, A. V. Mikulich¹, V. A. Orlovich¹

¹ *B. I. Stepanov Institute of Physics, National Academy of Sciences of Belarus, 68 Nezavisimosti Ave., Minsk, 220072, Belarus*

² *Belarusian State Agricultural Academy, 5 Michurin Str., Gorki, 213410 Belarus*
e-mail: v.plavskii@ifanbel.bas-net.by

In this work, for the first time, comparative studies of biological activity of low intensity continuous, quasi-continuous and pulsed laser radiation of nano- and picosecond time ranges with the same average power density ($3,0 \text{ mW/cm}^2$) are carried out. Zooplankton (branchiopod crustaceans) *Artemia salina L.* and sturgeon sperm were used as objects. As a test, to check the action of laser radiation, percentage of nauplii hatched from cysts (protective shells) after activation of eggs in salt water in a stable thermal regime was chosen. The indicators of biological action on fish sperm were the data on duration of sperm motility as well as their curvilinear velocity after activation with water. Analysis of motility parameters was performed programmatically based on an assessment of their trajectory. The value of photobiological effect (dose curve) was evaluated in comparison with control intact objects. The exposure was realized using the second-harmonic radiation (wavelength – 532 nm, average output power $\sim 30 \text{ mW}$) of Nd:YAG-lasers working in continuous and quasi-continuous (pulse repetition rate – $F = 1 \text{ kHz}$, pulse duration – $\tau = 100 \text{ ns}$) modes, as well as in pulsed mode with generation of nanosecond ($\tau = 15 \text{ ns}$, $F = 10 \text{ Hz}$) and picosecond ($\tau = 60 \text{ ps}$, $F = 20 \text{ Hz}$) pulses. Comparative studies upon exposure to radiation of red spectral region (superbright LEDs, $\lambda = 632 \text{ nm}$, power density – 3 mW/cm^2) were also carried out.

It is shown, for the first time, that, despite the significant differences in peak values of intensity of acting factor, both continuous and quasi-continuous radiation and radiation of nano- and picosecond ranges are able to have both stimulating and inhibiting effects on all investigated parameters of functional activity of biological systems in a certain range of dose rates. For example, using the aforementioned parameters of acting factors the optimal stimulating dose when controlling the sperm motility is 135 mJ/cm^2 for continuous radiation; 90 mJ/cm^2 - for quasi-continuous and nanosecond and 60 mJ/cm^2 – for picosecond radiation. At the same time, maximal stimulating effect (compared to the control) is $140 \pm 6\%$ for continuous; $163 \pm 9\%$ – for quasi-continuous; $122 \pm 6\%$ – for nanosecond and $115 \pm 7\%$ – for picosecond modes. Even more pronounced stimulating effect ($180 \pm 9\%$) has a continuous radiation of red spectral region.

It is typical that stimulating effect in the case of nano- and picosecond modes is observed in a very narrow dose interval: $30\text{--}60 \text{ mJ/cm}^2$. The rapid suppression of functional characteristics of biological systems is observed upon increasing the dose: at a dose of 1.8 J/cm^2 duration of sperm motility reduced more than two times compared to the control.

Similar bell-shaped dose curves are registered when controlling the curvilinear sperm velocity and percentage of nauplii hatched from cysts after activation of eggs in salt. This type of dose curves testifies to “soft” regulatory nature of biological action of laser radiation. On the other hand, similar nature of dose curves upon control of functional characteristics differing in their

ORAL AND POSTER SESSION

structural organization of biological systems (zooplankton and fish sperm) is evidence of biological significance of the results obtained.

OD2

3D IMAGING OF CHITINOUS STRUCTURES USING NONLINEAR LASER SCANNING MICROSCOPY

Aleksandar Krmpot¹, Mihailo Rabasović¹, Branislav Jelenković¹, Srećko Ćurčić², Maja Vrbica², and Dejan Pantelić¹

¹ Institute of Physics, University of Belgrade, Pregrevica 118, 11080 Belgrade, Serbia

² Institute of Zoology, University of Belgrade - Faculty of Biology, Studentski Trg 16, 11000 Belgrade, Serbia
e-mail: krmpot@ipb.ac.rs

Various advanced optical microscopic techniques are in use today for the full characterization of micro-sized samples, giving different and mutually compatible information. In nonlinear microscopy (NLM), the information on oriented structures, refraction index variation, and fluorescent properties are obtained by detecting the signal produced by nonlinear optical effects: two photon excitation fluorescence (TPEF), second harmonic generation (SHG) and third harmonic generation (THG) during the scanning of the sample by laser beam [1]. The nonlinear optical effects are efficiently produced only in the focus of the laser beam where the intensity is high enough. High intensity is achieved by tight focusing using high numerical aperture objectives and ultra short laser pulses.

NLM experimental setup is employed for 3D imaging of chitinous structures of the specimens of endemic cave-dwelling insects *Pheggomisetes ninae* and *Plusiocampa christiani* from Southeast (the former species) and East Serbia (the latter species) [3]. The results are obtained using homemade experimental setup consisting of two femtosecond lasers, Ti:Sa (840 and 930 nm) and Yb:KGW (1040 nm). Properties of autoTPEF and SHG signal of chitin are examined and found suitable for 3D imaging in entomology. Also, images of compound eyes of the Small White butterfly (*Pieris rapae*) and some other species of butterflies (*Lepidoptera*) will be presented.

We have demonstrated the possibilities of using NLM in entomology and for 3D imaging of chitinous structures. The advantages are deep penetration into the sample and improved axial resolution in comparison with confocal microscopy. Obtained images are clear, well contrasted showing numerous details of the samples that can be used for the characterization of the insect organs and species determination.

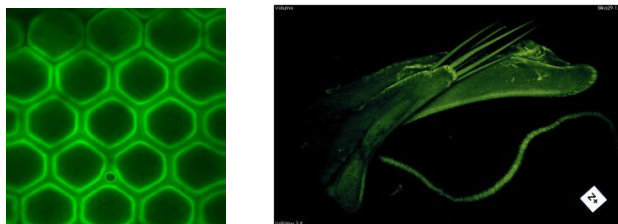


Figure 1. Images of the compound eye part of *Pieris rapae* (left) and aedeagus of *Pheggomisetes ninae* in alteral view (right) obtained by TPEF modality of NLM.

ORAL AND POSTER SESSION

References:

- [1] R. Carriles, D. N. Schafer et al, Rev Sci Inst, 80081101, (2009).
- [2] Barry R. Masters and Peter So, Handbook of Biomedical Nonlinear Optical Microscopy, Oxford University Press, (2008).
- [3] S. B. Ćurčić, H. Schönmann et al, Arch. Biol. Sci. Belgrade 56, 109-113, (2004).

Acknowledgements: We are thankful for financial support by the Ministry of education and science of Republic of Serbia, under grants III45016 and OI171038, and SNF-Scopes Grant IZ 76Z0 147548/1.

PE1

IMPROVED FAR-FIELD MODEL OF SIMPLE TWO-LEVEL ANNULAR BEAMS

Dimo N. Astadjov

*Metal Vapour Lasers Department, Georgi Nadjakov Institute of Solid State Physics,
Bulgarian Academy of Sciences, 72 Tzarigradsko Chaussee, Sofia 1784, Bulgaria
e-mail: asta55@issp.bas.bg*

Improved far-field distribution model of simple (uniform flat) two-level (low-intensity core and high-intensity ring) annular beams is presented. The model involves analytic solution of Fourier transform for such an annular beam near-field and digital integration of the far-field distribution yielded.

Beam output power parameters as dependents of annularity (input near-field annulus ratio of inside/outside radii) parameter are compared for dark (zero-intensity core) annular beam with an earlier model [1-3] which was entirely based on discrete (matrix) approach and issues are discussed.

We found that both models are adequate and conclusions from the earlier discrete approach are still valid. Yet new values of the power parameters of far-field output are being calculated and given here. We regard the new model (referred to as ‘semi-continuous’) as more precise than the discrete model because of very nature of the last (pixelation issues, roughness of definitions, etc.). Nevertheless the semi-continuous and the discrete approaches give similar results which are assessed to be within a tolerable deviation of ± 0.1 from each other.

The increased accuracy does not change the trends and whole picture of the behavior of the parameters which had been investigated and reported in our earlier publications [1-4]. The improved semi-continuous approach helped simulation accuracy made higher.

References:

- [1] D. N. Astadjov, “Fourier Transform of Annular Beams”, <http://arxiv.org/pdf/0904.1911v1>, Apr 13, (2009).
- [2] D. N. Astadjov, “Energy Focusability of Annular Beams”, AIP Conf. Proc., Vol. 1203, 472-476, (2010).
- [3] D N Astadjov and S V Nakhe, “CuBr laser beam transformations”, Journal of Physics: Conference Series, Vol. 253, 012076, (2010).
- [4] D N Astadjov, Om Prakash, “Experimental verification of focusability of coherent annular laser beams”, Proc. SPIE Vol. 8770, 87701O, (2013).

Acknowledgements: This work was supported by BIn#3/07 Grant of Ministry of Science and Education of Republic of Bulgaria.

PE2

DETERMINATION OF SPATIALLY-RESOLVED ELECTRON TEMPERATURE IN POWERFUL GAS-DISCHARGE LASERS

K. A. Temelkov¹, T. P. Chernogorova², S. I. Slaveeva¹, N. K. Vuchkov¹

¹*Metal Vapour Lasers Laboratory, Institute of Solid State Physics, Bulgarian Academy of
Sciences, 72 Tzarigradsko Chaussee, 1784 Sofia, Bulgaria*

²*Faculty of Mathematics and Informatics, Sofia University, 3 James Bourchier, 1164 Sofia,
Bulgaria
e-mail: stisl80@abv.bg*

Electron temperature together with gas temperature and electron density are the most fundamental plasma parameters in gas discharges and play a very important role in understanding of numerous phenomena in gaseous discharges, laser physics, plasma technologies, gas-discharge mass spectroscopy, absorption and emission spectroscopy, and plasma in general.

Elastic and inelastic electron-heavy particle collisions, such as electron impact excitation, de-excitation, and ionization, as well as three-body recombination, depend on the electron temperature. Measurements of electron temperature by Langmuir probe are not suitable for pressure of helium (He) or neon (Ne) above 10 Torr, especially in high-voltage and high-current nanosecond pulsed longitudinal discharges. Laser Thomson scattering measurements of electron temperature have been proved to be effective but challenging because of the low signal and excessive stray light, as well as the complicated experimental setup. In the literature there are several models of varying degrees of complexity, which predict, among the other parameters, values of electron temperature with considerable variation, and furthermore there is no overlap.

Under conditions of Local Thermodynamic Equilibrium measurement of the relative intensities of some He and Ne spectral lines, originating from different upper levels, enabled us to determine the stationary electron temperature, as well as the time-resolved electron temperature in the discharge afterglow, in a nanosecond pulsed longitudinal discharge (NPLD) in He, Ne and Ne-He mixtures. This type of discharge is widely used for excitation of powerful metal and metal halide vapour lasers, oscillating in deep ultraviolet (DUV), visible, near infrared (NIR) and middle infrared (MIR) spectral ranges.

Using time-resolved measurement of electrical discharge parameters, such as tube voltage and discharge current, electron temperature and electron density were also determined in the discharge period of NPLDs, exciting He-Sr⁺ recombination, DUV Cu⁺ Ne-CuBr and He-Hg⁺ lasers. The obtained results were in fairly good agreement with the existing self-consistent models or with the theoretical estimations.

Using the results obtained for stationary electron temperature and analytically solving steady-state heat conduction equation for electrons as well, radial distribution of electron temperature, i.e. spatially-resolved electron temperature, is also obtained for a number of high-power metal and metal halide vapour lasers.

PE3

COMPARISON BETWEEN A LASER Nd: YAG AND Nd, Cr: YAG PUMPED BY FLASH LAMP

R. Bouadjemine, D. Louhibi

*Division Milieux Ionisés et Laser, Centre de Développement des Technologies Avancées
 CDTA BP 17, Cité du 20 Août 1956, Baba Hassan, Alger
 e-mails : rbouadjemine@cdta.dz, dlouhibi@cdta.dz*

The major disadvantage for a Nd: YAG laser pumped by a flash lamp is the low pumping efficiency. Only a small fraction of the emission spectrum of the flash (figure 1.a) is absorbed by the bands pumping of the active medium (figure 1b).

Flash lamps allow a homogeneous pumping and allow the design of more economic flash especially for large power systems.

The co-doping Chrome neodymium allows better improvement of the pumping efficiency by transferring excitation bands chromium pumping to higher levels of the neodymium laser. It is noted that the absorption bands of chrome covers a large part of the emission spectrum of the flash (Figure 1.c), with a transfer coefficient of about 80% [1]. The laser rods Nd:YAG codoped chrome constitute excellent candidate for solar pumping lasers and quasi-solar [2-4].

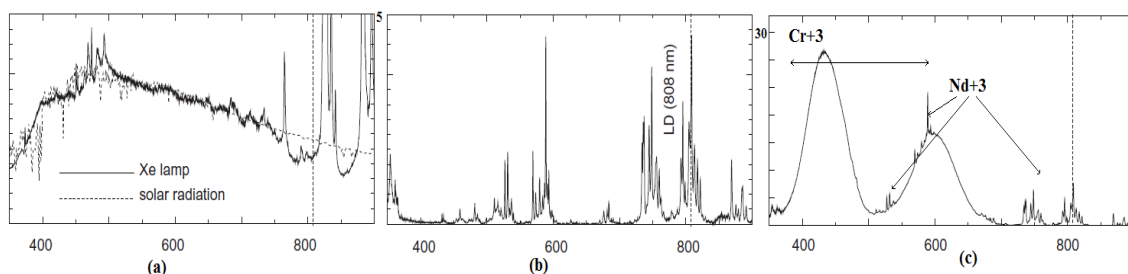


Figure 1. (a) Emission spectrum of the flash lamp and sun. (b, c) Absorption spectrum of Nd: YAG, Nd,Cr :YAG.

In our work, we simulated our dynamic laser oscillator Nd: YAG and Nd, Cr: YAG pumped by flash.

The parameters used in the simulation are:

$\zeta = 1$, $b=0.1$, $L_C = 0.60$ m, $L_b = 0.065$ m, $c = 3.10^8$ m/s,
 $\sigma_{21} = 6 \cdot 10^{-23}$ m², $n_{tot} = 1.38 \cdot 10^{26}$ atomes/m³, $R_1=90\%$,
 $\gamma = 0.20$, $\tau_C = 1.95$ ns, $n_{S0} = 0.30 \cdot 10^{21}$ atomes/m³.
 Nd :YAG : $\tau_f = 230 \cdot 10^{-6}$ s.
 Nd,Cr:YAG: $\tau_f = 600 \cdot 10^{-6}$ s, $W_p(Nd,Cr) = W_p(Nd)*50$.

The Result is in accordance with experiment.

References:

- [1] Masamori Endo, "Optical characteristics of Cr+3 codoped Y3Al5O12 ceramics", Optics and laser technology, 42, 610-616, (2010).
- [2] Koechner W. "Solid-state laser engineering", 6th ed. U S A, Springer, (2006).
- [3] Taku Saiki, "Disk-type Nd/Cr:YAG ceramic lasers pumped by arc-metal-halide-lamp" Optics Communications 268, 155–159, (2006).

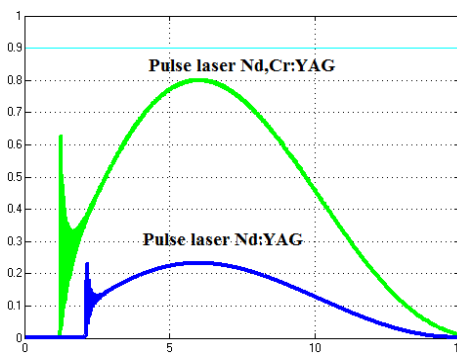


Figure 2. Pulse laser for Nd:YAG and Nd, Cr: YAG.

ORAL AND POSTER SESSION

[4] Hideki YAGI, “Highly Efficient Flashlamp-Pumped Cr³⁺ and Nd³⁺ Codoped Y₃Al₅O₁₂ Ceramic Laser”, Japanese Journal of Applied Physics Vol. 45, No. 1A, pp. 133–135, (2006).

PE4

POLYMERS IN LENS DESIGN FOR LASER APPLICATIONS

Stefka Kasarova¹, Nina Sultanova¹, Ivan Nikolov²

¹ Department of Mathematics and Physics, “Prof. Assen Zlatarov” University of Bourgas
1 Prof. Yakimov Str., Bourgas-8010, Bulgaria

² Department of Optics and Spectroscopy, “St. Kliment Ohridsky” University of Sofia
5 J. Bourchier Blvd., 1164 Sofia, Bulgaria
e-mail: kasarova_st@yahoo.com

In the last two decades application of optical polymers grows in popularity. Plastics have several key advantages over glass as low manufacturing cost, low weight and design flexibility. Injection moulding technology of fabrication of optical elements allows for reproducing aspheric, toric and other complex geometric surfaces which broadens application of polymers not only in consumer but in precision optics, too.

Successful application of polymers in lens design is based on knowledge of their optical as well as some material properties. We have measured refractive indices of more than twenty types of transparent plastic materials including principal and some new development polymers [1]. Different measuring techniques are applied to obtain precise refractometric data. Transmission and dispersion have been also investigated not only in the visible but also in the near-infrared region [2, 3]. Refractive and dispersive characteristics are reported to confirm usage of polymers in the design of optical systems for laser applications. Refractive indices at many laser emission wavelengths of polymers are presented. The data is intended for designers and technologists of laser optical systems.

Examples of optical design of all-plastic laser beam expanders on base of Galilean type optical scheme are presented. Suitable polymer materials are selected on base of our refractive index measurements and calculated dispersive characteristics. Ray trace, spot-size and wavefront analysis are carried out and optimization of the aberrations is proposed.

References:

[1] N. Sultanova, C. Ivanov, I. Nikolov, “Measuring the refractometric characteristics of optical plastics”, Opt. Quant. Electron., Vol. 35, pp. 21-34, (2003).

[2] S. Kasarova, N. Sultanova, C. Ivanov, I. Nikolov, “Analysis of the dispersion of optical plastic materials”, Opt. Mater., Vol. 29, No 11, pp. 1481-1490, (2007).

[3] N. Sultanova, S. Kasarova, I. Nikolov, “Characterization of optical properties of optical polymers”, Opt. Quant. Electron., Vol. 45, pp. 221-232, (2013).

PE5

DYNAMIC LASER SPECKLE MEASUREMENT WITH ENHANCED VIZUALIZATION OF ACTIVITY MAP

Elena Stoykova, Nataliya Berberova, Tanya Nikova

*Institute of Optical Materials and Technologies, Bulgarian Academy of Sciences, Acad.
Georgi Bonchev Str., Bl.109, 1113 Sofia, Bulgaria
e-mail: natali.berberova@gmail.com*

Capture of 2D laser speckle patterns in time provides means to recognize regions of high or low physical or biological activity within an object through statistical description of speckle dynamics on its surface [1]. Sensitivity and reliability of the dynamic speckle method depend on the applied processing algorithm. In the ideal case, the estimate should give a quantitative high contrast detailed 2D map that adequately reflects the spatial distribution of activity at non-uniform illumination and varying reflectivity across the object surface as well. To improve the contrast of the built activity map, recently we proposed pointwise correlation-based processing [2]. If N patterns of size $N_x \times N_y$ are acquired for time T at a sampling rate $1/\Delta t = N/T$ and a pixel period Δ , $N_x \times N_y$ time sequences of 8-bit encoded intensities $I_{kl,n} \equiv I(k\Delta, l\Delta, n\Delta t)$, $k = 1, 2, \dots, N_x$, $l = 1, 2, \dots, N_y$, $n = 1, 2, \dots, N$ are formed. They allow for building a pointwise estimate of a correlation or structure function by averaging over T .

Speckle nature of the acquired patterns leads inevitably to strong fluctuations of the estimates across the sample. This is valid for all processing algorithms. The aim of the present paper is to find out effective way to enhance visualization of the activity map obtained by correlation-based processing. As a first task we studied statistical properties of the built estimates and found out that the normalized estimates of the correlation function were negatively biased. The structure function algorithm provided a non-biased estimate with a better contrast of the activity map at the expense of requirement for uniform luminance across the captured speckle images. Both correlation and structure function estimates exhibited fluctuations which were increasing with the time lag. Therefore, as a second task, we applied approaches for smoothing the activity map by filters for signal dependent noise. Figure 1 depicts the smoothed 2D distribution of a structure function for a time lag equal to $10 \Delta t$ in the case of a sample with four different regions of activity. As a third task we considered building a map of a parameter related to the correlation radius of the temporal correlation function of the processes undergoing within the sample. The results are verified both by simulation and experiment.

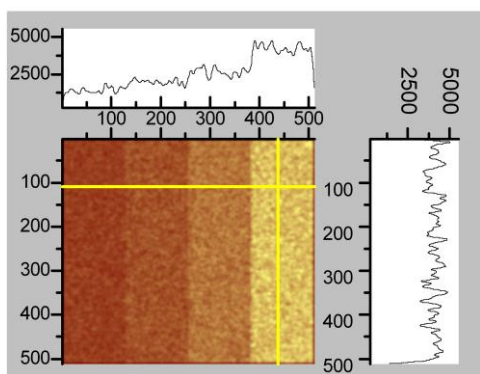


Figure 1. Enhanced visualization of activity map of a structure function estimate for a sample with four regions of different activity.

References :

- [1] E. Stoykova, B. Ivanov, and T. Nikova, "Correlation-based pointwise processing of dynamic speckle patterns, " *Opt. Lett.*, 39, 115-118 (2014).
- [2] H. Rabal, R. Braga (Eds.), "Dynamic laser speckle and applications", CRC Press, (2009).

PE6

BIREFRINGENCE INDUCED IN AZOPOLYMER (PAZO) FILMS WITH DIFFERENT THICKNESS

Lian Nedelchev^{1,2}, Dimana Nazarova¹, Georgi Mateev¹, Nataliya Berberova¹

¹*Institute of Optical Materials and Technologies – Bulgarian Academy of Sciences,
Acad. G. Bonchev Str., bl. 109, P.O Box 95, 1113 Sofia, Bulgaria*

²*College of Telecommunications and Post, 1 Acad. St. Mladenov Str., 1700 Sofia, Bulgaria
e-mail: dimana@iomt.bas.bg*

In this article we present a study of the photoinduced birefringence (Δn) in films of a water soluble azopolymer: poly[1-[4-(3-carboxy-4-hydroxyphenylazo)benzene sulfonamido]-1,2-ethanediyl, sodium salt] (PAZO). Varying the concentration of the azopolymer in the solution, films with wide range of thicknesses are obtained – from 50 to 2500 nm. The film thickness is determined with a Talystep precision profilometer, as illustrated in Fig. 1.

Birefringence is measured using a polarimetric setup (Fig. 2) with a recording laser at 473 nm and probe He-Ne laser at 633 nm. As shown experimentally, the birefringence value is relatively high for all of the investigated samples and is of the order of $\Delta n = 0.07$. The obtained results are analyzed and compared with published data for the same [1] or similar azopolymers [2,3].

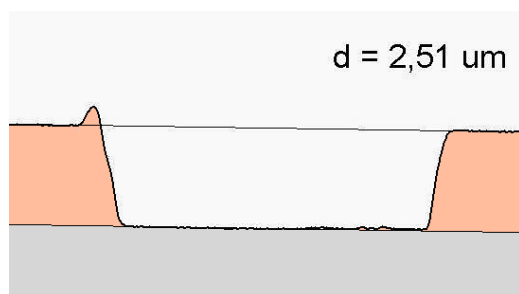


Figure 1. Example of a thin film groove profile obtained with the Talystep profiler.



Figure 2. Experimental setup for photoinduced birefringence measurement.

References:

[1] Q. Ferreira, P. Ribeiro, O. Oliveira, Jr., M. Raposo, “Long-Term Stability at High Temperatures for Birefringence in PAZO/PAH Layer-by-Layer Films” *ACS Applied Materials & Interfaces* Vol. 4, No. 3, 1470-1477, (2012).

[2] B. Lachut, S. Maier, H. Atwater, M. de Dood, A. Polman, R. Hagen, S. Kostromine, “Large Spectral Birefringence in Photoaddressable Polymer Films” *Adv. Mater.*, Vol. 16, No. 19, 1746–1750, (2004).

[3] L. Nedelchev, A. Matharu, S. Hvilsted, P.S. Ramanujam, “Photoinduced anisotropy in a family of amorphous azobenzene polyesters for optical storage” *Appl. Opt.*, Vol. 42, No. 29, 5918-5927, (2003).

Acknowledgements: Support from COST Action MP1205 is gratefully acknowledged.

PE7

AQUEOUS SOLUTIONS OF $\text{MgSO}_3 \cdot 6\text{H}_2\text{O} : \text{M}$ (M = Co, Ni OR Co+Ni) AND NONLINEAR OPTICS

P. Petkova¹, M. Mustafa¹, P. Vasilev¹, V. Nedkov², J. Tacheva¹, and Youri Tzukrovski³

¹Shumen University “Konstantin Preslavsky”, 115 Universitetska street, 9712 Shumen, Bulgaria,

²Department of Physics, Faculty of Sciences and Engineering sciences, University “Mohamed Khider” 07000 Biskra, Algeria

³Dept. of Radiophysics and Electronics, Faculty of Physics, Sofia University “St. Kliment Ohridski”, James Boucher 5, 1164 Sofia
e-mail: Petya232@abv.bg

In this work, the absorption of the complexes $[\text{Co}(\text{H}_2\text{O})_6]^{2+}$, $[\text{Ni}(\text{H}_2\text{O})_6]^{2+}$ $[\text{Co}+\text{Ni}(\text{H}_2\text{O})_6]^{2+}$ is measured in the spectral region 400 – 800 nm. The aqueous solutions of $\text{MgSO}_3 \cdot 6\text{H}_2\text{O} : \text{M}$ (M = Co, Ni or Co+Ni) are prepared with the concentration 2%. The energies of the electron transitions in M are calculated. The role of the spin-orbit interaction and Jahn-Teller effect is evaluated also. Zeeman splitting which is characteristic for M is determined and discussed.

References:

[1] R. Drago, “Physical Methods in Chemistry”, (University of Illinois), Urbana, (1981).

[2] C. J. Ballhausen, “Introduction to Ligand Field Theory”, (Mc Graw – Hill Book Company) Inc., New York, (1964).

[3] G. S. Nikolov, “Structure and Properties of the coordination compounds”, Publishing house Science and Art, Sofia, (1977).

Acknowledgements: Partial financial support by a project of Shumen University (2014) is gratefully acknowledged.

PE8

GENERATION OF MODULATED MICROCHIP LASER PULSES

F. Almabouada, D. Louhibi

*Centre de Développement des Technologies Avancées, Division Milieux Ionisés & Laser
Cité du 20 Août 1956, BP n° 17 Baba Hassen, 16303 Algiers, Algeria
e-mail: falmabouada@cda.dz*

This paper describes the results obtained with a microchip Nd:YVO₄ laser and KTP crystal pumped by 808 nm laser diode to generate modulated laser pulses. The interest is due to the efficiency of this type of laser in several fields such as telecommunication, spectroscopy and medical applications [1-3]. The electrical circuit of the laser diode was designed allowing to change their drive current according to the type of modulation.

The laser pulses obtained, at a repetition rate of 10 kHz, detected with a PIN photodiode are represented on the lower traces of figures 1-a and 1-b. The upper traces are the laser diode

ORAL AND POSTER SESSION

drive signal which can be a square or sine waveforms. Burst mode has been also obtained as represented on the lower traces of figures 2-a and 2-b. The repetition rate of the pulses is up to 58 kHz. Varying the peak drive current, the duty cycle and the number of pulses allow to set the laser energy. For the burst mode experiment the energy obtained by pulse equal to 1.2 μ J.

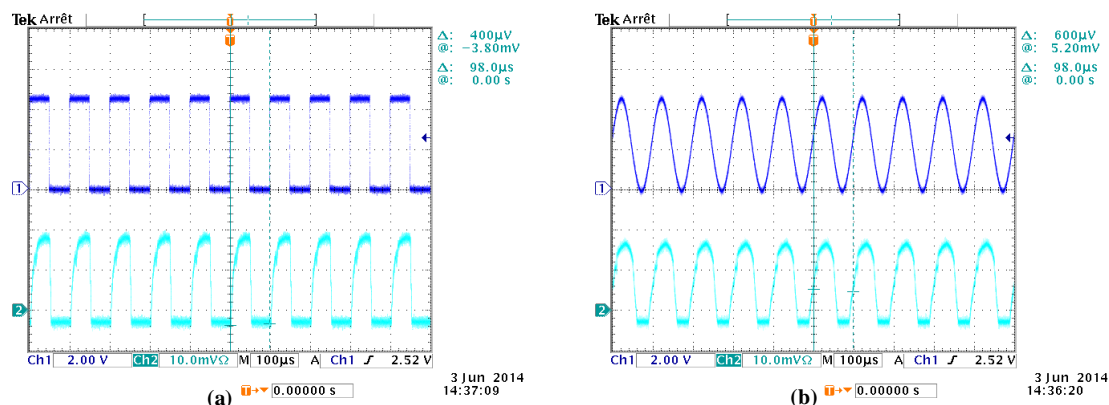


Figure 1. Laser diode drive signal and laser pulses.

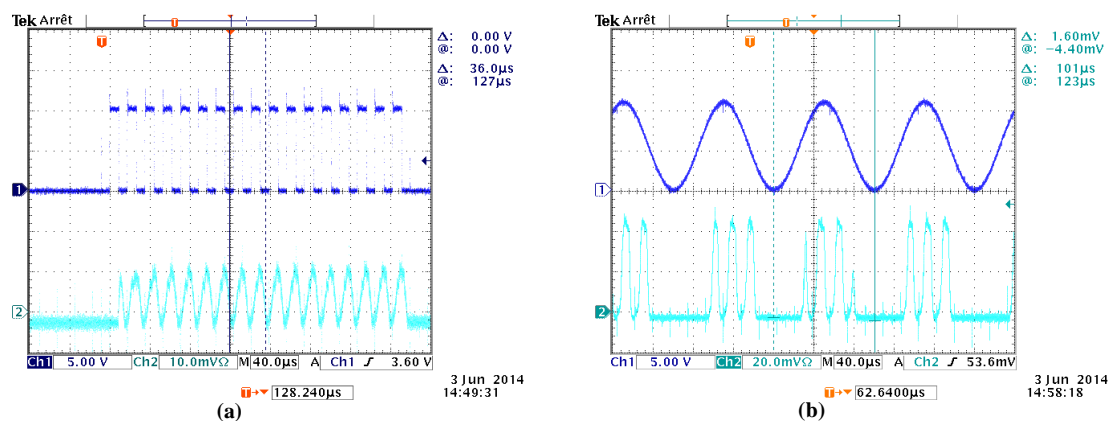


Figure 2. Burst mode pulses.

References:

- [1] R. Conroy, “Microchip lasers”, Doctoral Thesis, University of St. Andrews, Scotland (UK), (1998).
- [2] B. Cochenour, L. Mullen, and J. Muth, “A modulated pulse laser for underwater detection, ranging, imaging, and communications”, Proc. SPIE Vol. 8372, 1-10, (2012).
- [3] W. Koechener, “Solid-state Laser Engineering”, 6th edition, Springer Verlag, New York, (2006).

PE9

ANALOGIES AND DISTINCTIONS BETWEEN HYDRODYNAMIC SUPERCONTINUUM AND SUPERCONTINUUM GENERATION IN OPTICAL FIBERS

Armando Mena Contla¹, Ricardo Darío Peña Moreno¹, V. A. Pinaev², and V. N. Serkin¹

¹ Benemerita Universidad Autonoma de Puebla, 72001, Puebla, Mexico

² Kutateladze Institute of Thermophysics, Siberian Branch of
the Russian Academy of Sciences, Novosibirsk, Russia
e-mail: vsarkin@yahoo.com

The interpenetration of the main ideas and methods being used in different fields of science and technology has become one of the decisive factors in the progress of science as a whole. Completely different systems can be described by similar mathematical models, and generalized analogies between different fields have proven to be extremely fruitful.

As one of the most important example, we consider the hydrodynamic supercontinuum discovered recently in [1]. In [1], the authors presented the experimental observations of higher-order solitons in a water wave tank and show that a higher-order water wave soliton can also split into fundamental solitons and generate a broad and continuous spectrum in the same way as seen in optics. By analogy with the corresponding optical phenomenon [2], in [1], the authors theoretically described this effect and proposed to call it as a hydrodynamic supercontinuum.

There is one basic question to be answered. What happens if an arbitrary high-energy wave packet (for example, the high-order water soliton or laser beam/pulse) approaches the parameters region of the exact integrability of the model under consideration [3-5]?

The main goal of our work is to investigate main features of supercontinuum in the parameter regions closed to the exact integrability of the mathematical model.

References:

- [1] A. Chabchoub, N. Hoffmann, M. Onorato, G. Genty, J. M. Dudley, and N. Akhmediev, “Hydrodynamic Supercontinuum”, *Phys. Rev. Lett.*, 111, 054104-5 (2013).
- [2] J. M. Dudley and J. R. Taylor, Eds., “Supercontinuum Generation in Optical Fibers”, Cambridge University Press, (2010).
- [3] V. N. Serkin and A. Hasegawa, “Novel soliton solutions of the nonlinear Schrödinger equation model,” *Phys. Rev. Lett.*, 85, 4502–4505, (2000).
- [4] V. N. Serkin and A. Hasegawa, “Soliton management in the nonlinear Schrödinger equation model with varying dispersion, nonlinearity, and gain”, *JETP Lett.*, 72, 89–72 (2000).
- [5] V. N. Serkin, A. Hasegawa, and T. L. Belyaeva, “Nonautonomous Solitons in External Potentials”, *Phys. Rev. Lett.*, 074102 (2007).

PE10

ANALOGIES BETWEEN SOLITONIC BIO-ENERGY TRANSPORT ALONG POLYPEPTIDE CHAINS AND NONAUTONOMOUS OPTICAL SOLITONS IN STRUCTURATED NONUNIFORM FIBERS

Laura Moreno Lara¹, Ricardo Darío Peña Moreno¹, V.A. Pinaev², and V. N. Serkin¹

¹ Benemerita Universidad Autonoma de Puebla, 72001, Puebla, Mexico

² Kutateladze Institute of Thermophysics, Siberian Branch of
the Russian Academy of Sciences, Novosibirsk, Russia

e-mail: vserkin@yahoo.com

The interpenetration of the main ideas and methods being used in different fields of science and technology has become one of the decisive factors in the progress of science as a whole. Mathematical analogies between different physical systems can be extremely fruitful in understanding the novel physical concepts. Recently, the new theory of bio-energy transport along protein molecules in living systems, where the energy is released by hydrolysis of adenosine triphosphate (ATP), has been proposed [1]. In [1], Pang Xiao-feng introduced the new modified Davydov soliton with so larger lifetime that it can play an important role in biological processes and can be considered as a candidate of the bio-energy transport mechanism in protein molecules. The most important properties of this soliton transport of bio-energy are related with the influences of structure nonuniformity in protein molecules.

By analogy with the corresponding optical phenomena in inhomogeneous optical fibers with varying properties along the length [2], we study the main features of modified Davydov soliton on the basis of the unified nonautonomous nonlinear Schrodinger model in the parameters region of the exact integrability of the model under consideration.

References:

[1] Pang Xiao-feng, “The properties of bio-energy transport and influence of structure nonuniformity and temperature of systems on energy transport along polypeptide chains”, *Progress in Biophysics and Molecular Biology*, 108, 1-46, (2012).

[2] V. N. Serkin and A. Hasegawa, “Novel soliton solutions of the nonlinear Schrödinger equation model,” *Phys. Rev. Lett.*, 85, 4502–4505, (2000).

[3] V. N. Serkin, A. Hasegawa, and T. L. Belyaeva, “Nonautonomous Solitons in External Potentials”, *Phys. Rev. Lett.*, 074102, (2007).

PE11

“WATER WAVES” IN OPTICAL FIBERS: NONLINEAR TUNNELING OF HYDRODYNAMICAL AND OPTICAL SOLITON SUPERCONTINUA

Armando Mena Contla¹, Ricardo Darío Peña Moreno¹, V. A. Pinaev², and V. N. Serkin¹

¹ Benemerita Universidad Autonoma de Puebla, 72001, Puebla, Mexico

² Kutateladze Institute of Thermophysics, Siberian Branch of the Russian Academy of Sciences, Novosibirsk, Russia
e-mail: vserkin@yahoo.com

Mathematical analogies between different physical systems can be extremely fruitful in understanding the novel physical concepts. Recently, the so-called hydrodynamic supercontinuum has been discovered [1]. In [1], the authors presented the experimental observations of higher-order solitons in a water wave tank and show that a higher-order water wave soliton can also split into fundamental solitons and generate a broad and continuous spectrum in the same way as seen in optics. By analogy with the corresponding optical phenomenon [2], in [1], the authors theoretically described this effect and proposed to call it as a hydrodynamic supercontinuum.

There are two basic questions to be answered. What happens if an arbitrary high-energy wave packet (for example, the high-order water wave soliton or laser beam/pulse) approaches the classically forbidden potential barrier? In particular, what happens in the case of the nonlinear tunneling of the sequence of two or more isolated in space and time solitons with different self-interaction (binding) energies, and what happens in the opposite case of the tunneling of strongly overlapping in one space point N solitons? More generally, how does the wave-particle duality demonstrate itself for arbitrary high-order soliton bound states? What other analogies for N -soliton bound states have not been established so far?

In our work we provide a new framework for understanding of nonlinear tunneling mechanisms, and clarify the profound physical linkage between the quantum-mechanical tunneling and soliton continua tunneling through classically forbidden and localized potential barriers.

References:

- [1] A. Chabchoub, N. Hoffmann, M. Onorato, G. Genty, J. M. Dudley, and N. Akhmediev, “Hydrodynamic Supercontinuum”, *Phys. Rev. Lett.*, 111, 054104-5 (2013).
- [2] J. M. Dudley and J. R. Taylor, Eds., “Supercontinuum Generation in Optical Fibers”, Cambridge University Press, (2010).

PE12

FORMATION OF STABLE LORENTZIAN TYPE FILAMENT FROM INITIAL FS PULSE WITH GAUSSIAN SHAPE

V. Slavchev, L. Kovachev

*Institute of electronics, Bulgarian Academy of Sciences
72 Tzarigradsko shossee, 1784, Sofia, Bulgaria
e-mail: lubomirkovachev@yahoo.com
e-mail: valio5@mail.bg*

One of the basic methods for transformation of an initial Gaussian femtosecond pulse to stable filament is by using long-focus lens ($f = 3-5m$) and gradually increasing the intensity up to $I_{cr} = 1 \cdot 10^{12} W/cm^2$ [1, 2]. The long-focus lens prevents the strong self-focusing and the formation of plasma in the nonlinear focus. On the other hand the weak self-focusing broadens the spectrum of the femtosecond pulse which leads to the formation of a stable filament.

In the present work is studied numerically the process of formation of stable filament with theoretical model based on the vector generalization of the nonlinear amplitude equation.

References:

[1] A. Couairon, A. Mysyrowicz, “Femtosecond filamentation in transparent media” Physics Reports, 441, 47-189 (2007).

[2] G. Mechain, A. Couairon, Y.B. Andre, C. D’Amico, M. Franco, B. Prade, S. Tzortzakis, A. Mysyrowicz, R. Sauerbrey, “Long-range self-channeling of infrared laser pulses in air: a new regime without ionization”, Appl. Phys B, 79, 379-382 (2004).

PE13

FILAMENT AS VECTOR SOLITON WITH LORENTZIAN PROFILE. ONDITIONS FOR STABILITY

A. Dakova and L. Kovachev

*Institute of Electronics, Bulgarian Academy of Sciences
72 Tzarigradsko shossee, 1784 Sofia, Bulgaria
e-mails: anelia.dakova@abv.bg, lubomirkovach@yahoo.com*

In resent experiments on filamentation the following basic characteristics of a stabile filament are observed: broad-band spectrum [1], asymmetrical spectral and temporal shape associated with the Lorentzian profile [1], rotation of the vector of polarization [2], coherent GHz and THz generation [3].

These experimental results cannot be explained in the frames of well-known scalar models describing the process of filamentation and a vector generalization is required. By using a vector models it can be accounted the effects like rotation of the vector of polarization of the pulses and the reduction of the number of filaments observed during multi-filamentation [4].

ORAL AND POSTER SESSION

As it is shown in [5], the coupled vector equations have analytical solutions with Lorentzian profile for A_+ and A_- components of the electric field.

In our work the stability of these solutions under small perturbation of the amplitude and the phase is numerically investigated.

References:

- [1] Couairon A., Mysyrowicz A., “Femtosecond filamentation in transparent media”, *Physics Report* 441, 47-189 (2007).
- [2] Olga Kosareva, Nikolay Panov, Vladimir Makarov, Igor Perezhogin, Claude Marceau, Yanping Chen, Shuai Yuan, Tiejun Wang, Heping Zeng, Andrey Savelev, See Leang Chin, “Polarization rotation due to femtosecond filamentation in an atomic gas”, *OPTICS LETTERS* / Vol. 35, No. 17 / September 1, (2010).
- [3] S. Tzortzakis, G. Méchain, G. Patalano, Y.-B. André, B. Prade, M. Franco, A. Mysyrowicz, J. M. Munier, M. Gheudin, G. Beaudin, and P. Encrenaz, “Coherent subterahertz radiation from femtosecond infrared filaments in air”, *Opt. Lett.*, 1944-1946, (2002).
- [4] Daniela A. Georgieva, Liubomir M. Kovachev, “Energy transfer between two filaments due to degenerate four-photon parametric process”, *In Press* (2014).
- [5] Annual Report of the Institute of Electronics, Bulgarian Academy of Sciences, (2013).

PE14

COMPARISON OF SOLITON SOLUTIONS OF THE NONLINEAR SCHRÖDINGER EQUATION AND THE NONLINEAR AMPLITUDE EQUATION

A. Dakova and D. Dakova

*Faculty of Physics, University of Plovdiv “Paisii Hilendarski”,
24 Tsar Asen Str., 4000 Plovdiv
e-mails: anelia.dakova@abv.bg, ddakova2002@yahoo.com*

It is known that the Nonlinear Schrödinger equation (NLSE) very well describes the evolution of nano- and picosecond pulses in isotropic nonlinear dispersive medium [1, 2]. For exploration the propagation of femtosecond and attosecond light pulses it is necessary to be used the more general nonlinear amplitude equation [2, 3]. Therefore it is important to clarify the difference between the solutions of these two equations.

In the present work are investigated the one-dimensional soliton solutions of the NLSE and the nonlinear amplitude equation describing the evolution of optical pulses in a single-mode fiber with negative dispersion of the group velocity. It is shown that for a fundamental soliton the main difference between the two solutions is in the phases of the pulses.

References:

- [1] Agrawal, G. P., *Nonlinear fiber optics*, Academic Press, INC, New York (2007).
- [2] Boyd, R.W., *Nonlinear optics*, Academic Press, (2003).
- [3] Aneliya M. Dakova, Diana Y. Dakova, Finding a soliton solution of the nonlinear amplitude equation describing the evolution of optical pulses in a single-mode fiber, *Scientific Researches of the Union of Scientists in Bulgaria-Plovdiv, Series C. Natural Sciences and Humanities*, vol. XVI, ISSN 1311-9192 (2013).

PE15

INTRAPULSE RAMAN SCATTERING IN THE PRESENCE OF LINEAR AND NONLINEAR GAIN AS WELL AS SPECTRAL FILTERING

Ivan M. Uzunov¹, Zhivko D. Georgiev², Todor N. Arabadzhev¹

¹*Department of Applied Physics, Technical University Sofia, 8 Kl. Ohridski Blvd., Sofia 1000, Bulgaria,*

e-mails: ivan_uzunov@tu-sofia.bg, tna@tu-sofia.bg

²*Department of Theoretical Electrical Engineering, Technical University Sofia, 8 Kl. Ohridski Blvd., Sofia 1000, Bulgaria*

e-mail: zhdgeorg@tu-sofia.bg

In this paper we present numerical investigation of the influence of intrapulse Raman scattering (IRS) [1] on the stable stationary pulses. Our basic equation, namely cubic-quintic Ginzburg-Landau equation [2] describes the propagation of ultra-short optical pulses under the effect of IRS in the presence of linear and nonlinear gain as well as spectral filtering [3]. Our aim is to examine numerically the influence of IRS, on the stable stationary pulses in the presence of constant linear and nonlinear gain as well as spectral filtering. Numerical solution of our basic equation is performed by means of the “fourth-order Runge-Kutta method in the interaction picture method” method [4]. We found that the small change of the value of the parameter which describes IRS leads to qualitatively different behavior of the evolution of pulse amplitudes. In order to study the observed strong dependence on the IRS perturbation method of conserved quantities of the nonlinear Schrodinger equation [5] is applied. The bifurcation analysis of the derived nonlinear system of ordinary differential equations has shown that our numerical findings are related to the existence of the Poincare-Andronov-Hopf bifurcation [6] and the appearance of the unstable limit cycle.

References:

- [1] G. P. Agrawal, *Nonlinear Fiber Optics*, third ed., Academic Press, San Diego, (2001).
- [2] N. N. Akhmediev and A. Ankiewicz, *Dissipative solitons in the complex Ginzburg-Landau and Swift-Hohenberg equations*, in: N. N. Akhmediev and A. Ankiewicz (eds.), *Dissipative Solitons*, Springer, Berlin, (2005).
- [3] S. C.V. Latas and M.F.S. Ferreira, *Soliton propagation in the presence of intrapulse Raman scattering and nonlinear gain*, *Opt. Commun.*, 251, 415- 422 (2005).
- [4] J. Hult, “A Fourth-Order Runge–Kutta in the Interaction Picture Method for Simulating Supercontinuum Generation in Optical Fibers”, *J. Lightwave Technology*, 25, 3770-3775, (2007)
- [5] A. Hasegawa and Y. Kodama, *Solitons in Optical Communications*, Clarendon Press, Oxford, (1995).
- [6] S. Wiggins, *Introduction to Applied Nonlinear Dynamical Systems*, second ed., Springer, New York, (2003).

PE16

SOLITON SELF-FREQUENCY SHIFT IN THE PRESENCE OF LINEAR AND NONLINEAR GAIN, THIRD-ORDER DISPERSION AND SELF-STEEPENING EFFECT

Ivan M. Uzunov¹, Todor N. Arabadzhev¹, Zhivko D. Georgiev²

¹*Department of Applied Physics, Technical University Sofia, 8 Kl. Ohridski Blvd., Sofia 1000, Bulgaria,*

e-mails: ivan_uzunov@tu-sofia.bg, tna@tu-sofia.bg

²*Department of Theoretical Electrical Engineering, Technical University Sofia, 8 Kl. Ohridski Blvd., Sofia 1000, Bulgaria*

e-mail: zhdgeorg@tu-sofia.bg

We study soliton self-frequency shift due to the intrapulse Raman scattering (IRS) [1] in the presence of linear and nonlinear gain, spectral filtering, third-order of dispersion and self-steepening. The model which describes this phenomenon generalizes the cubic-quintic Ginzburg-Landau equation [2-3]. We first analyze the influence of third-order of dispersion and self-steepening on the soliton self-frequency shift IRS by means of the perturbation method of conserved quantities of the nonlinear Schrodinger equation [4]. Conditions are determined for reduction of soliton self-frequency shift. Further in order to verify the obtained results, numerical solution of generalized cubic-quintic Ginzburg-Landau equation is performed by means of the fourth-order Runge-Kutta method in the interaction picture method [5].

References:

- [1] G. P. Agrawal, *Nonlinear Fiber Optics*, third ed., Academic Press, San Diego, (2001).
- [2] P.-A. Bélanger, On the profile of pulses generated by fiber lasers: the highly – chirped positive dispersion regime (similariton), *Opt. Express* 14 12174-12182, (2006).
- [3] S. C. V. Latas, M. F. S. Ferreira, M.V. Facao, Impact of higher-order effects on pulsating, erupting and creeping solitons, *Appl. Phys. B* 104, 131-137, (2011).
- [4] A. Hasegawa and Y. Kodama, *Solitons in Optical Communications*, Clarendon Press, Oxford, (1995).
- [5]. J. Hult, “A Fourth-Order Runge–Kutta in the Interaction Picture Method for Simulating Supercontinuum Generation in Optical Fibers”, *J. Lightwave Technology*, 25, 3770-3775, (2007).

PE17

**FAR-FIELD DIFFRACTION OF SINGULAR DARK BEAMS BY
 COMPUTER-GENERATED HOLOGRAMS WITH ENCODED
 OPTICAL VORTICES**

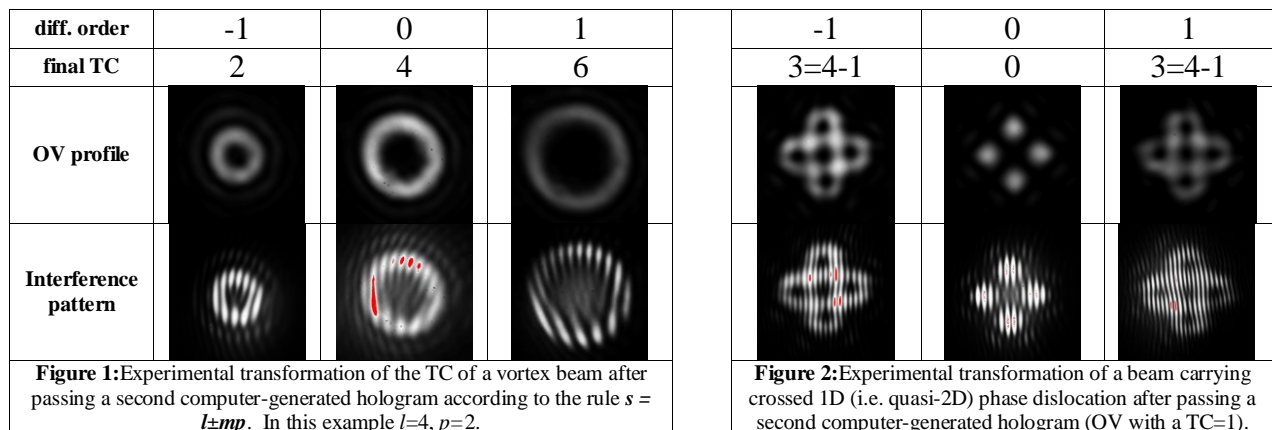
L. Stoyanov¹, S. Topuzoski², G. Maleshkov¹, I. Stefanov¹, L. Janicijevic², A. Dreischuh¹

¹*Department of Quantum Electronics, Faculty of Physics,
 Sofia University "St. Kliment Ohridski," Sofia-1164, Bulgaria*

²*Faculty of Natural Sciences and Mathematics, Institute of Physics,
 University "Ss. Cyril and Methodius," Skopje-1000, Republic of Macedonia
 e-mail: l_stoja@yahoo.com*

Optical vortices (OVs) are intriguing objects that attract much attention and display fascinating properties with possible applications in the optical transmission of information and in guiding and trapping of particles [1]. OVs are associated with isolated point singularities with helical phase profiles around them. The central singular point of the helix possesses no defined phase and therefore the intensity must vanish, leading to a characteristic toroidal intensity profile [1]. Such beams carry photon angular momentum, which can also be transferred to matter [2]. The angular momentum is referred to the topological charge (TC) l , which corresponds to the total phase change $2\pi l$ over the azimuthal coordinate φ . The far-field diffraction of an incident optical vortex with a TC l by a fork-shaped grating encoding an OV with a TC p and the resulting beam's topological charge $s=l\pm mp$ has been analyzed in [3].

Here we report experimental data (Fig. 1) confirming the predicted transformation of the TC of the input OV beam [3] after a second fork-shaped binary computer-generated grating. The radii of the transformed OVs also agree fairly well with these predicted from the analytical theory.



Further we conducted experiments in which, in the first grating, we encoded crossed 1D (i.e. quasi-2D) phase dislocation. The second hologram was fork-shaped, thus encoding an OV with a TC=1. The result (see Fig. 2) was very intriguing: Four new OVs were born from the crossed 1D phase dislocations. Additional experimental data will be presented and discussed too.

References:

- [1] A. Dreischuh, S. Chervenkov, Dr. Neshev, G. G. Paulus and H. Walther, *J. Opt. Soc. Am. B* **19**, 550-556, (2002).
- [2] A. S. Desyatnikov, Yu. S. Kivshar, and L. Torner, *Progress in Optics* **47**, 291-391, (2005).
- [3] H. He et al., *Phys. Rev. Lett.* **75**, 826-829, (1995).
- [4] S. Topuzoski and L. Janicijevic, *J. Modern Optics*, **58**, 138-145, (2011).

PE18

PULSE FRONT TILT MEASUREMENT OF FEMTOSECOND LASER PULSES

N. Dimitrov¹, L. Stoyanov¹, I. Stefanov¹, A. Dreischuh¹, P. Hansinger^{2,3}, G. G. Paulus^{2,3}

¹Department of Quantum Electronics, Faculty of Physics, Sofia University, Sofia, Bulgaria

²Institute for Optics and Quantum Electronics, Friedrich-Schiller-University, Jena, Germany

³Helmholtz Institute Jena, Jena, Germany

e-mail: nrd@phys.uni-sofia.bg

The pulse front tilt (PFT) is a specific spatio-temporal distortion of (ultra)fast optical pulses - the pulse front is tilted with respect to the direction of beam/pulse propagation, while its phase front remains perpendicular to it. In some cases the PFT is useful – e.g. for an efficient phase-matched terahertz radiation generated by optical rectification of femtosecond laser pulses down to near-single-cycle terahertz pulse durations.

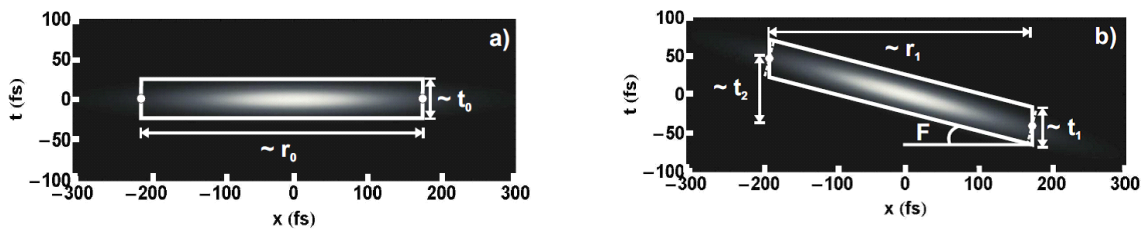


Figure 1. (a) Intensity distribution of a Gaussian pulse/beam with a time duration t_0 and beam width r_0 . (b) Effective pulse/beam dimensions t_1 , r_1 , and t_2 of the same pulse/beam envelope rotated at a PFT at an angle F .

In this work we report experimental measurement of an intentionally introduced pulse front tilt on femtosecond laser pulses by using an inverted field correlator/interferometer. The results obtained with two low-dispersion diffraction gratings are in good qualitative agreement with the data from a previously developed analytical model and from an independent interferometric measurement.

ORAL AND POSTER SESSION

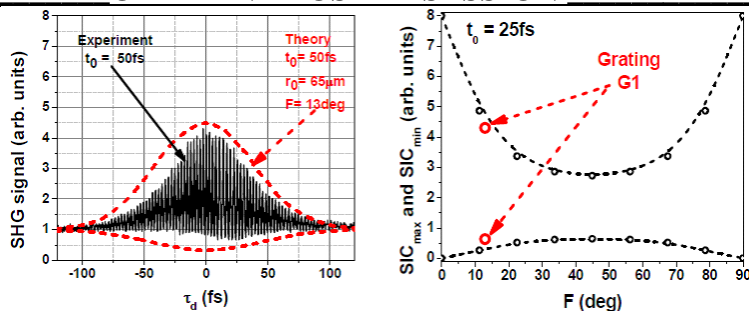


Figure 2. **Left:** Comparison between the experimentally measured interferometric correlation (IC) and the envelope of the simulated IC (SIC). **Right:** Location of the maximum and of the minimum of the experimentally obtained IC on the theoretically predicted dependence of the minimum and maximum of the SIC vs. PFT angle F .

These results provide a valuable criterion for the precision in aligning (in principle) dispersionless systems for manipulating ultrashort pulses, as well as in cases when the pulse front tilt is a result of a desired spatio-temporal coupling.

PE19

SPATIAL FILTERING OF WIRE LASER RADIATION

E. E. Orlova

*Institute for Physics of Microstructures RAS, Russia 60395, N. Novgorod GSP-105
e-mail: orlova@ipm.sci-nnov.ru*

Radiation structure of wire lasers (long lasers with subwavelength transverse dimensions) differs drastically from that of the lasers with transverse dimensions much larger than the wavelength [1,2]. High divergence and non-uniformity of the wave front of wire laser radiation hinders their application in imaging and remote sensing. On the other hand wire lasers are attractive for many applications due to their miniature size, high efficiency and low power consumption. Terahertz wire lasers are especially important for applications due the lack of convenient laser sources in this frequency region. It has been shown recently that radiation structure of wire lasers can be significantly improved using a special design of laser cavity [3-5]. Conventional methods of laser beam shaping [6] developed for the sources with transverse dimensions larger than the wavelength can not be directly applied to wire lasers. Here we show how spatial filtering of wire laser radiation can be achieved using spherical lenses, specially designed phase plates and a diaphragm, leading to concentration of a considerable part of the power emitted by a wire laser in a directive beam with the uniform phase front.

References:

- [1] E. E. Orlova, J. N. Hovenier, T. O. Klaassen, I. Kasalynas, A. J. L. Adam, J. R. Gao, T. M. Klapwijk, B. S. Williams, S. Kumar, Q. Hu, J. L. Reno, Phys. Rev. Lett., 96, 173904 (2006).
- [2] A. J. L. Adam, I. Kasalynas, J. N. Hovenier, T. O. Klaassen, R. Gao, E. E. Orlova, B.S. Williams, S. Kumar, Q. Hu, J. L. Reno, Appl. Phys. Lett., 88, 151105, (2006).
- [3] M. I. Amanti, M. Fischer, G. Scalari, M. Beck, J. Faist, Nature Photonics, 3, 586, (2010).

ORAL AND POSTER SESSION

[4] L. Mahler, A. Tredicucci, F. Beltram, C. Walther, J. Faist, H.E. Beere, D. A. Ritchie, D. S. Wiersma, *Nature Photonics*, 4, 165, (2010).

[5] T.-Y. Kao, Q. Hu, J. L. Reno, *Optics Letters*, 37, 2070, (2012).

[6] Laser beam shaping: theory and techniques ed F M Dickey and S C Holswade (New York: Marcel Dekker), (2000).

Acknowledgements: The work is supported by RAS, NATO SfP 984068 grant, RFBR project 14-02-00979a.

PE20

SUBPICO SECOND Z-SCAN METHOD

G. Yankov, T. Petrov

*Institute of Solid State Physics, Bulgarian Academy of Sciences, 72, Tzarigradsko
Chaussee, Blvd., 1784 Sofia, Bulgaria¹
e-mail: gjankov@issp.bas.bg*

Nonlinear optical properties – nonlinear refractive index n_2 and multi-photon absorption coefficient β were studied by new developed z-scan method. The introduced z-scan method has the following advantages:

- avoid the diffraction problems by applying CCD camera instead typically used power meter and diaphragm;
- simultaneous measurement of the nonlinear constants;
- by using fs laser, the influence of any thermal effects are minimized.

The developed setup was validated by measuring of nonlinear optical parameters of known materials from the literature (**fused silica** and **B₂F**). The values of n_2 and β of the glasses were determined.

OE1

IONIZATION-FREE FILAMENTATION. VECTOR MODEL AND VECTOR ROTATION

Lubomir M. Kovachev

*Institute of Electronics, Bulgarian Academy of Sciences,
Tzarigradsko shossee 72, 1784 Sofia, Bulgaria
e-mail: lubomirkovach@yahoo.com*

We present an analytical approach to the theory of propagation in air of femtosecond optical pulses with broad-band spectrum. The vector character of the nonlinear third order polarization is investigated in details, taking into account the carrier to envelope phase. This additional phase transforms the third harmonic term to GHz term, which starts to generate radiation when the pulse duration reaches the femtosecond range. Thus, the corresponding vector amplitude equations admit GHz oscillated terms, which creates a rotation of the vector

ORAL AND POSTER SESSION

of the electrical field in a plane, orthogonal to the direction of propagation. Exact vector soliton solutions of Lorentz type, which present this rotation, are obtained.

OE2

VECTOR GENERALIZATION OF THE FILAMENTS INTERACTION

Daniela A. Georgieva¹ and Lubomir M. Kovachev²

¹*Faculty of Applied Mathematics and Computer Science, Technical University of Sofia, 8,
Kliment Ohridski Blvd., 1000 Sofia, Bulgaria*

²*Institute of Electronics, Bulgarian Academy of Sciences,
Tzarigradsko shossee 72, 1784 Sofia, Bulgaria
e-mails: dgeorgieva@tu-sofia.bg; lubomirkovach@yahoo.com*

We investigate the filament as a vector field. We consider the interaction between the filaments by using generalized nonlinear polarization operator of the kind $\vec{P}_{nl} = n_2(\vec{E} \cdot \vec{E})\vec{E}$. The vector representation removes the disadvantages from the scalar theory and describes a mechanism of polarization rotation and energy exchange between the vector fields.

AUTHOR INDEX

A

Amoruso S., 20
Agustsson S., 28
Alexandrov M., 41,43
Aliosman M., 73
Alipieva E., 57
Almabouada F., 98
Andreeva Ya., 83
Angelov D., 30
Angelov I., 73,74,86
Angelova L., 84
Antoniou Ch., 77
Antonopoulou-Athera N., 78
Arabadzhev T., 105,106
Archer J., 65
Asimov M., 85,86
Asimov R., 86
Astadjov D., 92
Atanasov P., 40,42,44
Atanasova G., 40,43
Avdeev G., 40
Avramov L., 75,82,83,84

B

Balis D., 28
Barbucha R., 38
Barulin N., 89
Batay L., 89
Batsi O., 77
Berberova N., 49,96,97
Bialous A., 18
Bianchi G., 28
Bliznakova I., 39
Bock W., 88
Boevski I., 41
Borisova E., 74,75,83,84
Bouadjemine R., 94
Brabant D., 54
Bruzzese R., 20
Burdonsky I., 47

C

Calabrese R., 28
Carotta M. C., 20
Cartaleva S., 23,50,51,52,58,59,63
Chatzitheodoridis E., 76,78
Chernogorova T., 93
Christofidou E., 77

Contla A., 100,102
Corradi L., 28
Ćurčić S., 90

D

Dainelli A., 28
Dakova A., 103,104
Dakova D., 104
Danchovski V., 67
Daskalova A., 39
Delchev V., 53
Deleva A., 67,71
Demetzos C., 80
Dergachev A., 34
Derkachov G., 65
Dikovska A., 40,43
Dimitrov I., 41
Dimitrov N., 108
Dimitrov Sl., 87
Domcke W., 53
Doulgerides M., 78
Drakaki E., 77
Dreischuh A., 107,108
Dreischuh T., 68,69,70,82
Dutta M., 44
Dyankov G., 37,49
Dzhagarov B., 64

E

Eftimov T., 37,54,88
Eneva I., 74
Entin V., 58
Esman S., 85
Evangelatos Ch., 78
Evgenieva Ts., 66,67,68

F

Fukata N., 19,44

G

Garasz, 38
Gateva S., 51,54,59,61
Genova Ts., 75,83
Georgiev Zh., 105,106
Georgieva D., 111
Gergova R., 87
Ghosh P., 23,50
Gisbrecht A., 85,86

AUTHOR INDEX

Glódz M., 27,54
Gogyan A., 22
Goltsov A., 47
Gozzini S., 59
Grabchikov A., 89
Grigorov I., 67,71
Grochowska K., 18,46
Grujić D., 81
Grujić Z., 55
Gueaorgieva Tz., 87
Gurdev L., 69,70,82

H

Hakhumyan G., 21
Hansinger P., 108
Husinsky W., 39

I

Ionin A., 34
Ivanov D., 67

J

Jakubczyk D., 65
Janicijevic L., 107
Janowicz M., 27
Jelenković B., 55,62,90
Jendrzewski R., 45

K

Kalatzis I., 77
Kancheva P., 53
Kandidov V., 34
Karachalios I., 79
Karashanova D., 41
Kasarova S., 95
Katsambas A., 77
Keremedchiev M., 75,84
Khadasevich I., 89
Khanbekyan A., 22,28
Knyukshto V., 64
Kocik M., 38
Kolarov G., 71
Kolev N., 66,67,71
Koleva M., 40,44
Kolwas K., 65
Kolwas M., 65
Kostova I., 54
Kovachev L., 103,110,111

Kowalski K., 27,54
Krasteva A., 23,50,51,63
Krmpot A., 62,90
Kussovski V., 73,74

L

Lara L., 101
Lekić M., 55
Leonov A., 47
Lettieri S., 20
Leusenko I., 64
Louhibi D., 94,98
Lucchesini A., 59

M

Maddalena P., 20
Majumdar S., 46
Makarov K., 47
Makrelov I., 37
Makropoulou M., 77,80
Maleshkov G., 107
Mamilov S., 85
Mantareva V., 73,74
Margalit L., 25
Marinelli C., 28,51,59
Marinkov N., 41
Mariotti E., 28,51,61
Marmugi L., 28,51,59
Mateev G., 97
Mathes D., 79
Mazzocca G., 28
Merlemis N., 77
Mikulich A., 64,89
Mitra S., 23,50
Mitsou G., 79
Moi L., 28,51
Mokrousova D., 34
Moreno R., 100,101,102
Mourelatou E., 80
Movsisyan M., 22
Mustafa M., 98

N

Nasyrov K., 24,58
Nathala C., 39
Nazarova D., 97
Nedelchev L., 97
Nedkov V., 98

AUTHOR INDEX

Nedyalkov N., 40,41,42,44
Nikolov A., 41
Nikolov I., 95
Nikolov N., 58
Nikolova V., 50
Nikov R., 41
Nikov Ru., 42
Nikova T., 56,96

O

Orlova E., 109
Orlovich V., 89

P

Pallotti D., 20
Pantelić D., 81,90
Papoyan A., 22
Pashova T., 54
Paulus G., 108
Pavlova E., 84
Penchev E., 88
Peshev Z., 68,69
Petkov D., 66,67
Petkova P., 98
Petrov N., 58
Petrov T., 38,110
Pinaev V., 100,101,102
Plachkova V., 37
Plavskaya L., 64,89
Plavskii V., 64,89
Polischuk V., 63

R

Rabasović M., 90
Radojičić I., 55
Radonjić M., 55
Radzewicz C., 38
Ray B., 23,50
Ricci L., 28
Rosenbluh M., 25
Rubinov A., 86

S

Sargsyan A., 21,52
Sarkisyan D., 21,52
Savov P., 67
Sawczak M., 42,46
Schaefer K., 42

Seleznev L., 34
Semyachkina-Glushkovskaya O., 75
Serafetinides A., 29,76,77,78,80
Serkin V., 35,100,101,102
Sharlandjiev P., 49
Shlenov S., 34
Shmavonyan S., 22
Shustikova A., 34
Sianoudis I., 77, 79
Šibalić N., 62
Sinitsyn D., 34
Slavchev V., 103
Slaveeva S., 93
Slavov D., 23,39,50,63
Śliwiński G., 18,42,45,46
Spyratou E., 80
Stefanov I., 107,108
Stoyanov D., 68,69,70,71,82
Stoyanov L., 107,108
Stoykova E., 56,96
Stratigos A., 77
Sultanova N., 95
Sunchugasheva E., 34
Szonert J., 27,54

T

Tacheva J., 98
Tański K., 38
Taskova E., 57
Taslakov M., 61
Temelkov K., 93
Timofeev I., 47
Todorov G., 57,63
Todorov P., 23,50
Tomassetti L., 28
Tonchev D., 54
Topuzoski S., 107
Tretyakova A., 64,89
Tsvetkov S., 59,61
Tuna D., 53
Tzukrovski Yo., 98

U

Uzunov I., 105,106
Uzunov Tz., 86

AUTHOR INDEX

V

Valais I., 79
Vankov O., 82
Vartanyan T., 26,63
Vasilev P., 98
Vasiljević D., 81
Vladimirov B., 75
Vladimirov D., 86
Vladimirova J., 32
Vodchits A., 89
Vrbica M., 90
Vuchkov N., 93

W

Wilson-Gordon A., 25,52
Woźniak M., 65

Y

Yankov G., 110
Yufa V., 47

Z

Zadkov V., 32
Zekou E., 76
Zhelyazkova A., 75,83,84
Zhelyazkova K., 49
Zlatković B., 62
Zmuda-Trzebiatowska I., 42



NOTES

